From Percutaneous to Transcutaneous Hearing Implants:

Surgical Techniques, Osseointegration, and Microbiological Insights

Marsel Ganeyev

Department of Biomaterials

Institute of Clinical Sciences

Sahlgrenska Academy, University of Gothenburg

UNIVERSITY OF GOTHENBURG

Gothenburg 2025

Cover illustration: *Toluidine blue–stained section of peri-implant bone and soft tissue adjacent to a transcutaneous implant in the ovine model. Dark purple indicates soft tissue, light purple corresponds to mature bone, and the lightest purple highlights newly formed bone.*

© Marsel Ganeyev 2025
marsel.ganeyev@biomaterials.gu.se

ISBN 978-91-8115-348-4 (PRINT)
ISBN 978-91-8115-349-1 (PDF)

Printed in Borås, Sweden 2025
Printed by Stema Specialtryck AB

In an attempt to observe my inner self as a sensation,

or as a hard-working osteocyte.

ABSTRACT

From the moment a person decides to change their life and steps into the operating room to (re)gain one of the most vital senses—hearing—through to their return to daily routines, multiple factors shape both the decision-making process and overall experience. Thus, optimising functional outcomes in implantable bone conduction devices (BCD) requires a patient-centred approach that integrates clinical insights with advanced diagnostic, surgical, and analytical methods to examine the interplay between biological responses, surgical execution, and the microbiome. This thesis explores these aspects in four studies. Paper I analyses retrieved percutaneous implants, linking clinical symptoms with structural, histological, and microbiological findings. Paper II investigates the peri-abutment microbiome, showing how staphylococcal colonisation, biofilms, and antibiotic resistance drive soft tissue complications. Paper III evaluates the mechanical and thermal effects of different drilling protocols on bone trauma. Lastly, Paper IV introduces a surface-modified transcutaneous implant and a less invasive implantation alternative with translational potential.

The first two studies expand our understanding of tissue–implant interactions by investigating the role of the colonising microbiome and integrating clinical findings with structural and microbiological analyses. Findings from Paper I revealed that pain and infection are the most common factors affecting implant success and are influenced by both patient-related and microbiological factors. Paper II demonstrated that biofilm formation and antibiotic resistance in staphylococci colonising percutaneous implants are key drivers of adverse soft tissue outcomes. Paper III examined the thermal and mechanical effects of a single-drill system, highlighting its impact on heat generation and bone preservation. Finally, Paper IV identified surgical bone preparation—rather than surface modification—as the determining factor in early new bone formation and fibrous encapsulation, extending research strategies established in percutaneous implants to transcutaneous implants and providing new evidence to guide their future clinical development. Together, these results support evidence-based refinements in BCD practice and guide the development of next-generation implants with greater longevity, fewer complications, and improved patient outcomes.

***Keywords**: biomaterials, bone conduction device (BCD), bone-anchored hearing system (BAHS), percutaneous implants, transcutaneous implants, osseointegration, inflammation, pain, infection, Staphylococcus aureus, Staphylococcus epidermidis, biofilm, antimicrobial resistance (AMR), minimally invasive surgery, drilling protocols.*

SAMMANFATTNING

Hörselimplantat – en resa genom vetenskap, kirurgi och mikrobiologi

Att förlora hörseln påverkar inte bara kommunikationen, utan kan leda till betydande negativa effekter på livskvaliteten. För många innebär ett benledningsimplantat (BCD) en chans att återfå ett av våra mest grundläggande sinnen. Men vägen från beslutet att inoperera et benledningsimplantat till att återgå till vardagen är komplex och påverkas av många faktorer: kroppens biologiska reaktioner, kirurgiska tekniker, och till och med de mikroorganismer som lever på vår hud.

Denna avhandling tar ett helhetsgrepp på hur benledningsimplantat fungerar i praktiken, och hur vi kan förbättra dem. Genom fyra olika studier undersöks allt från bakterier och vävnadsreaktioner till kirurgiska metoder och ny implantatdesign.

Från patientens upplevelse till mikroskopiska detaljer

I den första studien analyserades uttagna implantat från patienter, främst på grund av komplikationer som smärta och inflammation. Genom att koppla ihop patienternas symtom som smärta och infektion med strukturella och mikrobiologiska fynd, kunde det visas att trots komplikationer med bakteriell närvaro och smärta så var implantaten väl förankrade i benvävnaden. Både individens egna förutsättningar och bakteriernas närvaro spelar en avgörande roll för behandlingen.

Den andra studien gick ännu djupare in i mikrobiologin. Här undersöktes bakterierna som koloniserade runt implantatet. Resultaten visade att vissa stafylokocker bildar biofilmer – ett slags skyddande skikt – som gör dem svåra att behandla med antibiotika. Dessa bakterier bidrar till mjukdelskomplikationer och kan påverka behandlingen negativt. Vidare så uppstod ofta resistens mot antibiotika, vilket förvärrades med bakteriens förmåga att bilda biofilmer.

Teknikens roll i kroppens reaktion

I den tredje studien riktades fokus mot själva operationen. Genom att jämföra olika borrtekniker kunde vi visa att en enklare, enstegsmetod minskar värmeutvecklingen och bevarar benvävnaden bättre. Detta är viktigt eftersom överhettning och mekanisk stress kan försämra läkningen och påverka hur väl implantatet fäster.

Den fjärde och sista studien introducerade ett nytt implantat med modifierad yta, samt en mindre invasiv operationsmetod. Här visade resultaten att det inte är ytan på implantatet som är den dominanta faktorn för inläkningen utan hur benytan förbereds kirurgiskt. Dock med viss tendens till större bentillväxt och benkontakt mot den modifierade ytan trots de relativt korta uppföljningstiderna. Denna insikt kan bana väg för framtida implantat med mindre invasiv operation.

Mot framtidens hörselimplantat

Tillsammans ger dessa fyra studier en bred och djup förståelse för hur benledningsimplantat fungerar, från det mänskliga perspektivet till det mikroskopiska. Genom att kombinera kliniska insikter med avancerad analys av vävnad, bakterier och kirurgiska metoder, bidrar avhandlingen till utvecklingen av nästa generations implantat. Målet är tydligt; färre komplikationer, längre hållbarhet och ökad livskvalitet för patienterna.

LIST OF PAPERS

This thesis is based on the following studies, referred to in the text by their Roman numerals.

I. **Ganeyev, M**., Ben Amara, H., Monksfield, P., Hol, M., Stokroos, R., Hultcrantz, M., Savage Jones, H., Trobos, M., Thomsen, P., Palmquist, A., Johansson, M.L. Pain and infection are the primary reasons for elective retrieval of bone-anchored implants. Submitted manuscript.

II. **Ganeyev, M.**, Morales-Laverde, L., Hoffman, M., Hultcrantz, M., Palmquist, A., Thomsen, P., Johansson, M.L., Trobos, M. Staphylococcal persistence and biofilm resistance in bone-anchored hearing systems: Clinical impact. Submitted manuscript.

III. **Ganeyev, M.**, Shah, F.A., Thomsen, P., Palmquist, A., Johansson, M.L. Mechanical and thermal efficiency of a single drill system for bone-anchored hearing implants. *PLOS ONE* 2025; 20(5): e0311026.

IV. **Ganeyev, M.**, Pollaers, K., Monksfield, P., Emanuelsson, L., Ben Amara, H., Thomsen, P., Palmquist, A., Johansson, M.L. Comparative evaluation of machined and laser-ablated transcutaneous implants with recessed and non-recessed placement in a sheep model.

CONTENTS

Abbreviations iv
1 Introduction 1
1.1 Bone conduction devices (BCD) 2
1.2 Evolution of percutaneous bone-anchored hearing systems (BAHS) and transcutaneous bone conduction devices (tBCD) 3
1.2.1 Evolution of BAHS 4
1.2.2 Introduction of tBCD 10
1.3 Challenges in BAHS 11
1.4 Challenges in tBCD 15
1.5 Research gaps & strategies for optimisation in BAHS and tBCD 16
2 Aims 19
3 Materials and methods 21
3.1 Experimental study design 22
3.2 Materials used in the studies 26
3.3 Material characterisation 29
3.4 Bone-implant interactions and structural analysis 31
3.5 Microbiological techniques 34
3.6 Mechanical and thermal evaluation of bone drilling 37
3.7 Ethical considerations 37
3.8 Statistical analysis 38
4 Results 40
4.1 Paper I 40
4.2 Paper II 42
4.3 Paper III 46
4.4 Paper IV 48
5 Discussion 53
5.1 Understanding implant success and failure: a holistic perspective 53
5.2 Drilling the bone and its implications 56
5.3 Percutaneous and transcutaneous systems as complementary solutions. 59

5.4 Methodological considerations and limitations 61
5.5 Translational aspects 63
6 Summary and conclusions 65
7 Future perspectives 67
Acknowledgements 69
References 71

ABBREVIATIONS

AMR	Antimicrobial resistance
AES	Auger electron spectroscopy
BA	Bone area
BAHS	Bone-anchored hearing system
BCD	Bone conduction device
BIC	Bone-to-implant contact
BHX	Laser-ablated Ponto implant (Oticon Medical)
BSE-SEM	Backscattered electron scanning electron microscopy
BV	Bone volume
cgMLST	Core-genome multilocus sequence typing
CGRP	Calcitonin gene-related peptide
CLI	Clindamycin
CoNS	Coagulase-negative staphylococci
cp-Ti	Commercially pure titanium
CR	Congo Red
CT	Computed tomography
CV	Crystal Violet
DAB	Diaminobenzidine
DLC	Diamond-like carbon (coating)
DP	Drilling protocol

ECM	Extracellular matrix
EPS	Extracellular polymeric substances
FBR	Foreign body reaction
FOX	Cefoxitin
FUS	Fusidic acid
FUS^R	Fusidic acid resistance
GD	Guide drill (MIPS system)
HA	Hydroxyapatite
HBS	Hank's balance salt solution
HRP	Horseradish peroxidase
IL	Interleukin
iNOS	Inducible nitric oxide synthase
IPS scale	Inflammation-scale, Pain-scale and Skin height/numbness-scale
La	Laser-ablated implant
LEVO	Levofloxacin
LZD	Linezoid
Ma	Machined implant
MBEC	Minimum biofilm eradication concentration
MDR	Multidrug resistant
MIC	Minimum inhibitory concentration
MIPS	Minimally Invasive Ponto Surgery

MLST	Multilocus sequence typing
MMP	Matrix metalloproteinase
MONO	Single-step drill system
MRC1	Mannose receptor C-type 1
MRI	Micro-computed tomography
NBF	Neutral buffered formalin
NB	New bone
NB.Ar	New bone area
OB	Old (native) bone
OD	Optical density
OXA+	Oxacillin
PBS	Phosphate-buffered saline
PCR	Polymerase chain reaction
PIA	Polysaccharide intercellular adhesin
RIF	Rifampicin
ROI	Region of interest
ROS	Reactive oxygen species
R^2	Coefficient of determination (regression)
S_a	Arithmetical mean height, μm
S_d	Developed interfacial area ratio, %
SEM	Scanning electron microscopy

SMI	Structure model index
ST	Soft tissue / Sequence type (depending on context)
ST.Ar	Soft tissue area
SXT	Trimethoprim-sulfamethoxazole
tBCD	Transcutaneous bone conduction device
TiO_2	Titanium dioxide
TLR	Toll-like receptor
TISA	Transcutaneous Implant Skin Anomalies
TSB	Tryptic soy broth
OB	Old (native) bone
VAN	Vancomycin
VAS	Visual Analog Scale
Vd.Ar	Void area
VEGF	Vascular endothelial growth factor
VOI	Volume of interest
WD	Widening drill (MIPS system)
3D	Three-dimensional/three dimensions

1 INTRODUCTION

Restoring essential functional capabilities is a central goal in applied clinical sciences, whether by enabling a patient to walk again, eat independently, or regain hearing. Bone-anchored implants are well-established solutions with applications in orthopaedics, dentistry, and hearing rehabilitation.

Hearing loss is a major global health concern, currently affecting over 466 million individuals worldwide – a number projected to nearly double by 2050 [1]. For people affected by conductive or mixed hearing loss, as well as those who have single-sided deafness [2,3], bone conduction devices (BCD) represent an effective and well-established treatment option. BCD convert sound waves to mechanical vibrations and transmit them through the skull bone to the cochlea by means of bone conduction, thereby bypassing the outer and middle ear. These systems are available either as non-surgical solutions, externally worn using an elastic soft band or similar support, or as implantable systems.

There are two primary configurations of implantable BCD that are clinically used (**Fig. 1a,b**): percutaneous bone-anchored hearing systems (BAHS), in which the external sound processor connects directly to a skin penetrating abutment; and transcutaneous bone conduction devices (tBCD), where the sound processor is retained using a magnetic coupling between the sound processor and the subcutaneously positioned implant, thereby leaving the skin intact [4]. Percutaneous implants have been used for hearing rehabilitation since the late 1970s, and transcutaneous implants became available in the early 2010s. The clinical success of these implants is built on decades of research focused on improving not only the technology and hearing performance but also patient clinical outcomes and understanding of the underlying mechanisms of implant integration and failure. Critical factors include the biological response at the tissue–implant interface, as well as the influence of material properties, implant geometry, surface characteristics, surgical protocols, and postoperative care.

While much of the existing research has addressed these factors in isolation, focusing either on clinical performance or on fundamental biological and material science questions, this thesis aims to bridge these perspectives. By systematically investigating various aspects of implantable BCD performance through a range of analytical and clinical methodologies, this work seeks to provide an integrated understanding that connects experimental findings to clinically observable outcomes.

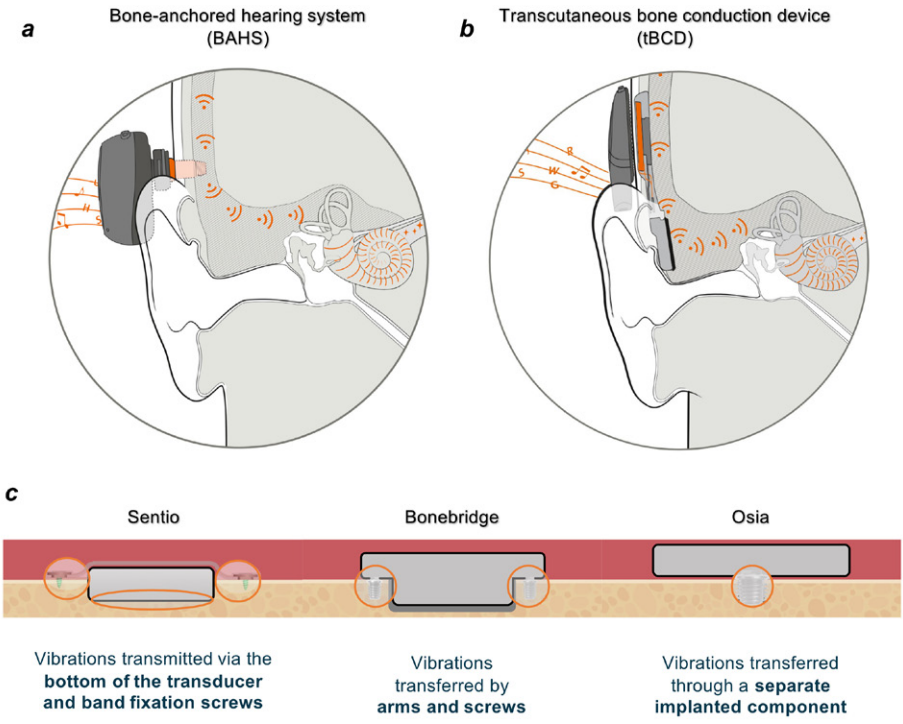

Fig. 1 Bone-anchored hearing systems (BAHS) and transcutaneous bone conduction devices (tBCD). (*a*) Percutaneous BAHS, where vibrations generated in the external sound processor are transmitted directly to the skull bone through a skin-penetrating abutment; **(*b*)** Active tBCD, where the power and sound signal are transferred across intact skin via an inductive link to the implanted transducer; **(*c*)** Different transcutaneous implant designs: Sentio™ (Oticon Medical, Sweden); Bonebridge (Medel Austria); and Osia® (Cochlear, Sweden). Images reproduced with permission from Oticon Medical©.

1.1 Bone conduction devices (BCD)

Terminology

In this thesis, the term *bone conduction device (BCD)* is used when referring to bone conduction systems in general, while a clear distinction is made between *bone-anchored hearing systems (BAHS)* for percutaneous solutions and *transcutaneous bone conduction devices (tBCD)* for active transcutaneous systems. This terminology ensures consistency, avoids reliance on trademarked names, and reflects the diversity of current devices and technologies.

Across the included studies, terminology is applied systematically. In **Papers I–III**, which investigate percutaneous implant design, surgical technique, and clinical retrievals, the term *BAHS* is used. In **Paper IV**, where a transcutaneous implant is evaluated, the term *tBCD* is applied.

Overview: Components, function, and clinical applications

First introduced in 1977 [5], BAHS consist of a screw-shaped titanium (Ti) implant placed in the temporal bone behind the ear (**Fig. 1a**). A skin-penetrating abutment connects the implant to an external sound processor, enabling direct mechanical vibration transfer. This configuration provides reliable and superior direct sound transmission and has demonstrated long-term implant survival rates of up to 98%, particularly with the adoption of wide-diameter implants and surface-enhancing modifications [6-8]. Today, over 400,000 patients globally benefit from this technology [7]. In addition to improving hearing function, BAHS significantly enhance patients' quality of life [6,7,9,10].

Transcutaneous bone conduction devices (tBCD) were introduced more recently and can be categorised as either active or passive. In passive systems, the transducer is integrated within the external sound processor, whereas in active systems, it is implanted beneath the skin. The passive systems are however used clinically to a much lesser extent today, primarily because of the sound attenuation of up to 20 dB [4,11], this thesis therefore focuses on the active devices. In these systems, the transducer is placed subcutaneously and anchored to the bone, with signal and power transmission achieved via an inductive link through intact skin. By avoiding a skin-penetrating abutment, active tBCD may reduce the risk of infection and offer improved cosmetic outcomes (**Fig. 1b**). The first clinically adopted transcutaneous implants became available in the early 2010s [12], and current solutions are illustrated in **Fig. 1c** and described in more detail in the subsequent chapters.

1.2 Evolution of percutaneous bone-anchored hearing systems (BAHS) and transcutaneous bone conduction devices (tBCD)

Over the years, the design of the BAHS' components has been continuously refined, including the implant, abutment, and sound processor, as well as surgical techniques. These advancements have focused on improving hearing outcomes, reducing the size and complexity of the system, improving patient comfort and outcomes, and simplifying the surgical procedure to make it more efficient, less invasive, and to reduce post-operative complications.

1.2.1 Evolution of BAHS

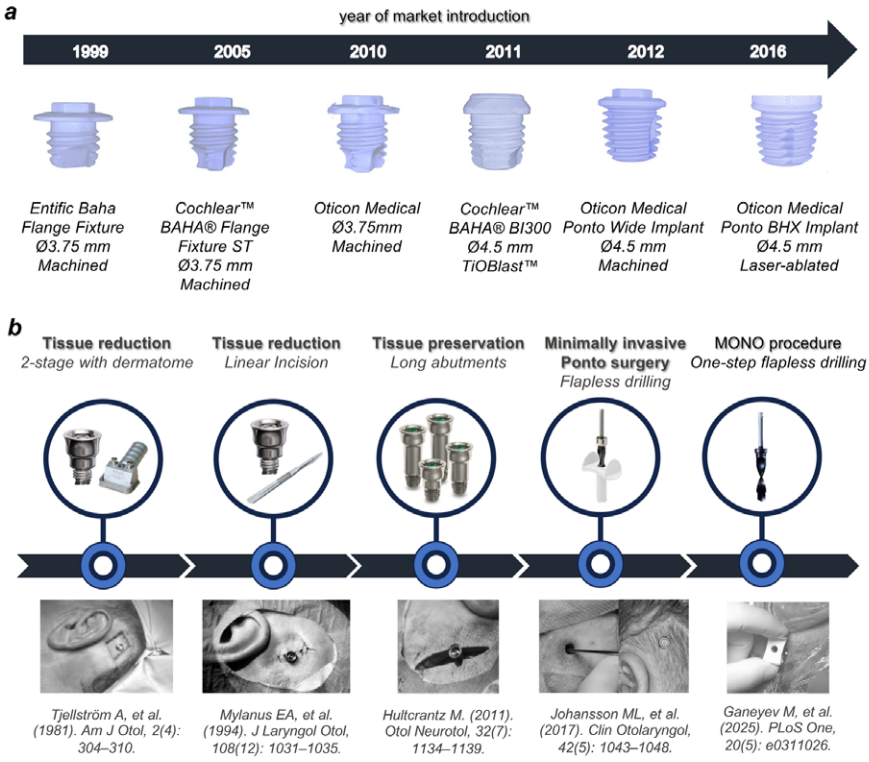

Fig. 2. Evolution of bone-anchored hearing implant design and surgical procedure. (*a*) Timeline showing the market introduction of various percutaneous bone-anchored hearing system (BAHS) implants, highlighting advances in geometry, surface modifications, and implant diameter. **(*b*)** Key milestones in the development of surgical techniques for BAHS, from early tissue-reduction approaches using dermatome and linear incisions to tissue-preservation methods with long abutments, minimally invasive flapless drilling (MIPS), and the most recent MONO single-step flapless procedure.

Implant

Bone-anchored hearing implants are made of commercially pure titanium grade 4 (cp-Ti). These devices were first introduced following the discovery of the osseointegration phenomenon, whereby direct structural and functional contact is established between living bone and the surface of a load-bearing implant [13], both at the micro- and nano-scales [14,15]. Moreover, in load-bearing bone-anchored implants, mechanical stability must be accompanied by predictable integration with bone. Thus, in its fullest definition, osseointegration involves: (1) the ability to provide stable, immobile support for a prosthesis under functional loading; 2) the direct contact of newly formed and remodelled bone with the implant surface,

without any intervening connective tissue; 3) the absence of detectable movement between the implant and surrounding bone during function; and 4) histological evidence of normal bone and marrow immediately adjacent to the implant [16-19].

To optimise the physicochemical and biological performance of Ti implants, a variety of surface modification techniques have been developed over the years [20-22]. These methods can be broadly divided into three categories:

(i) Mechanical methods – including grinding, polishing, and blasting to create defined surface textures.

(ii) Physical methods – such as applying surface coatings or depositions to increase wear resistance and improve biocompatibility.

(iii) Chemical methods – involving acid etching, alkali treatment, hydrogen peroxide exposure, or electrochemical processing, all of which alter the surface chemistry, produce tailored topographies and improve biological compatibility.

In modern clinical practice, cp-Ti and its alloys are among the most commonly used metallic biomaterials because of their excellent biocompatibility, resistance to corrosion, and favourable mechanical strength [23]. Corrosion resistance is especially important for long-term implants, as it prevents material degradation and protects surrounding tissues from potentially harmful reactions. When exposed to air, titanium forms a stable oxide layer (TiO_2) on its surface. This layer improves corrosion resistance and enhances the bioactivity of the implant [24,25].

Following implantation, osseointegration is initiated, beginning with blood clot formation and adsorption of proteins to the implant surface, similar to that in bone fracture healing [26]. However, in the presence of the implant interface, this early phase is followed by the recruitment of osteoprogenitor cells and the differentiation of osteoblasts, which deposit an unmineralised osteoid matrix directly onto the implant surface. As mineralisation progresses, primary woven bone forms, bridging the gap between the host bone and the implant. Over time, this immature bone undergoes remodelling, a dynamic process in which osteoclast-mediated resorption and osteoblast-mediated bone formation occur in coupled cycles. Woven bone is gradually replaced by highly organised lamellar bone, with its collagen fibres oriented according to local mechanical loads [19,26]. This remodelling increases bone-to-implant contact (BIC) and enhances the mechanical anchorage of the implant. The stability of the bone–implant interface depends not only on the surgical procedure and implant design but also on the

biological balance between bone resorption and formation during functional loading. Excessive mechanical stress, infection, or inflammation can shift this balance towards resorption, potentially leading to implant failure.

Since their clinical introduction, BAHS have undergone substantial development in terms of implant geometry and surface treatments (**Fig. 2a**). Early systems utilised narrow Ø3.75 mm machined fixtures, while the currently available implants have a wider diameter of Ø4.5 mm with surface modifications aimed at enhancing osseointegration for increased stability and survival rate as well as to allow for one-stage surgery and earlier loading. Such modifications include blasted surfaces (TiOblast™, BI300, Cochlear, Sweden) [27,28] and laser-ablated textures (Ponto BHX, Oticon Medical, Sweden) [29,30].

Abutment

An integral component of percutaneous devices is the skin-penetrating abutment, which traverses the skin and connects the sound processor with the osseointegrated implant. The biological response of the surrounding soft tissue is, therefore, a critical determinant of long-term function. Similar to the implant screw fixture, the abutment is made of cp-Ti grade 4 and has undergone multiple design iterations aimed at improving clinical outcomes, but to date, it remains suboptimal.

Under normal circumstances, when the skin is breached, the body initiates a tightly regulated wound-healing cascade consisting of four overlapping phases: (1) homeostasis (starts immediately and lasts from a few hours to 2 days); (2) inflammation (starts on day one, lasting up to 8 days); (3) proliferation (starts on 3–10 day and lasts until day 25); and (4) remodelling (starting on 21–23 day, and lasting for up to 2 years) [31]. The initial coagulation phase involves platelet aggregation and fibrin clot formation, providing a provisional matrix for incoming cells. This is followed by the inflammatory phase, which functions as an innate immune defence triggered by tissue damage. During this phase, neutrophils (polymorphonuclear leukocytes) are the first to infiltrate the wound, releasing proteolytic enzymes and reactive oxygen species (ROS) to combat pathogens. Neutrophils are subsequently joined by monocytes that differentiate into macrophages, orchestrating tissue repair through phagocytosis of debris, release of pro-inflammatory and anti-inflammatory cytokines (e.g., TNF-α, TGF-β1, IL-1, IL-6, and IL-8), and recruitment of additional immune cells. Lymphocytes, including both T and B cells, may also be involved, contributing to adaptive immune surveillance and antibody-mediated responses. The proliferative phase is characterised by fibroblast migration, deposition of extracellular matrix (ECM) components such as type III collagen, and angiogenesis driven by vascular

endothelial growth factor (VEGF). Finally, in the remodelling phase, some of the type III collagen is replaced by the mechanically stronger type I collagen, often leading to scar tissue formation.

When a skin-penetrating abutment is present, however, this normal wound healing sequence is interrupted. Due to the foreign material and the breach of the skin barrier, the wound cannot fully re-epithelialise, and a persistent breach in the skin barrier is maintained. This leads to a chronic foreign body reaction (FBR) [32]. A hallmark of FBR is the recruitment of macrophages that fuse into multinucleated foreign body giant cells at the tissue–implant interface. Although fibrous encapsulation is never fully realised in percutaneous abutments [33], over time, newly accumulated fibrous tissue around the abutment can contract, creating mechanical stresses and micro-gaps between the tissue and the abutment surface. These gaps serve as niches for bacterial colonisation, often leading to biofilm formation and recurrent local inflammation. From a mechanistic perspective, the percutaneous abutment creates a permanently vulnerable interface between the external environment and underlying tissues. This interface is neither fully healed nor functionally integrated with the surrounding dermis and epidermis. One proposed strategy to improve clinical outcomes is to achieve a robust "material–soft tissue seal," where the implant surface promotes stable epithelial or connective tissue attachment. However, in the anatomical context of the skin around BAHS and given the drastically different biological and mechanical properties of the soft tissue and the metallic abutment surfaces, a perfect seal has not yet been achieved in clinical practice. Current research continues to explore surface modifications, coatings, and design geometries that may attenuate the inflammatory response and improve tissue integration, but the fundamental challenge remains in the unique biological environment of a chronically breached skin barrier.

In BAHS, abutment designs have undergone several iterations, involving changes in geometry, the introduction of various profiles, and surface modifications aimed at improving soft tissue response. Some approaches have focused on establishing a tighter seal between the skin and abutment, whereas others have prioritised developing surfaces less susceptible to bacterial colonisation and easier to maintain. Examples include hydroxyapatite (HA)-coated abutments (BIA400, Cochlear, Sweden) [34] and machined or polished Ti abutments [35], intended to reduce inflammation and improve hygiene. The studies demonstrated that peri-abutment host inflammatory responses vary with abutment surface properties [35-38]. Electropolished abutments were associated with elevated inflammatory cytokines (IL-8, IL-1β, IL-10) and toll-like receptor expression (TLR-2, TLR-4) in peri-abutment fluid, alongside higher tissue expression of genes linked to soft

tissue regeneration (COL1A1, FOXO1). Additionally, HA coatings, while enhancing skin adherence and barrier formation, have produced mixed pre-clinical and clinical results [34,39-41].

Surgical techniques and osteotomy preparation

The surgical approach for implanting percutaneous BAHS has been modified and re-evaluated over several decades of clinical practices (**Fig. 2b**). In the past, since its introduction by Tjellström in 1977 [5], the procedure involved various tissue grafting methods, flap techniques and incisions [42-46]. In the course of development, the linear incision technique using a multi-step drilling protocol became the gold standard to prepare for implant installation [47,48]. This approach was paired with soft tissue reduction, where subdermal tissue was excised to minimise skin mobility around the abutment. While effective, this approach often resulted in aesthetic concerns, tissue overgrowth and prolonged healing [49]. Later, against the existing dogma, an evolutionary step was made, and clinicians moved towards linear incision surgery with soft tissue preservation, avoiding the undermining of the soft tissue around the abutment. This approach demonstrated significant improvements in the mitigation of soft tissue complications, improved patient satisfaction and aesthetic outcomes [50,51]. Importantly, this shift was made possible with the introduction of a longer abutment.

Minimally invasive techniques have since been introduced. One such advancement is the minimally invasive Ponto surgery (MIPS, Oticon Medical, Sweden), where site preparation is performed through a small circular skin biopsy and drilling is guided via a cannula, maintaining intact surrounding tissues [52,53]. Nevertheless, the transition to this flapless surgical technique has introduced new challenges. These include a learning curve and the necessity for specific surgical training to achieve consistent outcomes [54-57], as seen in flapless dental implantology. Risks include accidental inclusion of soft tissue in the osteotomy [54,58,59] and limited visibility during drilling, which may compromise irrigation and increase the risk of heat-induced bone osteonecrosis [60-64]. Despite this, the MIPS technique has shown significant patient benefits, including shorter operative times, improved or comparable soft tissue outcomes, enhanced cosmetic results, and reduced postoperative numbness around the abutment [52,65,66].

As noted above, MIPS requires proper surgical training due to limited visibility, restricted irrigation, and the risk of soft tissue entrapment in the osteotomy, all of which may impact heat generation and bone healing. Early reports highlighted a learning curve and high sensitivity to protocol deviations; a few centres experienced mixed implant loss rates, ranging between 0-4% [67-69] and 35% [52,70,71], prompting the re-evaluation of the technique. Modifications were subsequently

made to the MIPS protocol and drill design to improve its safety and reproducibility [65,72,73]. This experience highlights the critical importance of evaluating drilling protocols in terms of their clinical feasibility, mechanical and thermal performance, osteotomy precision, and the biological response of bone.

The development of less-invasive surgical techniques has ultimately led to the MONO technique, a next-generation flapless single-step drilling procedure that is also performed via a guide cannula. Initial results with MONO have shown significant reductions in skin-related adverse events, offering promising outcomes in terms of both surgical efficiency and patient satisfaction [74,75].

In summary, the evolution, from open surgery with tissue reduction to fully flapless minimally invasive techniques, illustrates a clear shift toward less invasive, patient-centred interventions.

Bone drilling effects

Osteotomy preparation by rotary drilling subjects bone tissue to both thermal and mechanical stresses. Friction generated between the drill bit, bone chips, and osteotomy walls primarily converts the applied energy into heat. The extent of the temperature increase is determined by factors such as the drilling protocol (single or multiple drilling steps), drill design, rotational speed, feed rate, irrigation efficiency, and density of the bone. Previous reports have proposed that when bone is exposed to temperatures above ~47–55 °C for longer than one minute, irreversible changes, including protein denaturation, collagen–mineral breakdown, osteocyte death, and thermal osteonecrosis, occur [61,76,77]. Such heat damage compromises bone viability at the implant interface, which may delay osseointegration and reduce long-term stability. Likewise, excessive drilling torque or feed rate can generate microcracks and local stress concentrations that elicit reparative processes, temporarily weakening primary stability. Consequently, an optimised drill design and drilling protocol together with adequate irrigation are critical for minimising surgical trauma.

Numerous investigations have examined how the drilling protocol, feed rate, drill geometry, bone substrate, and irrigation affect thermal generation through techniques such as thermocouple measurements, infrared imaging, and finite element simulations [53,78-81]. Yet, variations in methodology make it difficult to define universally optimal parameters applicable across implant systems, anatomical sites, and patient conditions. While a commonly cited threshold for thermal degradation is 47 °C maintained for more than one minute [61,76,77], other factors, including total drilling work, drill design, and irrigation, also influence thermal outcomes [82]. Another important consideration is the biological role of

bone debris produced during drilling. While thermal injury may lead to osteonecrosis and bone decomposition [78,83], some reports suggest that autologous bone chips may actually support osseointegration [83,84]. Despite the potential benefit, such debris is routinely removed before implant placement [85], leaving its precise role uncertain. On the other hand, efficient removal of the hot bone chips from the osteotomy site might be beneficial in terms of reduced heat generation [53].

1.2.2 Introduction of tBCD

tBCD were developed as an alternative to percutaneous solutions to address soft tissue complications by maintaining an intact skin barrier. Power and sound signals are transmitted inductively from an externally worn sound processor, retained on the skin by the magnet [86-89]. This design eliminates the skin-penetrating abutment of traditional percutaneous systems, potentially reducing the associated risk of infection and inflammation. Currently, three active tBCDs are in clinical use: Bonebridge (Medel, Austria) [12], Osia® (Cochlear, Sweden) [90] and Sentio™ (Oticon Medical, Sweden) [91,92]. Each device employs a distinct approach to bone fixation and vibration transmission, which are critical factors for optimal performance (**Fig. 1c**).

- The Bonebridge transducer is placed in a surgically created bone recess and secured with two screws through the transducer wings into cortical bone. At the initial stages, the implant does not require direct contact with the bone for vibration conduction [93].
- The Osia® system, by contrast, avoids recessing; its active implant is attached to a Ti screw implant anchored to the bone [94].
- The Sentio™ device is placed in a shallow recess and stabilised with a silicone over-moulded Ti fixation band spanning across the transducer casing and fixed with two self-drilling Ti mini-screws [91].

These three principles of stimulation modes, anchorage to the bone (one-point stimulation, two-point stimulation, and surface) and their influence on the transmission of vibrations, are currently being debated [91,95-97]. For both percutaneous and transcutaneous devices, a secure fixation of the implant and coupling to the skull is an important surgical requirement for effective vibration transmission and necessitates sufficient thickness of the bone at the implantation site.

As the implant is fully submerged under the skin, it undergoes fibrous tissue encapsulation as a part of the previously described foreign body reaction. The Osia® system uses a screw-shaped implant for anchorage to the skull bone,

reflecting the concept that osseointegration is essential for effective sound transmission in transcutaneous implants. The Bonebridge and Sentio™ systems are flat-shaped implants placed in a bone recess and rely on osseointegration of mini-screws for the fixation of the implant.

In active tBCD, the implanted component contains an active transducer (vibrator/actuator) that directly stimulates the skull bone, and the external processor sends signals and power across the skin via an inductive link. One study reported no detectable effect on output performance in connection with simulated tissue growth of up to 300 μm between the transducer and bone [91]. However, as shown with passive transcutaneous devices, where the transducer is housed in the external processor, vibration transmission is attenuated by the skin [11]. It is therefore plausible that in active systems, excessive soft tissue growth beneath the transducer casing could impair performance if the tissue surpasses a certain thickness. Nevertheless, to date, few studies have explored the subcutaneous implant–tissue interface in the context of tissue response around transcutaneous implants [98-101].

1.3 Challenges in BAHS

While enabling efficient direct sound transmission through a skin-penetrating abutment, percutaneous BAHS inherently breach the skin barrier, creating a pathway for bacterial colonisation and increasing the risk of inflammatory soft tissue reactions. The reported complications include infection, inflammation and soft tissue overgrowth [102-106], mechanical instability [103], chronic pain [103,107-109], and failed osseointegration [110]. Such adverse events may require surgical revision or, in severe cases, implant removal, as well as pharmacological treatment [111-113]. Despite these challenges, it is important to recognise recent long-term reports evaluating the newer generation, wide-diameter, surface-modified implants, which demonstrate excellent survival rates of over 95% at 5-10 years in adults [7,27,114] and reaching survival rates as high as 97% in more complex paediatric studies [30]. Similarly, with the introduction of tissue preservation techniques and minimally invasive surgical procedures, in combination with longer abutments, adverse soft tissue reactions have improved. A recent review of one available system reported adverse skin reaction rates (defined as Holgers score ≥2) of 5% across visits and in 15% of patients [7].

Loss of osseointegration

Loss of osseointegration is a risk with any type of bone-anchored implant and can occur at any stage after implantation [110]. Reported occurrence rates vary [115], depending on factors such as implant design, surgical technique, patient age,

comorbidities, length of follow-up and compromised situations, e.g., radiation therapy. Early implant loss is most often linked to insufficient or failed osseointegration or surgical trauma, whereas late loss is typically associated with more complex aetiologies, including infection, chronic inflammation, pain, and other contributing factors. In BAHS, the implant is subjected to repeated functional loading and a constant skin breach, which increases the risk of inflammatory and infectious complications that can compromise the bone–implant interface. Once osseointegration is lost, the implant becomes loosened and mobile, leading to device failure, necessitating surgical revision or re-implantation. Preventing this complication requires optimisation of surgical protocols, improvement of drilling protocols, good soft tissue care, and early detection of adverse peri-implant changes.

Inflammation and infection

At the skin–abutment interface of BAHS, histological investigations consistently demonstrate a state of subacute to chronic inflammation, reflecting the normal for FBR rather than complete wound resolution [36,52,116-118]. One characteristic finding is epithelial downgrowth [118], where the epidermis migrates along the abutment surface into the dermis, displacing the normal dermal–epidermal junction. In the subepithelial connective tissue, inflammatory infiltrates dominated by lymphocytes, plasma cells, and macrophages are commonly observed [119,120], often indicating a persistent low-grade inflammatory state [119,121,122].

When tissue equilibrium is compromised by factors such as excessive skin mobility, microtrauma, undermined surrounding soft tissue due to tissue reduction, or bacterial colonisation, the inflammatory reaction escalates, leading to a pathological state. Histologically, this is reflected by dense neutrophilic infiltration—often forming micro-abscesses—similar to findings from peri-implant interfaces in dental implants [123]. Activated immune cells release matrix metalloproteinases (MMPs) that degrade extracellular matrix components, weakening the epithelial barrier [124].

When microbial colonisation progresses to overt infection, it represents a major risk factor. Epidemiological studies in patients with BAHS report adverse skin reaction (Holgers ≥ 2) rates of 15% [7], and ranging between 2.4 and 38.1% [112], depending on the surgical technique, implant design, and length of follow-up. While many infections are superficial and manageable with topical antibiotics, recurrent or severe cases may cause chronic pain, persistent inflammation, and, in some cases, implant loss.

Microbiome and biofilms

Bacterial colonisation and biofilm formation are well-recognised challenges affecting the long-term success of BAHS. *Staphylococcus epidermidis* and *Staphylococcus aureus* are the most frequently identified species, present at both inflamed and clinically healthy sites [35-38,105,116,125]. While a case report has implicated *S. aureus* in adverse outcomes such as idiopathic pain, suggesting a potential pathogenic role [113], the direct contribution of bacterial flora to implant failure remains incompletely understood, partly due to the lack of comprehensive large-scale microbiological investigations.

Biofilm formation is a major virulence factor in staphylococcal infections associated with biomaterials. Biofilms are structured bacterial communities embedded in self-produced extracellular polymeric substances (EPS) and provide protection against host immune defences and antimicrobial agents [126,127]. The main polysaccharide in the EPS of staphylococcal species is the intercellular adhesin/poly-N-acetylglucosamine (PIA/PNAG), synthesised via the *icaADBC* operon [128].

Biofilm-associated infections remain notoriously difficult to treat because bacterial communities within biofilms adopt unique physiological states that promote tolerance and resistance to antibiotics [129,130]. Several mechanisms underpin the antimicrobial resistance (AMR) of biofilms. Close cell-to-cell proximity facilitates efficient horizontal gene transfer, promoting the spread and maintenance of resistance genes. The EPS physically restricts antibiotic penetration and can inactivate drugs through binding or enzymatic degradation [33]. Within the biofilm, gradients of nutrients and oxygen generate metabolically dormant subpopulations, including persister cells, which are inherently less susceptible to antimicrobials [33]. Compared to planktonic bacteria, biofilm bacteria often grow slower and show altered gene expression patterns [131,132]. Some cells can enter a dormant, metabolically inactive state, further reducing antibiotic susceptibility; these persister cells are considered critical in the persistence and recurrence of biofilm-associated infections [133]. To avoid immune clearance during biofilm development, *S. aureus* biofilms, for instance, modulate host immune responses, for instance by interfering with TLR-2 and TLR-9 signalling pathways, thereby reducing phagocytosis and promoting persistence [134]. Mature biofilms also enhance infection spread by releasing bacteria into the surrounding tissue. Upon dispersal, the planktonic bacteria acquire increased virulence, colonise new niches, and restart the biofilm cycle [132,135].

In vivo studies have confirmed the presence of biofilms on BAHS abutments and surrounding tissues [136], and isolates from biomaterial-associated infections often

exhibit strong biofilm-forming capacity [136]. Nevertheless, to our knowledge, no clinical studies have directly linked biofilm characteristics to patient outcomes with hearing implants.

Pain

Pain is a complication of BAHS during the postoperative course, with a prevalence of below 10% [7,51,114]. In most cases, postoperative pain diminishes within weeks as healing progresses; however, in a subset of patients, it persists as a chronic condition, leading to substantial discomfort, reduced quality of life, and in severe cases, elective implant retrieval. Chronic persistent pain may occur even in the absence of obvious pathological lesions, infection or inflammation, and has been reported to account for ~2% of implant removals [103,108,109]. While the most used scale to classify the soft tissue state is Holgers score [137], it lacks pain assessment. Thus, clinical assessment of patient-reported pain relies on standardised scales such as the Visual Analog Scale (VAS) and/or the Inflammation-scale, Pain-scale and Skin height/numbness scale (IPS scale) [138]. These scales allow clinicians to quantify pain intensity, evaluate progression over time, and guide targeted interventions.

Antibiotic therapy and antimicrobial resistance (AMR)

In clinical practice, antibiotic therapy is applied to manage soft tissue complications at several stages: topical treatment (often combined with corticosteroids) as preoperative and postoperative prophylaxis and for the management of soft tissue inflammation/infection, and systemic oral therapy when local interventions prove insufficient. Commonly used medical compounds include fusidic acid–based topical formulations (e.g., Fucidin®) [35] and antibiotic–corticosteroid ointments (e.g., Tri-Adcortyl, Terra-Cortril) [52,73,139], which are typically dipped in dressings and applied around the abutment, often under the healing cap. In selected cases, silver nitrate cautery may also be employed for soft tissue infection management [140]. Despite these options, antimicrobial susceptibility testing of the causative bacteria is rarely undertaken, and the role of biofilm-mediated resistance is generally overlooked in treatment planning. As a result, suboptimal therapeutic strategies may contribute to persistent inflammation, recurrent infections, and increased reluctance among patients to undergo BAHS implantation surgery, as concerns about surgical risks and skin-related complications remain high [141].

In comparison, these challenges are more systematically addressed in the management of orthopaedic device-related infections [142,143]. In research related to orthopaedic device-related infections, two testing protocols are available: 1) integrated minimum inhibitory concentration (MIC) testing, which challenges

planktonic bacteria to different antibiotic concentrations, and 2) the minimum biofilm eradication concentration (MBEC) assay, which is used to assess the susceptibility of grown biofilms. The MBEC assay has demonstrated that biofilms markedly increase bacterial tolerance to antibiotics compared to planktonic bacteria [142-144]. Adapting these diagnostic methodologies to BAHS could provide valuable insights into the relationship between microbial colonisation, biofilm-associated resistance, and treatment outcomes, ultimately informing more effective clinical strategies.

1.4 Challenges in tBCD

Surgical considerations

Since its introduction, one objective of active transcutaneous implants has been to broaden patient eligibility by lowering the threshold for treatment. Currently, transcutaneous implantation requires a more invasive procedure, comparing to BAHS, due to its size. Thus, additional anatomical and surgical parameters must be carefully considered. For example, adequate bone thickness is essential to ensure correct implant placement. In the case of the Bonebridge device, preoperative computed tomography (CT) scans are routinely performed to optimise implant positioning [145]. Another critical factor is osseointegration. For the Osia® system, which relies on the same screw implant used in the percutaneous systems for anchorage, successful osseointegration is considered essential for optimal device function. However, this requirement may not apply equally to other transcutaneous solutions, and to date, no studies have provided definitive evidence on this matter.

MRI compatibility and safety issues

Many hearing implant recipients require magnetic resonance imaging (MRI) examinations for ongoing diagnostics (typically due to neurological comorbidities), which makes MRI compatibility a crucial concern [146]. Compared to percutaneous systems, tBCD present specific challenges in this regard. Magnetic materials inside the transcutaneous implant, when subjected to MRI, will generate torque that can introduce risks, including displacement, demagnetisation, local pain, or tissue heating [95]. Furthermore, magnets generate significant image artifacts [147-149], which may obscure critical diagnostic details, especially in head and neck imaging.

To mitigate these risks, most devices are classified as *MRI-conditional*, meaning that scans can be performed only under restricted parameters, such as maximum allowable field strength, or they may require bandaging or temporary magnet removal before imaging [95]. While effective, these restrictions reduce diagnostic

flexibility and may require additional interventions—factors that must be carefully weighed when selecting implant types, particularly in patients likely to undergo frequent or high-resolution MRI examinations.

Infection, pain, and soft tissue inflammation

Although tBCD are frequently promoted as having reduced skin-related complications compared with percutaneous systems, their size and placement require a more invasive surgical procedure. Consequently, while some studies report reduced rates of skin reactions [150,151], complications such as skin ulcers, infection, inflammation, and pain persist. One systematic review reported a rate of 17.9% minor complications and 3.6% for major complications, which in fact led to implant removals [152]. The most common major complications are surgical wound infection, skin rupture and necrosis or skin ulceration, as well as pain and device extrusion. Another review analysing the FDA MAUDE database identified wound, pain, and infection as major skin complications [153]. In summary, these reports highlight that, while transcutaneous approaches may address some challenges of percutaneous systems, they introduce new risks that must be considered when determining patient candidacy and considering long-term outcomes.

Notably, the commonly used Holgers score for skin status in percutaneous implants is not suitable for tBCD as it overlooks key aspects relevant to transcutaneous implants. These include the inability to capture early wound-healing complications, the lack of pain assessment, and no assessment of skin height changes that may hinder processor coupling and require revision. Therefore, researchers have proposed other scales for these types of hearing implants, such as the IPS scale [138] and the recently proposed Transcutaneous Implant Skin Anomalies (TISA) scale [154].

1.5 Research gaps & strategies for optimisation in BAHS and tBCD

Despite the decades of progress made in the development of percutaneous and transcutaneous bone conduction systems, important gaps remain, particularly concerning device performance in patients, long-term clinical outcomes, and methodologies used to evaluate them.

Addressing implant failure – Structural integrity, stability, and patient-specific factors: Insights from retrieved implants have already driven improvements in design and materials. However, diagnostics for predicting implant failure and identifying which solutions are best suited for individual patients remain limited and require further refinement.

Studying the microbiome – Biofilms, antimicrobial resistance, and treatment efficacy: The peri-abutment microbiome, biofilm formation, and AMR are increasingly recognised as key contributors to infectious complications, yet systematic clinical studies are still rare. Better integration of microbiological assessments with clinical outcomes is needed to optimise treatment strategies.

Refining surgical procedures – Reducing complications and enhancing efficiency: While innovations such as MIPS and MONO involve less invasive procedures, complications still occur. Future developments may include self-drilling implants as well as less invasive procedures, further minimising surgical trauma and recovery time.

Translating lessons from percutaneous to transcutaneous systems: There is an ongoing trend toward more implantable solutions, with the active tBCD representing an initial step, relocating the transducer from the external processor into the implant casing. Experiences with percutaneous BAHS provide a valuable foundation for addressing the challenges associated with transcutaneous implants, particularly regarding surgical practices, osseointegration, infection control, and soft tissue management. Applying this knowledge may contribute to the optimisation of newer systems.

2 AIMS

This thesis aims to improve the clinical outcomes of percutaneous and transcutaneous hearing implants by investigating how tissue response, bacterial colonisation, and surgical technique influence implant integration, infection risk, and long-term stability. Drawing on clinical, microbiological, *ex vivo/in vitro*, and preclinical studies, the research focuses on advancing the development of next-generation implants with greater longevity, fewer complications, and improved patient outcomes.

The specific aims are as follows:

Paper I: To correlate clinical outcomes in patients with bone-anchored implants with structural and biological tissue-implant interactions, using a multimodal analytical approach on electively retrieved implants.

Paper II: To characterise the biofilm-forming capacity and antibiotic resistance profiles of *Staphylococcus* spp. isolated from patients with percutaneous bone-anchored hearing systems (BAHS), and to investigate their association with clinical signs of inflammation, pain, and debris accumulation, with the goal of improving infection management strategies.

Paper III: To compare the mechanical and thermal performance of a novel single-step guided drilling system (MONO) with a conventional two-step flapless system (minimally invasive Ponto surgery, MIPS) for BAHS site preparation. The study focuses on torque, heat generation, bone integrity, and the effects of irrigation and drilling duration to assess procedural safety.

Paper IV: To evaluate the impact of modified surgical implantation techniques (bone recess vs. non-recess) and implant surface characteristics (machined vs. laser-ablated) on transcutaneous implant integration in a preclinical ovine model.

3 MATERIALS AND METHODS

This thesis is based on four studies, which include various experimental and sampling methodologies: clinical case series with retrieved human samples [**Paper I**], microbiological characterisation of clinical bacterial isolates from patients with BAHS [**Paper II**], *in vitro/ex vivo* model evaluating drilling techniques [**Paper III**] and a preclinical model on transcutaneous implants [**Paper IV**] (**Table 1**).

***Table 1**. Overview of the studies included in the thesis.*

Paper	Experimental Model/Participants	Application	Material/Feature	Research Focus
Paper I – Retrieval study	Human (retrieved implants from clinical case series)	Clinical retrieval sampling & histological/ microbiological analysis	Various generations of bone-anchored hearing implants and abutments, made of cp-Ti, with machined, blasted, hydroxyapatite-coated, or laser-ablated surfaces	Clinical status, bone-implant interface, soft tissue inflammation, microbiota
Paper II – Clinical study	Human (prospective patient cohort)	Longitudinal assessment of clinical outcomes & microbiological profile	Wide Ponto 4 mm implants with 6-12 mm abutments, made of commercially pure titanium (cp-Ti) grade 4; MIPS technique	Clinical status, genome sequencing, biofilm formation, antimicrobial resistance
Paper III – *Ex vivo* and *in vitro* drilling study	Cow tibia & artificial bone blocks (Sawbones)	Mechanical and thermal evaluation of osteotomy drilling techniques	MIPS (two-step) vs. MONO (single-step) drill systems; stainless steel with a diamond-like carbon coating	Cutting efficiency, torque, temperature rise during drilling, bone distortion
Paper IV – Preclinical sheep study	Ovine (*in vivo*, calvarial implantation)	Assessment of osseointegration and soft tissue response	Custom disc implants (20.3 mm Ø), cp-Ti grade 4, machined or laser-treated surfaces; titanium fixation band with silicon moulding and titanium fixation screws	Bone ingrowth, tissue integration, implant surface interaction

Abbreviations: MIPS – Minimally Invasive Ponto Surgery; MONO – one-step drilling system; cp-Ti – commercially pure titanium.

3.1 Experimental study design

Implant retrieval network [Paper I]

In **Paper I**, we employed a structured logistical framework to analyse bone-anchored implants retrieved from six clinics: Karolinska University Hospital (Sweden), Maastricht University Medical Centre, Utrecht University Medical Centre and University Medical Center Groningen (The Netherlands), Midland Regional Hospital (Ireland) and University Hospitals Birmingham (UK). The clinical patient histories were correlated with morphological, cellular, and microbiological findings obtained through a combination of laboratory techniques. These included X-ray micro-computed tomography (microCT), histology and histomorphometry, immunohistochemistry, and microbiological culturing of clinical swabs taken during the explantations.

Implant retrieval was conducted independently by the treating clinicians at the participating centres, based solely on clinical indications and without any influence from the research team. The decision to perform a retrieval was guided by medical necessity, including factors such as chronic or idiopathic pain, suspected or confirmed infection, mechanical failure, device nonuse, or change of treatment. All procedures were performed in accordance with local surgical guidelines at the participating centres. Patient-related data were recorded by the clinical teams at the time of retrieval. This information included demographics (age, sex, smoking status), comorbidities (e.g., diabetes, neurological conditions, history of radiotherapy), implant-related characteristics (implant type, dimensions, surface treatment), surgical technique used at implantation, and time *in situ*. Importantly, the primary clinical indications for retrieval were documented, including any history of pain, recurrent infection, or inflammation at the implant site.

During the explantations, multiple types of samples were collected to enable comprehensive analysis of the tissue-implant interface. Typically, if the abutment was previously removed, a 5-mm biopsy of the soft tissue above the submerged implant was taken and immersed in a 10% neutral buffered formalin (NBF) and paraffin-embedded for histology and immunohistochemistry. Any excess soft tissue remaining on the top of the implant was also preserved. Swabs were obtained from the top of the implant and/or around the abutment and placed in transport medium for subsequent microbiological culturing. The implant and the surrounding bone were then retrieved *en bloc* by drilling with a small diameter round burr and submerged in NBF solution for further analysis (microCT and histology). The soft tissue samples and the implant-bone specimens were transported to the Department of Biomaterials at the University of Gothenburg (Gothenburg, Sweden), where the explants were entered into the biobank (ID

513). Since surgeons aimed to minimise bone removal during the explantation, not all implants were retrieved with a substantial amount of surrounding bone tissue, and soft tissue samples were not consistently preserved for every case.

Microbiological study of BAHS [Paper II]

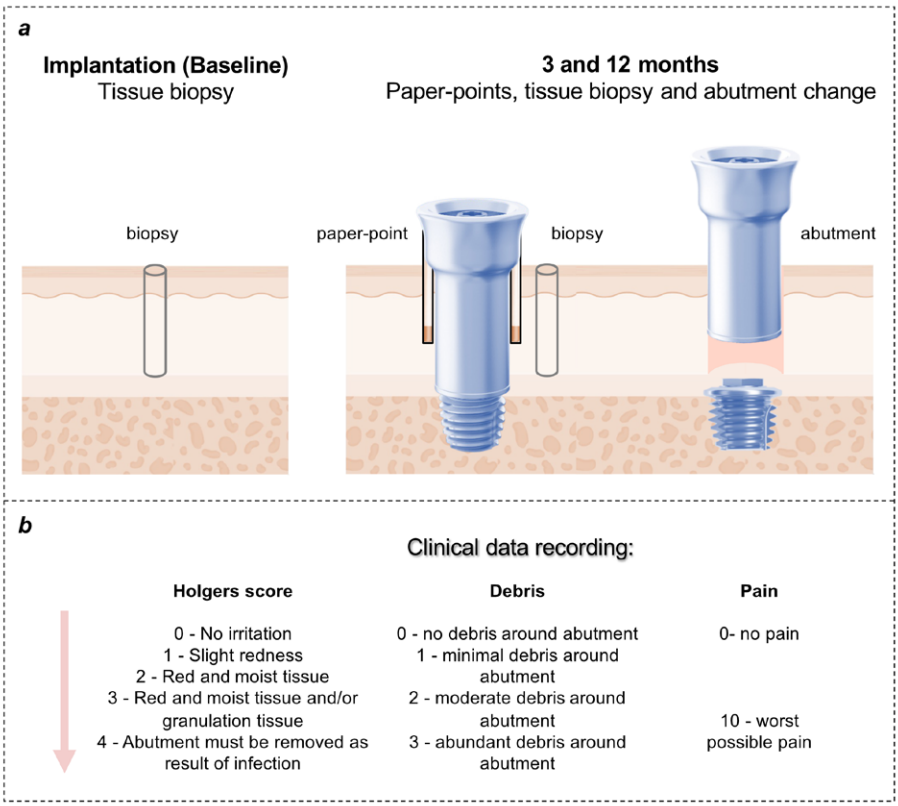

Fig. 3. Sampling and clinical evaluation scheme in the prospective clinical study [Paper II]. ***(a)*** Overview of sampling procedures at different time points. At baseline (implantation), a tissue biopsy was collected. At 3 and 12 months postoperatively, paper-point sampling, an additional tissue biopsy, and abutment sampling and exchange were performed. ***(b)*** Clinical data collection included the Holgers score (0–4), debris score (0–3), and pain score (0–10).

The single-centre, sponsor-initiated, prospective, controlled pilot case series was conducted over 12 months (**Fig. 3**). Sixteen adults received bone-anchored hearing systems, Wide Ponto 4 mm implants (Oticon Medical AB, Sweden) with 6-, 9-, or 12-mm abutments, via the minimally invasive Ponto surgery (MIPS) technique. One recipient was excluded due to early implant loss, leaving 15 patients for analysis. Clinical and microbiological assessments were conducted at

baseline, 3, and 12 months postoperatively. Demographics, hearing loss indications, and abutment lengths were recorded. Clinical assessments included Holgers scores [0 (no irritation) – 4 (abutment removed due to persistent infection)], pain scores [0 (no pain) – 10 (worst possible pain)], and debris scores [0 (no debris) – 3 (abundant debris around abutment)]. We evaluated microbiological samples from patients in relation to their clinical records collected during follow-up visits when clinical isolates were obtained.

Ex vivo/in vitro evaluation of bone drilling [Paper III]

In **Paper III**, the mechanical and thermal evaluation of a multi-step drilling sequence (MIPS) and a single-step guided drill system (MONO) was performed (**Fig. 4a,b**). Torque and force were measured using a customised test rig (Asset No. A069, Oticon Medical, Sweden) while drilling in fresh cadaveric cow tibia bone. The thermal evaluation was performed in artificial bone blocks (Sawbone PCF 50, Sawbones Europe AB, Sweden).

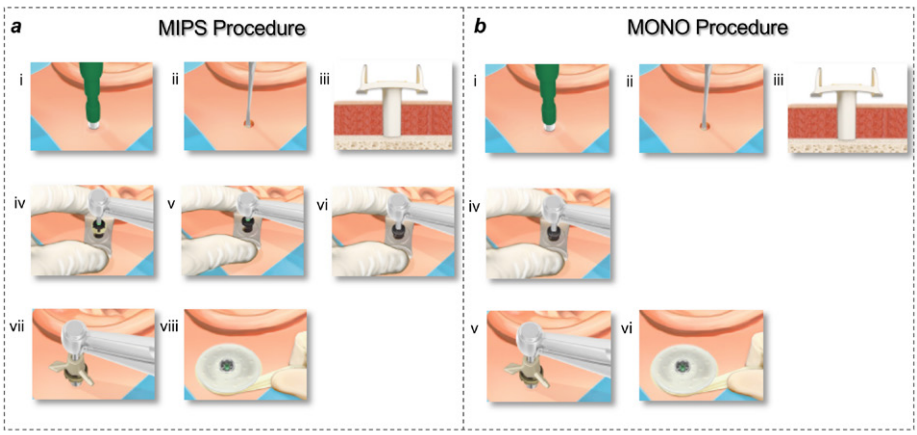

Fig. 4. Surgical techniques used in Paper III. (*a*) The minimally invasive Ponto surgery (MIPS): The procedure consists of the following steps: (i) a circular incision is made at the designated site using a biopsy punch, (ii) the periosteum is removed from the bone surface, (iii) the guide cannula is inserted into the incision to align the instruments, (iv) initial guide drilling is performed through the cannula, (v) after ensuring the sufficient bone thickness, the spacer is removed from the guide drill to accommodate a 4-mm implant, (vi) the osteotomy is enlarged using a widening drill, (vii) the cannula is removed and the implant is inserted through the circular incision, and (viii) a soft healing cap is placed on the abutment and a protective dressing is applied. **(*b*) The MONO surgical procedure** consists of the following steps: (i) a circular incision is made at the selected site using a biopsy punch, (ii) the periosteum is removed from the exposed bone surface, (iii) the guide cannula is inserted into the incision, (iv) the osteotomy is performed in a single step using the MONO drill, (v) the cannula is withdrawn, (vi) the implant is placed through the circular opening, and (vii) a soft healing cap is secured to the abutment and a dressing is applied. Images reproduced with permission from Oticon Medical AB©.

Five drilling protocols (DP1-DP5) were established to represent different clinical situations. The order reflects progressively higher expected heat generation due to increasing deviations from the recommended standard protocol, specifically regarding irrigation effectiveness and the duration of drilling.

DP1 (Standard procedure): Drilling was performed with continuous manual irrigation using tap water (22 °C) delivered via a 20 cc syringe. The cannula was prefilled before drill insertion, with continuous flow maintained throughout drilling and final flushing of the osteotomy after drill removal.

DP2 (No continuous irrigation): Similar to DP1, the cannula was prefilled before drilling, but continuous irrigation during drilling and post-drilling flushing were excluded.

DP3 (Idling): As in DP1, but each drill was left idling at 2,000 rpm for ~2 seconds at full depth before removal.

DP4 (Reduced irrigation + idling): Combined features of DP2 and DP3, excluding irrigation and including idling at depth.

DP5 (No irrigation, positive control): Drilling was conducted without any irrigation to simulate a worst-case scenario.

Drilling effects were further assessed by collecting the bone chips and the bone blocks containing the osteotomies for DP1, DP4 and DP5. Bone chips were retrieved from the osteotomy site and drill flutes; half was fixed in 4% paraformaldehyde for microCT and embedding, and the other half for Raman spectroscopy in Hank's Balanced Salt Solution (HBS). The bone blocks were longitudinally sectioned across the osteotomy and preserved in 4% paraformaldehyde or HBS for histological and Raman analyses, respectively.

Sheep model for transcutaneous implants [Paper IV]

Fourteen healthy female sheep (Blanche du Massif Central, 4.4 ± 0.8 years, 67.7 ± 5.7 kg) were included in the study. Prior to surgery, the health of the animals was checked, and they underwent fasting. General anaesthesia was induced with midazolam and propofol, maintained with isoflurane, and supplemented with local anaesthetics and analgesics. Antibiotic and analgesic treatments (cefazolin, morphine, fentanyl patch, and flunixin) were administered perioperatively and postoperatively.

Each sheep received three randomised titanium implants (machined or laser-modified; recessed or non-recessed) fixed on the frontal/parietal skull bone, either directly on the surface or in a 3 mm surgically created bone recess. The implants were secured with bands and self-drilling screws. Surgical sites were prepared under sterile conditions, and postoperative care included regular monitoring and pain management. The implantation procedure is presented in **Fig. 5**.

Four- and thirteen-weeks post-surgery, the animals were euthanised with intravenous pentobarbital. The implant sites were macroscopically examined and photographed. The implants, along with the surrounding bone and soft tissue, were extracted *en bloc* and fixed in 10% NBF for histological evaluation.

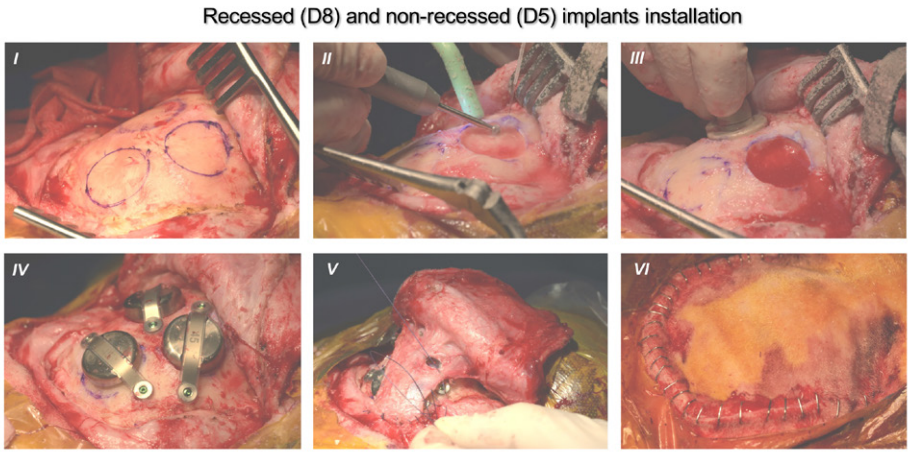

Fig. 5. Surgical technique used in Paper IV. The surgical procedure for transcutaneous implant placement involves the following steps: (i) the implantation site is prepared by making a skin incision and retracting a full-thickness flap that includes both the skin and underlying periosteum, (ii) a bone recess is drilled at the marked site, (iii) the shape and size of the recess are assessed using a custom template, (iv) the implant is secured to the bone using a fixation band and self-drilling screws, (v) the periosteum is sutured over the implant to provide coverage, and (vi) the closure is completed by sub-cutaneous sutures and stapling of the skin.

3.2 Materials used in the studies

Drill systems [Papers III and IV]

Drilling and implantation techniques were assessed *ex vivo* and *in vitro* [**Paper III**], and in preclinical *in vivo* models [**Papers IV**] to evaluate their mechanical and thermal performance and influence on subsequent implant stability and tissue response.

In **Paper III**, two commercially developed guided drill systems for BAHS placement were evaluated: the MIPS system and the more recently introduced single-step drilling MONO system (Oticon Medical, Sweden) (**Fig. 6a**). All drill components were manufactured from stainless steel and coated with a diamond-like carbon (DLC) layer to enhance durability and minimise friction. Both systems employ a flapless surgical approach, in which drills were inserted through a soft tissue punch and guided by a plastic cannula to reach the bone surface.

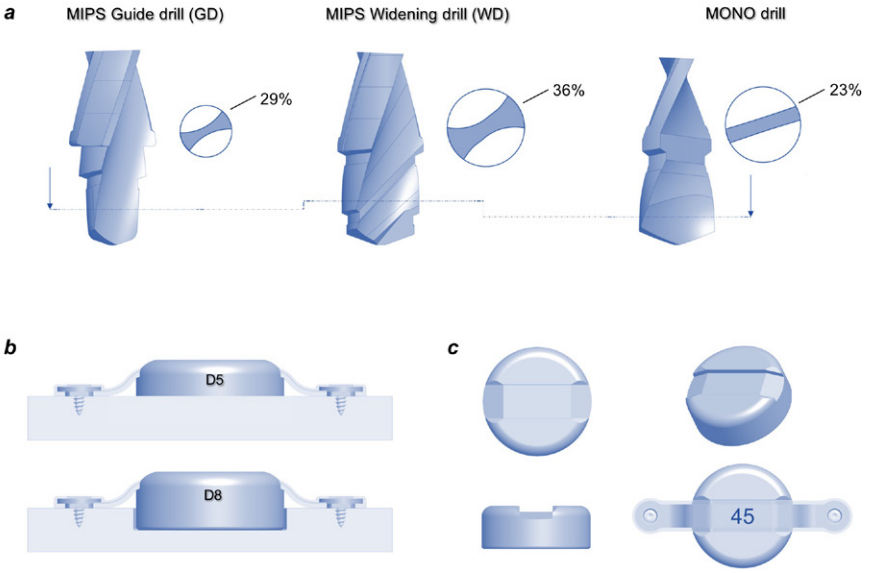

Fig. 6. Schematic overview of drills [Paper III] and implants [Paper IV]. ***(a)*** Geometry and cross-sectional area of the Guide Drill (GD) and Widening Drill (WD), and the single-step MONO drill. The MONO drill has the smallest cross-sectional area (23%), followed by the MIPS GD (29%) and the MIPS WD (36%). ***(b)*** Cross-sectional views of the two disc implant types used in the ovine model: D5 (5 mm thick, non-recessed) and D8 (8 mm thick, recessed in a 3 mm bone defect). ***(c)*** Top, angled, and lateral views of the disc implant geometry with a circumferential groove for fixation via a 45 mm silicone-coated titanium band and two mini-screws. *Abbreviations: MIPS – minimally invasive Ponto surgery; MONO – single-step drill system; GD – guide drill; WD – widening drill.*

The MIPS system replicates the traditional multi-step osteotomy preparation used in open surgical techniques, consisting of a guide drill (MIPS GD) and a widening drill (MIPS WD), all operated sequentially through the guide cannula. In contrast, the MONO system uses a single-step drilling approach using a twist drill with a parabolic geometry that enables complete osteotomy formation in one pass. This parabolic drill reduces the cross-sectional area, and thereby the bone-to-drill contact area, to approximately 23% of the osteotomy cross-section, compared

with 29% for the MIPS GD and 36% for the MIPS WD. This geometry is intended to optimise cutting efficiency, reduce frictional resistance, and enhance irrigation flow and the removal of the hot bone chips from the drill tract. Together, these properties help to minimise thermal damage, eliminating the need for sequential drilling steps.

In **Paper IV**, a drilling procedure was used for preclinical implantation in the ovine calvarium. Depending on the randomisation scheme, either one or two 3 mm deep recessed bone defects were created per animal using 3.2- and 6-mm round burrs, which was operated under continuous saline irrigation to prevent overheating. The implant sites were marked using a sterile template and positioned relative to anatomical landmarks on the frontal/parietal bone. In contrast to the guided systems in **Paper III**, these burr-based defects were prepared under direct visualisation through a linear incision with flap elevation. The created defects were used for recessed placement of 8 mm thick implants, whereas 5 mm thick implants were placed directly onto the calvarial surface without bone removal.

Implant and surface design [Papers I-IV]

A variety of implant designs were employed across the studies to reflect both clinical practice and experimental research aims. These included commercially available percutaneous systems used in patients [**Papers I** and **II**] and custom-made transcutaneous discs designed for preclinical evaluation [**Paper IV**].

In **Paper I**, the retrieved implants represented multiple generations of percutaneous BAHS. Implant geometries ranged from early Ø3.75 mm, machined, minimally roughened, commercially pure titanium (cp-Ti) designs to wider Ø4.5 mm fixtures incorporating surface modifications aimed at enhancing osseointegration. These included blasted surfaces, i.e., TiOblast™ (BI300, Cochlear, Sweden) and laser-ablated surfaces, i.e., Ponto BHX implant (Oticon Medical, Sweden). Various abutment designs were represented, including hydroxyapatite-coated variants (e.g., BIA400) and machined alternatives. Surgical protocols transitioned in parallel, from traditional soft tissue reduction to tissue preservation techniques, including the MIPS and MONO procedures, which aim to shorten surgical time and improve postoperative outcomes.

In **Paper II**, all patients received the Wide Ponto implant (Oticon Medical, Sweden), a 4 mm diameter, screw-type cp-Ti fixture with a moderately rough surface. The implants were paired with straight-profile abutments that were 6-, 9- or 12-mm in length, and were selected based on soft tissue thickness. All

procedures were conducted using the MIPS technique, consistent with current clinical standards for minimally invasive BAHS placement (**Fig. 1a**).

In the preclinical model of **Paper IV**, two types of custom-designed disc-shaped implants were manufactured by Oticon Medical (Sweden) using commercially pure Grade 4 titanium (**Fig. 6b,c**). Both implant types had a diameter of 20.3 mm but differed in thickness: the 5 mm variant (D5) was placed sub-periosteally on the bone surface, while the 8 mm version (D8) was recessed into a surgically prepared 3 mm deep bone defect. Both implant types featured a 6.2 mm wide circumferential groove designed to accommodate a 45 mm long silicone-overmoulded titanium fixation band, which was anchored to the bone using two Ø1.1 × 4 mm self-drilling titanium mini-screws.

Two distinct surface topographies were evaluated in **Paper IV**: machined (control) and laser-ablated (test) surfaces with a circular pattern. The laser-modified surfaces were produced on the bone-facing side of the implant using a Yb optical fibre laser (TruMark Station 5000, Trumpf, Germany) with a wavelength of 1062 ± 3 nm. Laser parameters included a 124.7 mm focus distance, 45% maximum pulse energy, 6.0 kHz frequency, and a scanning speed of 60 mm/s. The ablation pattern consisted of a circular spiral with 25% overlap from the periphery toward the centre of the disc, resulting in macro- and nano-scale texture features designed to promote osseointegration.

3.3 Material characterisation

Surface morphology and roughness [Papers III and IV]

Scanning electron microscopy (SEM) was employed to analyse surface morphology and roughness of bone chips and implants surfaces. By detecting different types of emitted electrons, this imaging technique enables complementary modes of analysis suited for both morphological and compositional characterisation.

Backscattered electron SEM (BSE-SEM) detects electrons reflected from the sample surface, with contrast proportional to atomic number. This makes it particularly useful for visualising compositional differences, such as distinguishing mineralised tissue from softer or less dense phases. In **Paper III**, four bone chip specimens were collected from every drill system during drilling with the standard protocol (DP1). These were embedded in resin, polished under wet conditions with silicon carbide grinding paper, and subsequently air-dried prior to imaging. BSE-SEM was performed using a Zeiss Leo Ultra 55 FEG SEM (Leo Electron

Microscopy Ltd, UK), operated at 20 kV. Qualitative shape-related differences between the bone chips groups were assessed at 100×, 200×, and 400× magnifications.

In **Paper IV**, SEM imaging was performed at 5 kV using a conventional secondary electron detector for low-resolution images and an in-lens detector for high-resolution images, across magnifications from 100× to 50,000×. Further, three-dimensional scanning electron microscopy (3D SEM) was performed for surface roughness quantification. This method combines stereopair image acquisition with digital reconstruction to generate quantitative topographical data, enabling surface roughness measurements beyond conventional 2D imaging. The stereopair images (–4° and +5° tilt) were acquired in secondary electron mode at 550× magnification using a Jeol JSM-7800F Prime (JEOL, Tokyo, Japan) operating at 5 kV. A 3D topographical reconstruction was generated using MeX® software (Alicona Imaging GmbH, Graz, Austria), with tilt correction to obtain S_a (arithmetical mean height) and S_{dr} (developed interfacial area ratio) values. Three regions (233 × 176 μm) were measured on three control and three test discs.

Raman spectroscopy [Paper III]

In **Paper III**, to assess the compositional changes of bone chips and bone adjacent to the osteotomy, micro-Raman spectroscopy was employed. This technique is used to identify molecular composition by detecting photon interactions with chemical bonds. When laser light strikes a sample, most photons are elastically scattered, but a small fraction undergoes inelastic (Raman) scattering, producing energy shifts that correspond to the unique vibrational fingerprints of specific molecules. The measurements were carried out using a confocal Raman microscope (Renishaw inVia Qontor) with a 633 nm laser and a ×50 objective. Spectra were collected with a cooled CCD detector and a 2400 g/mm grating, at ~15 mW laser power. The samples were analysed for each drilling system (MONO, MIPS) and protocol (DP1, DP4, DP5). Two points were located close to the drilled osteotomy (10–20 μm), and two were positioned further away (~500 μm). From these spectra, compositional parameters such as mineral crystallinity (1/FWHM of the ν_1 PO_4^{3-} peak), mineral-to-matrix ratio (ν_2 PO_4^{3-}/Amide III), and carbonate-to-phosphate ratio (ν_1 CO_3^{2-}/ν_1 PO_4^{3-}) were determined.

Auger electron spectroscopy [Paper IV]

Auger electron spectroscopy (AES) is a surface-sensitive analytical technique based on the emission of Auger electrons following core-level ionisation. Because the emitted electrons originate from only the top few nanometres of the sample,

AES provides detailed information on surface composition and elemental distribution. The method is widely applied to characterise thin films, interfaces, and surface modifications in materials research.

Surface chemical composition was determined using a PHI 700 Xi Scanning Auger Nanoprobe, which was used at 10 keV primary electron energy with a beam current of 10 nA. The quantitative chemical analysis was performed before depth profiling in areas of approximately 10×10 μm in size. The survey spectra were recorded between 30 and 1800 eV. Two implants of each type were examined, with four distinct regions analysed per implant. Oxide layer thickness was assessed via Auger electron spectroscopic (AES) depth profiling on two implants of each type, targeting three areas of each implant. Depth profiling was performed using 1 keV Ar+ ions with a beam current of 50 nA rastered over an area of 1×1 mm. The sputter rate was established using a standard sample with 24.4 nm SiO_2 on a Si substrate. The sputter rate for TiO at 2.19 nm/min was determined by multiplying the SiO_2 sputter rate at 4.05 nm/min by 0.52 [155].

3.4 Bone-implant interactions and structural analysis

Histology and histomorphometry [Papers I, III, and IV]

Histological and morphometric analyses were performed on resin- and paraffin-embedded samples to assess bone–implant interactions and peri-implant tissue organisation in **Papers I**, **III**, and **IV**. Where applicable, methodologies were harmonised across studies to enable inter-study comparisons.

Toluidine blue was used to provide general contrast and to visualise cell nuclei, osteoid, and overall tissue morphology. The combination of methylene blue and basic fuchsin enabled differentiation between mineralised and non-mineralised tissues, with mineralised bone appearing red/pink and soft tissues stained blue. In **Papers I** and **IV**, bone–implant specimens were fixed in formalin, dehydrated through a graded ethanol series, and embedded in LR White resin. Transverse ground sections were prepared using a precision cutting system (EXAKT® Apparatebau GmbH & Co, Germany). The sections were polished to a final thickness of 40–50 μm and stained with 1% toluidine blue and a combination of 1% methylene blue and 3% basic fuchsin for histological evaluation. In **Paper III**, bone half-blocks with pre-drilled osteotomies underwent an identical dehydration and resin-embedding process, followed by central ground sectioning and toluidine blue staining. Qualitative assessment of bone and osteotomy morphology was conducted using light microscopy (Nikon Eclipse E600; Nikon NIS-Elements software, Nikon Instruments Europe BV, The Netherlands) in all three studies.

In **Paper I**, soft tissue biopsies were embedded in paraffin, sectioned to 5 µm using a microtome (Leica RM 2255, Leica Biosystems, Germany), and stained with hematoxylin and eosin for general morphological evaluation. Selected sections were also stained with Giemsa to visualise potential bacterial colonies. A Nikon Eclipse E600 light microscope was used for qualitative analysis of both soft and hard tissues.

Quantitative histomorphometry was performed in **Papers I** and **IV**. In **Paper I**, image analysis software (Nikon NIS-Elements) was used to measure the bone-to-implant contact (BIC), the bone area (BA) within implant threads, and the vertical bone level relative to the implant flange. In **Paper IV**, transverse ground sections were scanned using a ZEISS Axioscan 7 slide scanner with a Plan-Apochromat 20×/0.8 objective (Zen software v. 3.10.103.01000, Carl Zeiss Microscopy GmbH, Germany). For each implant, three regions of interest—central (C), left peripheral (L), and right peripheral (R)—were defined, and 11 equidistant measurement points were placed per region. At each point, the perpendicular distance from the implant surface to (i) native bone and (ii) total bone (native + woven) was measured in micrometres.

To characterise the tissue composition further, the area between the implant surface and native bone was segmented into three compartments: the empty space (void), soft tissue, and woven bone. Manual segmentation was performed using the polygon region of interest (ROI) function in Zen software, and compartmental areas were exported to GraphPad Prism for calculation of compositional metrics (e.g., % woven bone = woven / [void + soft tissue + woven]). All measurements were performed by a single blinded operator, and regional comparisons were made to assess spatial differences in bone ingrowth and fibrous tissue encapsulation.

Immunohistochemistry [Paper I]

Immunohistochemical analysis was performed in **Paper I** to evaluate inflammatory and neuroimmune markers in peri-implant soft tissues. Paraffin-embedded soft tissue sections were first deparaffinised in xylene, rehydrated through a graded ethanol series, and rinsed in phosphate-buffered saline (PBS). Heat-induced antigen retrieval was carried out in citrate buffer at 90 °C for 20 min to unmask epitopes.

Following antigen retrieval, tissue sections were blocked for 30 min using 5% goat serum in 4% bovine serum albumin to reduce non-specific binding. Primary antibodies targeting specific immune and neuronal markers were applied for 2 h at room temperature. The panel included rabbit polyclonal antibodies against

inducible nitric oxide synthase (iNOS), mannose receptor C-type 1 (MRC1), CD3 (T lymphocytes), CD20 (B lymphocytes), and calcitonin gene-related peptide (CGRP).

Immunoreactivity was visualised using a horseradish peroxidase (HRP)-based detection system combined with a metal-enhanced diaminobenzidine (DAB) chromogen, following the manufacturer's instructions. Negative controls were included in each run by omitting the primary antibody to confirm staining specificity.

Whole-slide digital images were acquired using a Zeiss Axioscan 7 slide scanner (Carl Zeiss Microscopy GmbH, Germany) equipped with a Plan Apo 20x/0.8 objective. Quantitative analysis of immunopositive cells was performed in QuPath software (version 0.5.1) using the "positive cells detection" tool. Cell densities were reported for each marker to enable comparisons across specimens and correlation with clinical and histological outcomes.

Micro-computed tomography (microCT) [Papers I and II]

MicroCT is a non-destructive imaging technique that uses X-rays to generate high-resolution 3D reconstructions of samples. High-resolution microCT imaging was employed in **Papers I** and **III** to assess bone structure and morphology in relation to implant geometry and drilling protocols. Scanning was performed using the Skyscan 1172 microCT system (Bruker microCT, Kontich, Belgium) under optimised parameters tailored to each sample type.

In **Paper I**, embedded bone–implant specimens were scanned at 100 kV with a voxel resolution of 6.7 μm. Five images were averaged per 0.4° rotation step over a full 360° scan. Projection images were reconstructed using filtered back-projection algorithms and manually aligned along the long axis of the implant to facilitate region-specific analysis. A tapered cylindrical volume of interest (VOI) encompassing the threaded portion of the implant was defined, and bone volume within this VOI was segmented via manual global thresholding based on morphological features. The segmented binary images of the implant, surrounding bone, and designated ROI were analysed in 3D using the Bruker software suite (NRecon, DataViewer, CTAn, CTVox) to identify bone volume (BV). In addition, the vertical bone level relative to the implant flange was measured in two quadrants using orthogonal views in DataViewer to precisely localise the crestal bone margin.

In **Paper III**, the morphology of bone chips resulting from different osteotomy protocols were evaluated using the same Skyscan 1172 system, operating at 70 kV

with a pixel size of 6.98 μm. Each sample was scanned through a 180° rotation with frame averaging (3 frames per step) and 0.5° angular increments. Eight samples per drill system (MONO and MIPS) across three protocols (DP1, DP4, and DP5) were included. The microCT data were reconstructed and analysed using Bruker software to quantify total fragment volume and assess morphological features such as the size, density, and structure of the autologous bone debris. This allowed comparison of thermomechanical drilling effects across systems.

Together, these analyses were undertaken to provide both macro- and microstructural insights into bone integrity and drill-induced damage, complementing histological findings and enabling correlation with drilling performance and implant osseointegration potential.

3.5 Microbiological techniques

Patient sampling and bacterial identification [Papers I and III]

In **Paper I**, bacterial swabs were processed according to local routines at the participating hospital centres using the standard bacterial culturing techniques. In hospital settings, swab sampling for microbiological identification was typically performed during surgical or clinical procedures using sterile techniques. A sterile swab was gently rubbed from the cover screw or the top of the implant during explantation. The swab was then placed into a sterile tube containing transport medium (e.g., 200 μL of transport buffer) to preserve microbial cell viability and/or DNA. The samples were transported promptly to the microbiology laboratory, where DNA extraction was performed, followed by standardised molecular techniques, to identify bacterial species through polymerase chain reaction (PCR) amplification and capillary electrophoresis of 16S–23S rRNA interspacer regions. The results were analysed to determine the bacterial profiles.

In **Paper III**, quantitative culturing was performed on samples collected from the abutment surface, periabutment fluid, and soft tissue biopsies within 48 h of retrieval using selective agar media. From the staphylococci-selective medium, a single representative colony per patient, sample, and time point was subcultured and preserved for further analysis.

The clinical parameters recorded included Holgers scores (0 = no irritation to 4 = abutment removal due to persistent infection), pain scores (0 = no pain to 10 = worst possible pain), and debris scores (0 = no debris to 3 = abundant debris around the abutment).

Staphylococcal isolates were cryopreserved at –80°C in a biobank (ID 513) for future analysis. While clinical, microbiological, and molecular findings have been previously reported [35,36], the current investigation focused on evaluating the phenotypic and genotypic virulence profiles of the isolates and their associations with clinical outcomes.

Biofilm formation in vitro assays [Paper II]

The biofilm-forming capacity of the clinical bacterial isolates was evaluated using both quantitative and semi-quantitative methods. Biofilm biomass was assessed via the Crystal Violet (CV) microtiter plate assay. Overnight cultures grown in tryptic soy broth (TSB) supplemented with glucose were standardised, diluted, and inoculated into 96-well plates. After 24 h of incubation at 37°C, wells were gently washed, stained with 2% CV, and destained with an ethanol-acetone solution. Absorbance was measured at 595 nm to quantify biofilm biomass, and based on optical density thresholds by Baldassari *et al.* (2001) [156], the biofilm production ability of the strains was categorised.

Slime production was semi-quantitatively evaluated using Congo Red (CR) agar. The bacterial isolates were cultured on brain heart infusion agar enriched with sucrose and CR dye, then incubated at 37°C for up to 48 h. Following the predetermined colour scale by Arciola *et al.* (2002) [157], colony morphology and pigmentation were used to classify strains into non-producers, weak producers, or strong biofilm slime producers. An overview is presented in **Fig. 7a,b**.

Antimicrobial susceptibility testing [Paper II]

To characterise the antimicrobial resistance profiles of staphylococcal isolates, both planktonic and biofilm-associated susceptibility were assessed using standardised antibiotic testing methods. Antimicrobial susceptibility was tested using the broth microdilution method to determine the minimum inhibitory concentrations (MICs) of a panel of nine antibiotics. Standardised bacterial suspensions were incubated with predefined antibiotic concentrations in microtiter plates. MIC values were determined visually and interpreted based on established clinical breakpoints, allowing the categorisation of strains as susceptible, intermediate, or resistant. To evaluate antibiotic tolerance within biofilms, minimum biofilm eradication concentrations (MBECs) were determined using a specialised assay device. Biofilms were grown on peg lids for 24 h (MBEC Assay®, Innovotech Inc., Canada), exposed to antibiotics for 20 h, and then transferred to neutralising recovery media. MBEC values were recorded based on regrowth (visual turbidity) and compared with planktonic MICs to assess the level of biofilm-associated resistance. An overview is presented in **Fig. 7c,d**.

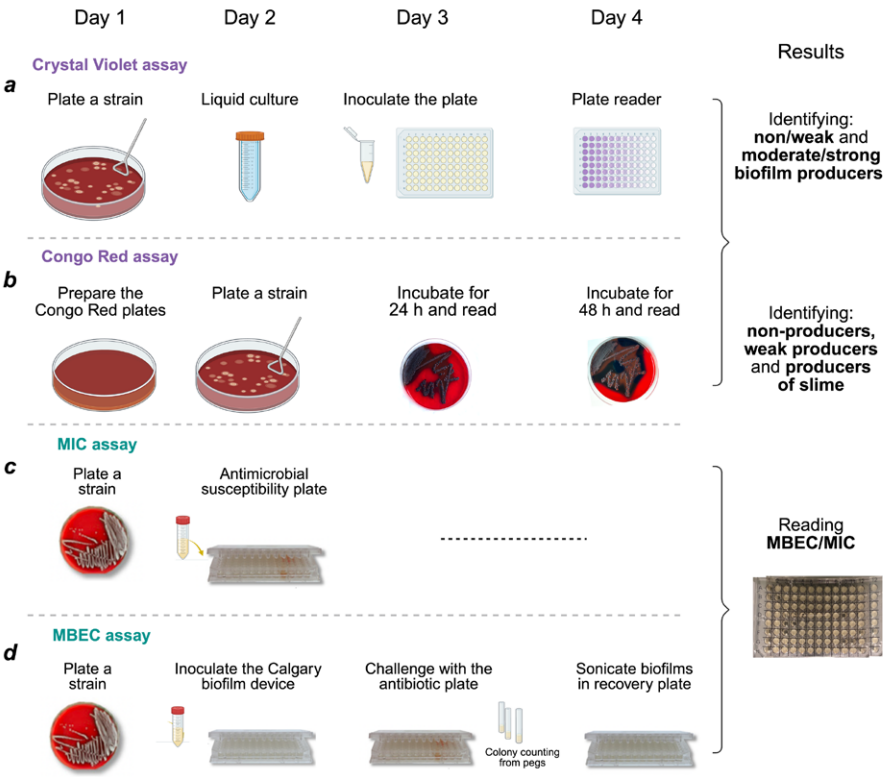

Fig. 7. Schematic overview of microbiological phenotypic assays used to assess biofilm formation and antimicrobial susceptibility [Paper II]. ***(a)*** The Crystal Violet assay was used to quantify biofilm biomass in 96-well plates over four days, classifying strains as non/weak or moderate/strong biofilm producers. ***(b)*** Congo Red agar enabled visual categorisation of slime production based on colony pigmentation after 24–48 h of incubation. ***(c)*** The Calgary Biofilm Device assay was used to measure the minimum biofilm eradication concentration (MBEC) by growing biofilms on pegs, exposing them to antibiotics, and analysing regrowth after sonication. ***(d)*** The minimum inhibitory concentration (MIC) assay was determined using the broth microdilution method to assess planktonic antibiotic susceptibility and establish the resistance profiles (antibiograms) of the bacterial strains. *Created with BioRender.com.*

Genomic DNA isolation and whole-genome sequencing [Paper II]

Whole-genome sequencing was performed to characterise bacterial isolates at the genetic level, allowing strain typing and detection of virulence and resistance-associated genes. Genomic DNA was isolated from bacterial strains using GenElute Bacterial Genomic DNA Kit (Sigma-Aldrich, USA), including the Gram-positive lysis protocol and enzymatic digestion steps to ensure effective cell wall disruption. DNA libraries were prepared using Nextera XT (Illumina, USA) and sequenced on MiSeq (Illumina, USA) using a short-read platform with a target

coverage of at least 40×. Bioinformatic analysis included species identification, multilocus sequence typing (MLST), phylogenetic clustering (core-genome MLST, cgMLST), and screening for virulence genes and regulatory loci. Sequence identity thresholds were applied to define gene presence, and genomic data were used to confirm epidemiologic clonality and contextualise phenotypic findings from the biofilm and resistance assays.

3.6 Mechanical and thermal evaluation of bone drilling

Ex vivo mechanical evaluation

The cutting performance of MIPS and MONO drill systems was assessed using a custom test rig (Asset No. A069, Oticon Medical, Sweden) in fresh cadaveric cow tibiae. Drilling was performed at 2,000 rpm across three feed rates (0.5, 1.0, and 2.0 mm/s). For each drill and condition, five sequences were recorded per set, totalling ten measurements per group. All the drills were tested via a guide cannula without irrigation at 22 ± 2 °C. The torque and axial force were measured, and the cutting power was calculated from these parameters to determine the mechanical efficiency.

In vitro heat generation evaluation

The thermal effects during osteotomy preparation were evaluated in artificial bone blocks (Sawbones PCF 50) using thermocouples positioned 0.5 mm from the osteotomy edge. Both MIPS (modified to two-step drilling, omitting the initial step with the spacer attached to the Guide drill) and MONO (single-step drilling) protocols were tested under five irrigation conditions (DP1–DP5), simulating increasing deviation from the clinical standard. The temperature was recorded at four depths using a TC-08 data logger at 10 Hz. Ten osteotomies were prepared for each combination of drill system and drilling condition, and drill bits were replaced after five uses.

Additionally, the influence of feed rate (0.5 and 2.0 mm/s) on heat generation was tested using the mechanical rig and protocols DP1, DP2, and DP5. MicroCT scans (Zeiss Metrotom 800) and 3D modelling software (Creo Parametric 7.0) were used to correct for thermocouple distance, enabling precise estimation of peak temperatures at 0.5 mm from the osteotomy wall.

3.7 Ethical considerations

Paper I: Six clinics participated in the network: Karolinska University Hospital (Sweden), Maastricht University Medical Centre, Utrecht University Medical Centre and University Medical Center Groningen (The Netherlands), Midland

Regional Hospital (Ireland), and University Hospitals Birmingham (United Kingdom). Ethical approvals for the analyses of explants were handled according to the respective national legislations. One sample was included from Karolinska University Hospital as part of a clinical investigation (Sponsor Oticon Medical, Askim, SE, Study ID C49); ethical approval was issued by the Regional Ethical Review Board of Stockholm, 2014/1566-31/2. One sample from Maastricht University Medical Centre was part of a clinical investigation (Sponsor Oticon Medical, Askim, SE, Study ID C50), with ethical approval ID NL50072.068.14/METC141007. One sample from Midland Regional Hospital (Ireland) was derived from material resected on clinical grounds, with patient consent for use in academic research, in accordance with the Irish Council of Bioethics (2005) and the HSE National Policy for consent in health and social research (2025). The remaining electively removed implants were exempt from ethical approval as they are considered waste material in the Netherlands. The samples from Birmingham, UK, are also considered waste materials according to the policy document (Policy on Human Tissue in Research, no. 063) and did not need separate ethical approval. The clinical data available were limited to sex, age, comorbidities, implant type, surgical implantation technique, time *in situ*, reason for explantation, and bacterial species (in cases of diagnosed infection). All samples were coded with these data in the biobank, with no access to patient identity or personal data.

Paper II: This prospective clinical pilot study was conducted in a specialised referral centre in Stockholm, Sweden. The study was registered with clinicaltrials.gov (NCT02304692).

Paper IV: This study was conducted according to the ISO 10993 Standard, Biological Evaluation of Medical Devices, Part 6 (2016): Tests for Local Effects after Implantation. The study protocol was approved by the NAMSA Ethical Committee, where each protocol is a part of a project authorisation that is reviewed every five years by the Ministry of Higher Education, Research and Innovation. The project authorisation number associated with this study is APAFIS#22914-2019091916114859 v13.

3.8 Statistical analysis

All statistical analyses were performed using GraphPad Prism (versions 10.0.0 or 10.1.1, GraphPad Software, USA) and, where specified, SPSS Statistics v29.0.1.1 (IBM Corporation). Data are presented as mean ± standard deviation (SD) unless otherwise indicated, and statistical significance was set at $p < 0.05$.

Data distributions were assessed using the Shapiro-Wilk test in **Paper III** and **Paper IV** to determine whether parametric or non-parametric methods were appropriate. When data were normally distributed, parametric tests such as independent samples *t*-tests, paired *t*-tests, and one-way or two-way ANOVA were applied. For non-normally distributed data, Wilcoxon signed-rank tests and the Kruskal-Wallis test were used [**Papers I** and **IV**].

In **Paper I**, the Kruskal-Wallis test was employed to compare BIC, BA, BV, and bone level to the flange across three implant design groups.

In **Paper II**, chi-square tests, Fisher's exact tests, and univariate logistic regression were used to analyse associations between bacterial species, biofilm properties, and tissue reactions. Intra-species variability in optical density (OD) in the CV assay was analysed using one-sample *t*-tests, while independent *t*-tests and one-way ANOVA were used to evaluate the inter-group differences in the CV OD and MBEC/MIC ratios.

In **Paper III**, two-way mixed ANOVA was used to assess the effects of drill type (MIPS GD, MIPS WD, MONO), feed rate (0.5, 1.0, 2.0 mm/s), and drilling protocol (DP1-DP5) on drilling force, torque, total work, and heat generation. Two analyses were conducted for heat: one using maximum temperature, and another using the average across thermocouples. The effect of feed rate on temperature was further analysed via one-way repeated-measures ANOVA with Bonferroni post hoc correction. The morphometric parameters of the bone chips (volume, surface area, thickness, and structure model index [SMI]) were compared using parametric *t*-tests. Raman spectroscopy data from surface and deep osteotomy regions were analysed using one-way ANOVA and the Wilcoxon matched-pairs signed-rank test.

In **Paper IV**, differences in surface purity and oxide thickness between machined and laser-ablated surfaces were analysed using paired *t*-tests or Wilcoxon signed-rank tests, depending on the type of distribution (e.g., normal). To evaluate the combined effects of implant type (D5 vs. D8) and surface treatment, mixed-model two-way ANOVA was applied with post hoc pairwise comparisons. Spearman's rank correlation and simple linear regression were used to assess relationships between implant–bone proximity and woven bone area.

4 RESULTS

4.1 Paper I

To evaluate the clinical outcomes of bone conduction devices, it is essential to investigate real-world retrieval cases and understand the factors contributing to their long-term success or failure.

The first study investigated the biological, structural, and microbiological characteristics of 21 electively retrieved bone-anchored implants from 19 patients. An overview of the results is presented in **Fig. 8.**

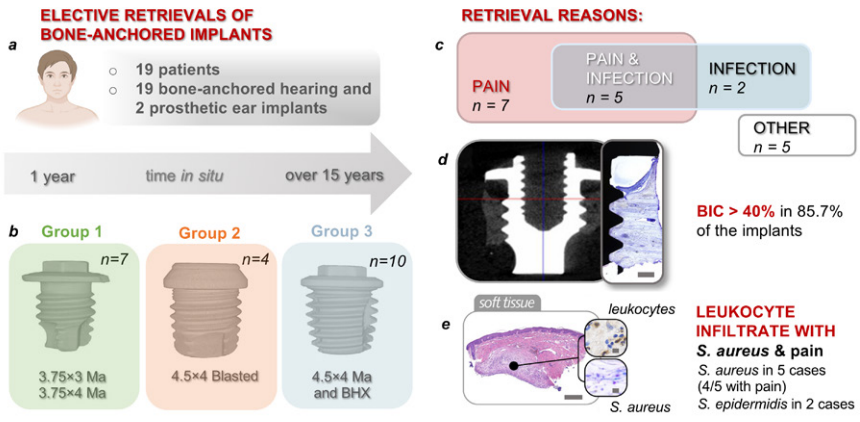

Fig. 8. **(*a*)** Summary of the elective retrieval study, including 19 patients with 19 bone-anchored hearing implants and 2 prosthetic ear implants. Implants had been *in situ* from 1 to >15 years. **(*b*)** Classification of retrieved implants by design and surface characteristics into three groups: Group 1 – 4.5×4 mm (n = 5) and 4.5×3 mm (n = 2) machined implants; Group 2 – 4.5×4 mm blasted implants (n = 4); and Group 3 – 3.75×4 mm machined implants (n = 8) and BHX implants (n = 2). **(*c*)** Clinical indications for implant removal included pain (n = 7), pain and infection (n = 5), infection alone (n = 2), and other causes including mechanical failure, non-use and change of treatment (n = 5). **(*d*)** MicroCT and histological section (toluidine blue and basic fuchsin stain) demonstrating bone–to-implant contact (BIC), which exceeded 40% in 85.7% implants. **(*e*)** Histological analysis of soft tissue (hematoxylin and eosin (left), Giemsa staining (top right), immunostaining (bottom right) revealed leukocyte infiltrates associated with pain and *Staphylococcus aureus* in 5 cases (4 with pain), and *S. epidermidis* in 2 cases. *Scale bars:* ***(d)*** *400 µm;* ***(e)*** *0.5 mm (left) and 10 µm (right). Abbreviations: Ma – machined; BHX – laser-ablated surface; BIC – bone–implant contact; microCT – micro-computed tomography.*

This study revealed that pain and infection were the most common reasons for bone-anchored implants elective retrieval, despite successful osseointegration.

Pain (63.2%) and infection (36.8%) were the most commonly reported indications for retrieval. In several cases, pain was present even in the absence of visible soft tissue inflammation or confirmed infection. Additional retrievals were due to mechanical failure (10.5%) or patient-requested removal for device nonuse or treatment changes (15.8%). The analysed implants had been *in situ* for 12 to 184 months (1 to over 15 years). All but three implants exhibited BIC above 40.5%.

Implants of various designs, ranging from early machined narrow types to modern surface-modified versions, showed similarly high levels of osseointegration.

The implants were grouped on the basis of their geometry design into three main categories: Group 1 – 4.5×4 mm (n = 5) and 4.5×3 mm (n = 2) machined implants; Group 2 – 4.5×4 mm blasted implants (n = 4); and Group 3 – 3.75×4 mm machined implants (n = 8) and BHX implants (n = 2). Despite differences in design and surface treatment, microCT and histomorphometry revealed no significant differences in bone-to-implant contact (BIC), bone area (BA), or bone volume (BV) fraction. Histology confirmed the maintained osseointegration even in cases where removal was indicated because of pain or infection. Notably, a lack of bone beneath the implant flange was frequently observed, regardless of the implant type.

Staphylococcal colonisation, especially by *S. aureus*, was associated with increased localised inflammation and persistent pain.

Swab culturing identified *S. aureus* in five cases, four of which were associated with chronic pain. *S. epidermidis* was found in two cases, whereas *S. capitis* and *Parvimonas micra* were each co-detected in patients with *S. epidermidis* and *S. aureus*, respectively. Among these cases, soft tissues obtained from four patients revealed distinct immune profiles. In *S. aureus*-positive cases associated with pain, dense inflammatory infiltrates dominated by neutrophils, iNOS+ macrophages, and CD3+/CD20+ lymphocytes were observed. In contrast, *S. epidermidis* and *S. capitis*-colonised tissues from a patient with resolved pain exhibited attenuated inflammation with weak immune marker expression.

A pro-inflammatory immune profile dominated *S. aureus*-positive cases, with limited evidence of neuroinflammatory signalling.

Quantitative immunostaining revealed strong expression of pro-inflammatory and adaptive immune markers (iNOS, CD3, CD20) in tissues colonised by *S. aureus*, but pro-regenerative macrophages (MRC1) were absent in these regions. Despite pain being the primary indication for implant retrieval, calcitonin gene-related peptide (CGRP) was detected in only one case.

4.2 Paper II

The biofilm-forming capacity and antibiotic resistance of colonising bacteria are critical determinants of soft tissue complications in patients with BAHS.

This study investigated the clinical relevance of *Staphylococcus* species colonising BAHS, focusing on their genetic profile, biofilm-forming ability, antimicrobial resistance (AMR), and association with soft tissue complications such as pain, inflammation (Holgers score), and debris accumulation. A total of 57 staphylococcal isolates from 15 patients were analysed through phenotypic assays and whole-genome sequencing. The overview of the results is presented in **Fig. 9**.

The most commonly identified species was *S. epidermidis*, which exhibited notable genetic diversity and persistence across time points and anatomical sites.

Among the isolates, *S. epidermidis* was the most frequently detected species (n = 32), followed by *S. aureus* (n = 16) and other coagulase-negative staphylococci (CoNS) (n = 9). Whole-genome sequencing revealed considerable clonal diversity. Six sequence types (STs) of *S. aureus* were identified, with ST1 and ST5 being the most common, each confined to individual patients. In comparison, *S. epidermidis* exhibited greater heterogeneity, encompassing 12 various STs, with ST7 as the most prevalent (33%, 10/32). Many of them persisted across multiple anatomical sites and time points, confirming long-term colonisation.

***S. aureus* was significantly associated with inflammation, whereas *S. epidermidis* was more common in patients with reported pain.**

Colonisation with *S. aureus* was significantly associated with peri-abutment inflammation (Holgers score > 0, $p = 0.0148$), whereas *S. epidermidis* was most frequently linked to patient-reported pain (76%, 13/17; $p = 0.0537$).

a

Bacterial species	**Biofilm formation (CV)**		**Slime production (CR)**	
	NP and WP	MP and SP	Non-slime producers	Slime producers
S. aureus (16), n (%)	2 (13)	14 (88)	0	16 (100)
S. epidermidis (32), n (%)	12 (38)	20 (63)	14 (44)	18 (56)
Other CoNS (9), n (%)	6 (67)	3 (33)	6 (67)	3 (33)
p-value	0.0228*		0.0002***	

Bacterial species	**Adverse events**				
	Holgers > 0	Pain	Debris	No adverse events	Any adverse event
S. aureus (16), n (%)	10 (63)	4 (25)	10 (63)	6 (38)	10 (63)
S. epidermidis (32), n (%)	7 (22)	13 (41)	11 (34)	14 (47)	18 (56)
Other CoNS (9), n (%)	1 (11)	0	4 (44)	5 (56)	4 (44)
p-value	0.0074**	0.0537	0.1713	0.2307	
Biofilm formation (CV)					
Non- and weak- producers (19), n (%)	6 (32)	9 (47)	8 (42)	7 (37)	12 (63)
Moderate- and Strong-producers (38), n (%)	10 (26)	8 (21)	17 (45)	18 (47)	20 (53)
p-value	0.7583	0.0646	0.8503	0.4503	
Slime production (CR)					
Non-slime producers (20), n (%)	3 (15)	7 (35)	4 (20)	11 (55)	9 (45)
Slime producers (37), n (%)	13 (35)	10 (27)	21 (57)	14 (38)	23 (62)
p-value	0.1323	0.5570	0.0114*	0.2682	

b

Minimum Inhibitory Concentration (MIC)	All strains (n=57)	*S. aureus* (n=16)	*S. epidermidis* (n=32)	Other CoNS (n=9)
MDR (resistant to ≥3 antimicrobial agents), n (%)	2 (4)	0	2 (6)	0

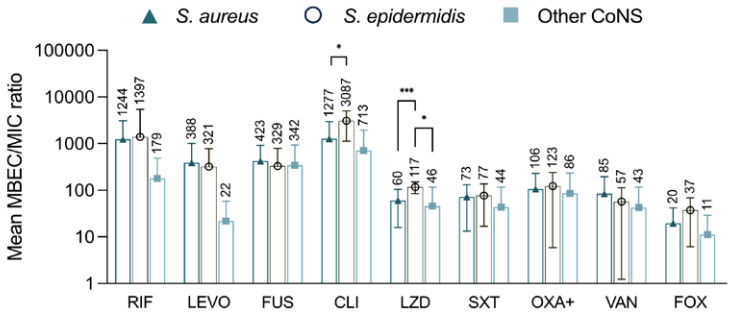

Fig. 9. ***(a)*** Biofilm-forming ability of *Staphylococcus aureus*, *S. epidermidis*, and other coagulase-negative staphylococci (CoNS), assessed via Crystal Violet (CV: non/weak producers and moderate/strong producers) and Congo Red (CR: non slime producers and slime producers) assays. Associations with clinical indications – Holgers score, pain, debris, and overall adverse events – are shown. Significant associations include *S. aureus* with Holgers score >0 ($p = 0.0074$) and slime production with debris accumulation ($p = 0.0114$). ***(b)*** The table shows multidrug resistance (MDR) prevalence, and the bar chart depicts the mean MBEC/MIC ratios for selected antibiotics. Compared with other species, *S. epidermidis,* as biofilm, exhibited significantly higher tolerance to clindamycin (CLI, $p < 0.05$) and linezolid (LZD, $^{**}p < 0.001$). MDR was observed in two *S. epidermidis* isolates (4%). *Abbreviations: NP – non-producers, WP – weak producers, MP – moderate producers, SP – strong producers (Crystal Violet); MBEC – minimum biofilm eradication concentration; MIC – minimum inhibitory concentration; MDR – multidrug resistant; RIF – rifampicin; LEVO – levofloxacin; FUS – fusidic acid; CLI – clindamycin; LZD – linezolid; SXT – trimethoprim-*

*sulfamethoxazole; OXA+ – oxacillin; VAN – vancomycin; FOX – cefoxitin. Statistical significance: *$p < 0.05$; **$p < 0.01$; ***$p < 0.001$.*

The majority of isolates demonstrated strong biofilm-forming ability, which was strain- and species-dependent.

The biofilm-forming ability of the strains was evaluated using both Crystal Violet (CV) and Congo Red (CR) assays. Overall, 67% of isolates were classified as moderate or strong biofilm producers (according to CV), and 65% demonstrated slime production (according to CR). Most *S. aureus* strains produced biofilm and slime (CV: 88%; CR: 100%) and all carried the *ica* operon responsible for polysaccharide intercellular adhesin (PIA)-mediated adhesion.

In *S. epidermidis*, biofilm production was also frequent (CV: 63%; CR: 56%), particularly in ST7 and ST297, which also carried the *ica* operon. Slime production correlated significantly with the presence of visible debris around the abutment ($p = 0.0114$). Patients with increased Holgers scores were predominantly colonised by biofilm-producing (62%) and slime-producing (81%) strains, while no clear association was observed between biofilm formation and reported pain.

Resistance to multiple antibiotics – particularly fusidic acid and tetracycline – was common and increased under biofilm conditions, particularly in *S. epidermidis* clones carrying multidrug resistance genes.

Antimicrobial susceptibility profiling revealed high degrees of resistance, especially to fusidic acid (54% of isolates), with *fusB* and *fusC* resistance genes commonly detected. *S. epidermidis* frequently harboured resistance genes for β-lactams (*blaZ*), tetracyclines (*tetK*), sulfonamides (*dfrS1*), fosfomycin (*fosB*), and macrolides (*msrA*, *mphC*). Two ST88 clonal isolates harboured both the *mecA* and *aadD/ant(9)-Ia* genes, providing resistance to methicillin and aminoglycosides, respectively, and were classified as multidrug resistant (MDR), showing resistance to three or more antibiotics.

MBEC assays demonstrated a marked increase in antibiotic resistance when the clinical strains were grown under biofilm conditions. For fusidic acid, resistance rose from 54% (MIC) to 97% (MBEC), with similarly elevated resistance to clindamycin and linezolid (>90%). MBEC/MIC ratio analysis highlighted significantly enhanced biofilm-associated resistance in *S. epidermidis*, particularly for clindamycin ($p = 0.0165$) and linezolid ($p = 0.0008$).

Both *S. aureus* and *S. epidermidis* isolates exhibited diverse genetics, resistance profiles, and virulence traits, with multiple clones linked to biofilm formation and antibiotic resistance.

The *S. aureus* strains showed diverse genetic and phenotypic profiles, with several clones (ST1, ST5) carrying virulence factors such as enterotoxins, leukocidins, superantigens, and immune evasion genes. All strains were slime producers and carried the *ica* operon. Resistance to fusidic acid was common, particularly in ST1 strains carrying *fusC*.

The *S. epidermidis* strains were genetically heterogeneous, with frequent detection of resistance genes (*blaI*, *fusB*, *dfrS1*, *fosB*, *msrA*, *mphC*, *tetK*, *mecA*), especially in ST88. Phenotypic resistance largely aligned with genotype. Some clones (ST7, ST297, ST278) produced slime via *ica*, whereas others (ST88, ST256) formed biofilms independently of *ica*.

4.3 Paper III

Bone drilling technique plays a key role in the success of implant installation; thus, it is vital to systematically evaluate the mechanical and thermal performance of drills utilised in BAHS site preparation.

The study compared a novel single-step drill system, MONO, with the conventional multi-step MIPS system in terms of mechanical performance, thermal effects, and bone distortion during osteotomy creation for percutaneous BAHS installation. An overview of the results is presented in **Fig. 10**.

MONO drilling generated higher force and torque but demonstrated greater mechanical efficiency at higher feed rates.

The MONO drill produced a gradual rise in both force and torque throughout the drilling depth. Across all feed rates tested (0.5, 1.0, and 2.0 mm/s), MONO drilling generated higher force and torque values than the MIPS WD but comparable or slightly higher than the MIPS GD. Notably, the total mechanical work required to create osteotomy decreased with the shortening of the drill sequence (increased feed rate) in both systems. At the highest feed rate (2.0 mm/s), the total energy required to complete the osteotomy was significantly lower with MONO drilling than with MIPS, suggesting a higher mechanical efficiency for the MONO drill despite creating osteotomy in a single step.

MONO drilling resulted in consistently lower temperature rises than MIPS under most irrigation scenarios.

Across the protocols, both drill systems maintained temperatures below the osteonecrosis threshold. Heat generation increased with reduced irrigation and longer drilling times, particularly with idling. The MONO system was less affected by reduced irrigation, with no significant difference between protocols with and without idling. Overall, temperature variation was higher for the MIPS procedure. Additionally, increasing the feed rate from 0.5 to 2 mm/s significantly reduced heat generation in both systems. At standard protocol, for MIPS, temperature increase dropped from 11.36 ± 1.48°C to 3.35 ± 0.70°C ($p < 0.0001$); for MONO, from 7.08 ± 0.56°C to 2.26 ± 0.47°C ($p < 0.0001$).

Only extreme drilling conditions caused detectable changes in bone composition.

Raman spectroscopy confirmed compositional changes in bone only under protocols with reduced or no irrigation (DP4 and DP5). For MIPS, mineral

crystallinity at the osteotomy site was elevated under no-irrigation conditions. In MONO drilling, the apatite-to-collagen ratio was higher at a greater distance from the osteotomy, and for DP5, the carbonate-to-phosphate ratio also increased at distal points.

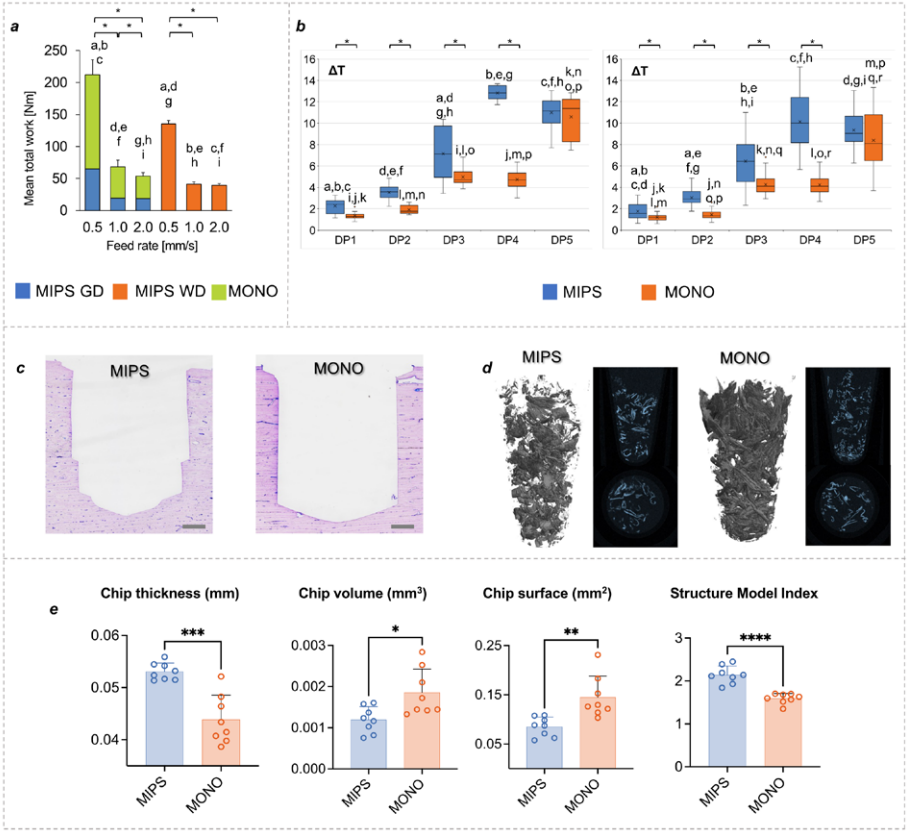

Fig. 10. ***(a)*** Mean total work (Nm) required to create an osteotomy at three feed rates (0.5, 1.0, and 2.0 mm/s) for MIPS Guide Drill (GD), MIPS Widening Drill (WD), and MONO drill. ***(b)*** Boxplots showing the highest mean temperature increase (left) and the mean temperature increase across all probes (right) (ΔT) for each drilling protocol (DP1–DP5). ***(c)*** Light microscopy images of osteotomy cross-sections created by MIPS and MONO drills, stained with toluidine blue, illustrating osteotomy morphology. Scale bars: 400 μm. ***(d)*** MicroCT renderings of bone chips retrieved from drilling, showing qualitative differences in chip morphology. ***(e)*** Quantitative evaluation of bone chips: thickness, volume, surface area, and structure model index (SMI). *Abbreviations: GD – guide drill; WD – widening drill; MIPS – minimally invasive Ponto surgery; MONO – single-step drilling system; DP – drilling protocol; microCT – micro-computed tomography; SMI – Structure Model Index. Statistical significance: *p < 0.05; **p < 0.01; ***p < 0.001; ****p < 0.0001.*

Bone chip morphology differed significantly between systems, with MONO drilling producing more homogenous, plate-like bone chips.

MicroCT and SEM analysis revealed that the MONO drill produced larger, thinner, and more homogenous bone chips with a plate-like morphology, whereas MIPS generated thicker and more variable bone chips. Quantitatively, chips from MONO drilling had significantly greater volume and surface area but lower structural model index (SMI), indicating a flatter geometry. Raman analysis of the bone chips revealed no significant compositional differences between drill types or irrigation protocols.

4.4 Paper IV

A novel, less invasive implantation technique for surface-modified transcutaneous implants was evaluated with respect to surgical feasibility and biological integration, thereby advancing the field of tBCD.

This preclinical study assessed the biological integration of transcutaneous disc-shaped titanium implants with either machined or laser-ablated surfaces, placed either directly on bone (non-recessed) or within a shallow bone recess (recessed). The implants were evaluated after 4 and 13 weeks *in vivo* in a sheep calvarial model using histological analysis and quantitative histomorphometry. The overview of the results is presented in **Fig. 11**.

Laser-ablated surfaces exhibited greater surface roughness and oxide thickness compared to machined controls.

SEM revealed differences in the surface morphology of the implants. Machined implants exhibited smooth concentric grooves, whereas laser-ablated surfaces demonstrated hierarchical topography combining macro- and microscale features. 3D SEM confirmed that laser-ablated implants had greater surface roughness (S_a = 2.18±0.09 μm; S_{dr} = 38.34±3.98%) compared with the machined controls (S_a = 0.54±0.07 μm; S_{dr} = 15.80±1.83%). Auger electron spectroscopy revealed that both surfaces were primarily composed of titanium, oxygen, and carbon, with trace amounts of calcium, phosphorus, and sulphur. The laser-ablated surfaces had significantly thicker oxide layers (13.1 ± 3.2 nm vs. 4.0 ± 0.05 nm, $p < 0.001$) and higher surface titanium content ($p < 0.001$).

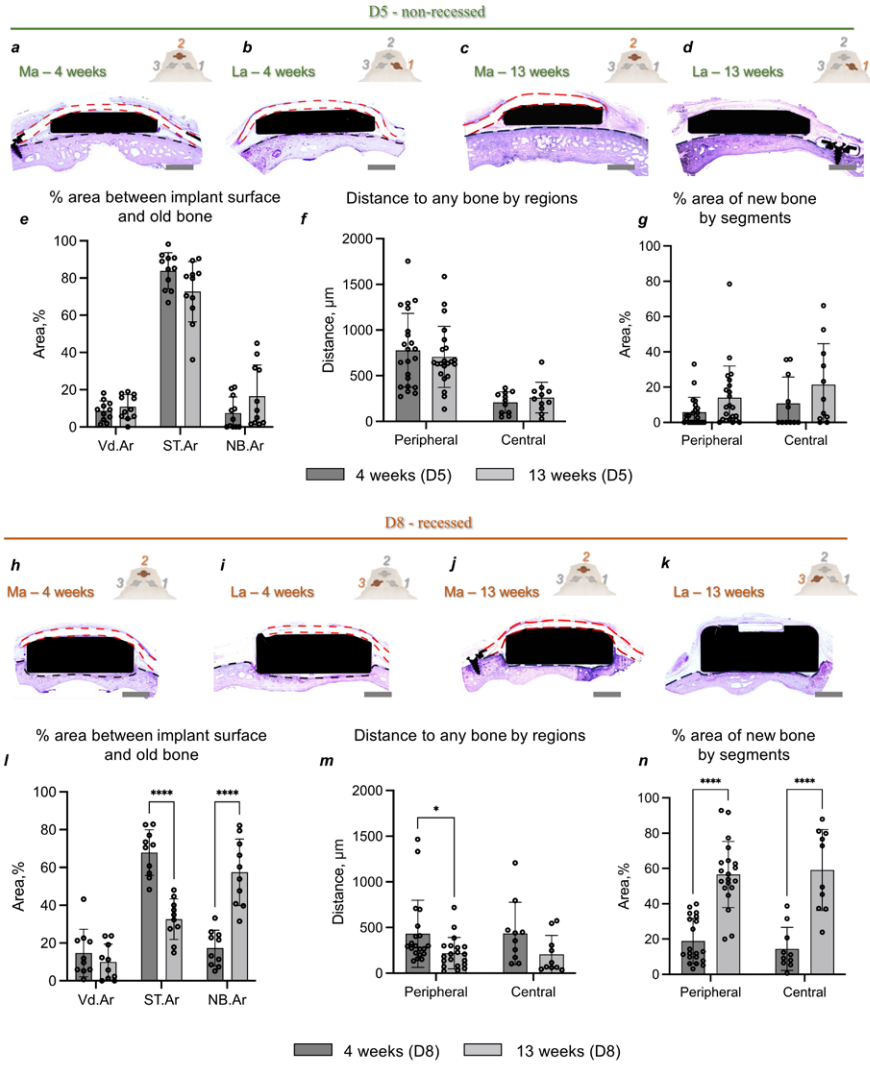

Fig. 11. Representative toluidine-blue sections of **(*a–d*)** non-recessed (D5) and **(*h–k*)** recessed (D8) implants with machined (Ma) or laser-modified (La) surfaces at 4 and 13 weeks; dashed red lines represent fixation band and dashed black line – bone surface. **(*e–g*)** Quantitative outcomes for D5, non-recessed implants: **(*e*)** percentage void (Vd.Ar), soft tissue (ST.Ar), and new bone (NB.Ar) between implant and old bone; **(*f*)** distance to any bone (old + new) by region (peripheral vs central); **(*g*)** segmental NB.Ar (peripheral vs central). **(*l–n*)** Quantitative outcomes for D8, recessed implants: **(*l*)** Vd.Ar, ST.Ar, NB.Ar (showing less ST.Ar and more NB.Ar at 13 weeks); **(*m*)** shorter distance to any bone (particularly peripheral) at 13 weeks; **(*n*)** greater NB.Ar at 13 weeks in both peripheral and central segments. *Abbreviations: Ma – machined surface; La – laser-ablated surface; D5 – non-recessed implant; D8 – recessed implant; Vd.Ar – void area; ST.Ar – soft tissue area; NB.Ar – new bone area. Statistical significance: *p < 0.05; ****p < 0.0001. Scale bars: 4 mm.*

All implants remained clinically stable, with uneventful healing and minimal complications observed.

No adverse tissue reactions occurred after 4 and 13 weeks. However, upon explantation, at 4 weeks, one machined non-recessed implant was found to have a loose fixation screw, and after 13 weeks, one machined non-recessed implant was loose, and two laser-ablated implants were dislocated. Gross examination and histology confirmed uneventful healing in all animals.

Non-recessed implants had higher central bone-to-implant contact (BIC) at 4 weeks, with recessed laser-ablated implants showing more consistent contact at 13 weeks.

Quantitative BIC analysis showed that at 4 weeks, non-recessed implants—particularly laser-ablated discs—had higher central BIC, with values reaching up to 29.1 ± 33.5%. In contrast, recessed implants rarely exhibited measurable BIC at this early stage (5–12.8%). By 13 weeks, the pattern shifted: all recessed laser-ablated implants and one machined disc displayed measurable BIC (mean 15.36 ± 21.74% and 10.46%, respectively). In contrast, only a few non-recessed implants retained limited BIC (2.5–24.8%), again localised mainly to central regions.

Recessed implants demonstrated greater new bone apposition and closer bone proximity than non-recessed implants.

Implant–bone proximity analysis showed that recessed implants had significantly shorter distances to any bone tissue (old + new) than non-recessed controls at both 4 weeks ($p = 0.024$) and 13 weeks ($p < 0.0001$). Surface modification (machined vs. laser-ablated) did not significantly influence proximity at either time point, although by 13 weeks, laser-ablated implants showed a trend toward increased new bone deposition.

Regionally, at 4 weeks, non-recessed implants exhibited closer proximity in the central segment ($p < 0.0001$), consistent with the observed BIC pattern, whereas recessed implants showed no segmental preference due to the flattened bone bed. By 13 weeks, recessed implants demonstrated uniformly reduced implant–bone distances across both central and peripheral regions, reflecting new bone infill within the recess.

Histomorphometric segmentation revealed that recessed implants promoted greater new bone apposition and reduced fibrous tissue infiltration compared with non-recessed implants.

Quantitative tissue composition analysis confirmed that recessed implants exhibited significantly more new bone ($p = 0.044$ at 4 weeks; $p = 0.0435$ at 13 weeks) and less soft tissue encapsulation ($p = 0.0007$ at 4 weeks; $p = 0.0007$ at 13 weeks) compared with non-recessed implants, while void space did not differ between the groups. Segmental analysis further demonstrated that recessed implants supported significantly greater new bone deposition in peripheral regions at 4 weeks ($p = 0.0015$) and in both peripheral and central regions by 13 weeks ($p < 0.0001$).

Generally, by 13 weeks, these trends became more pronounced. Recessed implants exhibited significantly greater amounts of dense, maturing new bone, reduced soft tissue encapsulation, and consistently shorter distances to any bone compared with non-recessed controls. Non-recessed implants, however, showed little progression over time, retaining fibrous tissue infiltration and limited new bone apposition.

Importantly, tighter bone apposition within recesses correlated with greater new bone formation. A significant negative association between implant–bone distance and new bone fraction was observed in recessed implants at 4 weeks ($R^2 = 0.067$, $p = 0.0034$), which became stronger by 13 weeks ($R^2 = 0.2163$, $p = 0.0096$).

Surface modification did not significantly affect tissue composition at either time point, although trends became more evident at 13 weeks.

At 4 weeks, machined and laser-ablated implants exhibited comparable proportions of woven bone, soft tissue, and void space within both recessed and non-recessed groups. By 13 weeks, however, laser-ablated implants in both the recessed (D5) and non-recessed (D8) groups showed a tendency toward increased woven bone area, though differences did not reach statistical significance.

5 DISCUSSION

5.1 Understanding implant success and failure: a holistic perspective

What underlies pain and infection in patients with bone-anchored hearing implants?

Pain has a subjective multifactorial nature, which makes its assessment inherently challenging. In BAHS, it may occur as acute post-operative discomfort or as chronic, localised pain around the abutment. Post-operatively, a commonly used soft tissue status evaluation method is the Holgers score [137], which primarily captures macroscopic inflammation but omits pain. The Inflammation-, Pain- and Skin height/numbness-scale (IPS scale) [138] offers broader coverage, including subjective pain and numbness, wound healing, and non-inflammatory changes, and may be a more comprehensive tool for post-implant assessment of pain. Nevertheless, pain is often a decision-making factor in the long-term use of percutaneous and transcutaneous implants and can ultimately lead to implant retrieval. In clinics, it is documented heterogeneously, described as a *chronic* [108,109,140], *intolerable burning sensation* [107], or simply as *persistent* and *idiopathic* [103,140]. In addition, unrecorded analgesic use could further confound interpretation.

In **Paper I**, we found that chronic localised pain was one of the main indications for elective implant removal and often co-occurred with infection, although the causal relationship between the two remains unclear. At the tissue level, the presence of an abutment disrupts the "steady state" of cutaneous immunity. Whereas intact skin over submerged fixtures shows sparse leukocyte infiltration, introduction of a titanium abutment doubles this cellularity and shifts it toward antigen-presenting immune cells and B-cells [117,158]. In our study, histological evaluation confirmed this disruption, showing dense immune infiltrates surrounding implants, consistent with prior reports [117,158]. Similarly, recent analyses of peri-abutment fluid and soft tissue biopsies, conducted in the same patient cohort from **Paper II**, have demonstrated prolonged inflammatory activity, upregulation of local immune responses, and ongoing tissue remodelling around the abutment following BAHS implantation [36,38]. These studies reported elevated expression of inflammatory cytokines (IL-8, IL-1β, IL-10) and bacteria-associated toll-like receptors (TLR2, TLR4) at 3 and 12 months compared with baseline implant surgery.

Another important discovery in the study [**Paper I**] was the association between *Staphylococcal* colonisation and pain. In cases where *S. aureus* was present, infiltrates rich in iNOS/CD3/CD20, phenotypically resembling those described in *S. aureus*–colonised atopic dermatitis lesions, were detected [159]. In contrast, the samples retrieved from a patient colonised by *S. epidermidis* and *S. capitis* exhibited

milder tissue reactions, which is consistent with the frequently commensal, skin-protective role of *S. epidermidis* [160]. However, this patient was fitted with a transcutaneous device, hence there was no skin-penetrating abutment.

Recent evidence suggests that staphylococcal infection can indirectly modulate the skin immune environment, triggering the release of calcitonin gene–related peptide (CGRP) from cutaneous sensory fibres, particularly T lymphocytes, under both steady-state and pathological conditions [161]. Additionally, virulence factors such as α-haemolysin and phenol-soluble modulins directly activate nociceptors [162,163]. However, in our subset of samples (Paper **I**), CGRP immunoreactivity was observed in only one *S. aureus*–positive case with pain, suggesting that, when the peri-implant niche is dominated by *S. aureus,* nociception may not always be CGRP-dependent. Interpreting pain data remains inherently complex, as nociception is a subjective experience. While Visual Analogue Scale provide a numeric measure, they capture only a transient perception influenced by factors such as mood and expectation [164]. Additional confounders, including unrecorded use of nonsteroidal anti-inflammatory drugs or opioids, may further obscure associations between microbial colonisation, histological findings, and reported pain. Consequently, the inconsistent detection of CGRP does not rule out a neurogenic component. Future investigations should combine multidimensional pain assessments with broader neuro-immune profiling (e.g., substance P, β-endorphin, nerve growth factor) to better characterise the molecular pathways underlying peri-implant pain. It is also important to acknowledge the limited number of available soft tissue samples in **Paper I**, which restricts the possibility of drawing strong conclusions or making broad generalisations.

Paper II further explored the role of the microbiome in soft tissue outcomes within a single clinical centre. Core genome multilocus sequence typing (cgMLST) revealed that patients often remained colonised by the same clone across sites and time points for up to 1 year post-implantation, indicating long-term colonisation or low-grade subclinical infection. *S. aureus* colonisation was significantly associated with higher Holgers scores, reflecting its strong pro-inflammatory potential [137]. This aligns with *S. aureus'* arsenal of virulence factors—including *scn* and *sak* (human-specific immune modulators) [165], leukocidins lukD/E, and enterotoxins—which enable persistent inflammation and keratinocyte invasion [166]. In contrast to **Paper I**, in this subset of patients, *S. epidermidis* colonisation was more often associated with post-operative pain than with overt inflammation, consistent with its role in subacute or chronic biomaterial-related infection [142,167-169]. This discrepancy may, however, be explained by differences in pain assessment, as **Paper I** relied on case reports from a cohort of electively retrieved implants, while **Paper II** systematically captured postoperative pain using standardised clinical scales. Although usually regarded as a commensal, *S. epidermidis* is also an opportunistic pathogen and a leading cause of periprosthetic

joint infections due to its strong biofilm-forming capacity [168]. Certain clones can exacerbate skin inflammation via cysteine protease production, highlighting the dual commensal and pathogenic potential [18].

Furthermore, **Paper II** demonstrated that the ability to form biofilms *in vitro* was widespread among the study subjects, with rates of 88–100% in *S. aureus* and 56–63% in *S. epidermidis* among the patients. The *ica* operon, central to polysaccharide intercellular adhesin (PIA)-mediated biofilm synthesis, was detected in all *S. aureus* isolates and in several *S. epidermidis* clones (ST7, ST297, ST278), suggesting that other clones relied on alternative mechanisms. Clinically, slime-producing strains correlated with peri-abutment debris, higher Holgers scores, and soft tissue complications. Biofilm formation also led to increased antimicrobial resistance, mirroring findings from orthopaedic device-related infections and highlighting the persistent challenge of treatment failure in BAHS [142,167-169]. Similarly, biofilm formation has been documented for cochlear implants, with *S. aureus* frequently implicated, further underscoring the role of biofilms in implant-related infection [170-172].

Are current clinical practices effective in targeting infection in BAHS?

In **Papers I** and **II**, antibiotics were used both prophylactically and for managing soft tissue complications. While antimicrobial resistance could not be assessed in **Paper I** due to the limited number of retrieved isolates, **Paper II** provides a detailed characterisation of the antimicrobial susceptibility of the BAHS-associated staphylococci.

A key concern identified in the cohort was the prevalence of fusidic acid resistance (FUS^R), detected in 54% of all bacterial isolates and in 72% of *S. epidermidis* isolates. This resistance pattern is likely linked to the widespread use of fusidic acid ointments as part of routine aftercare at the clinic where the study was conducted. Correspondingly, FUS^R genes (*fusB*, *fusC*) were frequently identified, and tolerance to fusidic acid increased dramatically under biofilm conditions (minimum biofilm eradication concentration, MBEC: 97% FUS^R). FUS^R shows considerable variability across infection settings, with rates of 0.3–52.5% for *S. aureus* [173-177] and 7.7–46% for *S. epidermidis* [178,179]. At a dermatology clinic in the UK, similarly high FUS^R in *S. aureus* led to initiatives aimed at reducing fusidic acid ointment use [180,181].

Resistance was not limited to fusidic acid. Tetracycline resistance genes were identified in 11% of *S. aureus*, 34% of *S. epidermidis*, and 11% of other CoNS. Notably, all patients in this cohort received prophylactic treatment with hydrocortisone–oxytetracycline ointment for up to 7 days post-surgery, suggesting that routine prophylaxis may contribute to resistance development.

This finding highlights the risks associated with prophylactic topical antibiotic use on antimicrobial resistance (AMR) evolution.

In addition to acquired resistance driven by clinical antibiotic use, biofilm formation substantially increased antimicrobial tolerance. The MBEC/MIC ratios demonstrated a striking increase in resistance levels under biofilm conditions, reaching 97% for fusidic acid, 92% for clindamycin, and 95% for linezolid. Particularly concerning was the high prevalence of rifampicin resistance—an antibiotic often regarded as an effective anti-biofilm agent—which was markedly higher in this cohort than in patients with periprosthetic joint infections [142,143]. These findings strongly suggest that conventional antibiotic regimens may be inadequate for managing BAHS-associated infections, especially in patients with adverse soft tissue responses such as pain, debris, and chronic inflammation. Addressing this challenge will require biofilm-targeted strategies, including rational antibiotic combinations and the development of biofilm-disrupting adjunctive therapies. Moreover, *S. epidermidis* displayed higher multidrug resistance than *S. aureus*, and frequently carrying multiple antimicrobial resistance genes—indicating a potential for treatment failure, which is in line with observations from other clinical contexts.

Taken together, **Papers I** and **II** suggest that pain, inflammation, and infection with BAHS are interrelated rather than separate complications. They arise from interactions between host immunity, microbial colonisation, and biofilm activity at the tissue–implant interface. These findings highlight the need to integrate clinical, histological, and microbiological assessments—beyond macroscopic inflammation scores alone—to capture the full spectrum of patient symptoms and tissue responses. The findings also align with experience from cochlear implants, where idiopathic pain and infection are among the leading causes of implant removal [182-185]. The bacterial species most commonly implicated include *S. aureus*, *S. epidermidis*, and *Cutibacterium acnes*.

5.2 Drilling the bone and its implications

What drives the efficiency and safety of osteotomy creation in bone?

The interaction between microbial factors and host tissue responses cannot be considered in isolation from the surgical trauma that initiates the peri-implant environment. While **Papers I** and **II** did not allow direct evaluation of surgical technique or drill systems—due to cohort heterogeneity in **Paper I** and the standardised use of MIPS in **Paper II**—these aspects were explored in **Paper III** using controlled *ex vivo*/*in vitro* methodologies. There, factors such as drill mechanics, thermal transfer to surrounding bone, and osteotomy geometry were

systematically assessed to clarify how drilling influences the conditions for implant integration.

Cutting efficiency

Unlike the minimally invasive Ponto surgery (MIPS) protocol, which requires two sequential drilling steps, the MONO system creates the full osteotomy in a single step while still maintaining force and torque within clinically acceptable limits. Importantly, MONO drilling required less total energy, indicating greater cutting efficiency.

One concern with higher feed rates and increased bone removal volumes is chip clogging, which can rapidly elevate torque and force [186]. In this study, maximum force and torque increased gradually with feed rate for all drills. No clogging was observed with MONO, even at the highest tested rate (2 mm/s). This may be explained by the osteotomy's shallow depth (4.75 mm) and the drill's design, which provides greater space for chip evacuation.

The performance of the MONO drill appears to stem from its geometry: less metal is in contact with the osteotomy wall during cutting and increased space for chip evacuation, reducing friction and energy demand [187]. While excessive friction can damage drill edges and impair cutting capacity [188], the MONO drill exhibited a more gradual torque increase compared with the sharper rise observed with MIPS drilling. Total work required for osteotomy creation also decreased as feed rate increased, particularly when drilling time was shortened from ~9.5 s at 0.5 mm/s to 4.8 s at 1 mm/s, with only marginal gains at the highest rate (2 mm/s).

Heat generation

Metal machining studies demonstrate that during drilling, most heat dissipates through chip evacuation rather than drill–substrate transfer [189,190]; therefore, efficient removal of hot chips is crucial for limiting bone heating. In this study, we showed that despite removing the entire osteotomy volume in a single-step, MONO drilling generated less heat than MIPS, which is in contrast to the dogma that a multi-step drilling procedure is needed to limit heat generation. This is likely due to its design, which provides greater flute space for chip evacuation and irrigation exchange while reducing drill–bone contact. In support of this finding, earlier reports indicated that single-drill protocols can yield lower temperatures than multi-step approaches when chip evacuation is efficient [191,192], whereas poor flute clearance or guided systems may increase frictional heating [193].

Drilling energy—the total work required to create an osteotomy—directly correlates with thermal output. In both systems, higher feed rates reduced energy

consumption and thereby heat generation, consistent with mechanical data and prior work [194-196]. Even though a higher feed rate increases the shearing force required to cut the bone, the drilling sequence is completed in a shorter time, leaving less time for heat generation and heat transfer.

Still, cooling efficacy remains critical. In guided systems, irrigation can be less effective due to limited fluid penetration and added drill–guide friction [197-199]. While both systems showed increased temperatures under reduced irrigation, MONO drilling demonstrated greater robustness. Since osteotomy is performed manually and operator technique varies, a system less sensitive to procedural deviations offers clear clinical advantages. Evidence from studies comparing the original MIPS protocol with the modified MIPS version further highlights that drill design directly influences heat generation [36,65].

Bone is known to tolerate drilling temperatures up to ~47–55 °C for less than one minute before necrosis occurs [200-202]. Although external irrigation mitigates thermal injury [203], some studies suggest that brief exposures above this threshold do not always result in permanent damage [204]. Among the tested protocols, differences in bone composition were most evident in reduced- or no-irrigation conditions, which produced the highest heat. In these cases, MIPS sites exhibited greater mineral crystallinity, whereas MONO sites retained more organic content, possibly reflecting selective phosphate loss and preserved collagen [84,203]. In this study, temperatures were recorded 0.5 mm from the osteotomy wall, and peak values at the interface may have been higher.

Finally, thermal effects may extend to the bone chips produced during drilling. While manufacturer protocols recommend flushing chips after each step [205], several studies argue that retaining viable bone chips may enhance osseointegration [206,207]. However, avoiding flushing can also increase local temperatures, as demonstrated in Paper III and by Johansson et al. (2019) [53], indicating that a threshold likely exists. The biological role of retained chips remains to be clarified, and their potential contribution to bone healing warrants further investigation.

5.3 Percutaneous and transcutaneous systems as complementary solutions

Osseointegration

What is the impact of implant design on osseointegration in percutaneous BAHS?

The evolution of BAHS spans not only different surgical procedures but also implant designs. In **Paper I**, we had the unique opportunity to examine retrieved implants with surrounding tissues from patients with BAHS, with durations *in situ* ranging from as little as 12 months to over 15 years. This enabled analysis across a broad spectrum of implant designs, reflecting the technological evolution of percutaneous BAHS. Histological and structural assessments revealed varying degrees of osseointegration across the three design groups (Ø4.5 mm machined surface, Ø4.5 mm blasted surface, Ø3.75 mm machined and laser-ablated BHX surface implants), yet no statistically significant differences were observed. Most implants exhibited substantial bone-to-implant contact, even in cases where pain or infection were reported.

Across all implant designs, considerable variability in bone marginal level relative to the implant flange was observed, with a consistent absence of bone beneath the flange—a finding in agreement with previous reports [109,208-212]. The pattern, progression, and underlying causes of marginal bone loss in dental implants have been extensively debated. The proposed mechanisms include bone resorption secondary to inflammation or infection, stress concentration at the implant–bone interface, incomplete implant insertion, and biofilm-related factors such as plaque accumulation and bacterial load [213]. While these discussions provide valuable insights, the exact aetiology remains unresolved. Importantly, although BAHS and dental implants both rely on stable osseointegration for function, their anatomical location and the surrounding molecular and microbiological environment differ considerably, limiting the validity of direct comparisons.

Transcutaneous implants

What does the future of transcutaneous bone conduction devices look like?

In much of the literature, transcutaneous systems are often presented in opposition to percutaneous solutions. Yet, they are not interchangeable and may not suit all patients—for example, those requiring stronger sound transmission, limited by bone thickness, or with specific preferences regarding sound quality and device management. Rather than viewing one as a replacement for the other, both solutions should be considered as complementary options, each addressing

distinct clinical needs. Selection must account for surgical factors and patient-specific characteristics and preferences, and although long-term data on transcutaneous implants are still emerging, both systems clearly retain an important role. Comparisons between the two are, nonetheless, valuable, as they expand the candidacy and allow insights from one system to inform improvements in the other.

In **Paper IV**, we built on two established trends from percutaneous systems—simplifying the implantation procedure through less invasive techniques (comparing recessed versus non-recessed placement) and incorporating surface modification—and applied them to the transcutaneous context, contributing to the ongoing evolution of this technology. While some transcutaneous bone conduction devices (tBCD) still depend on direct bone-to-implant contact (BIC), prior studies have shown that osseointegration is not essential for effective sound transmission [91,214]. However, passive transcutaneous systems, where the transducer is fully integrated into an external processor, reveal that the overlying skin attenuates vibration transfer [11]. Thus, reducing fibrous tissue interposition beneath transcutaneous implants may be critical for maintaining vibration fidelity and preventing a gradual decline in hearing performance.

Paper IV showed that although the mean distance to native bone did not differ between recessed and non-recessed implants at either 4 or 13 weeks, recess creation markedly altered the peri-implant environment. Recessed implants exhibited significantly greater new bone deposition and reduced soft tissue infiltration, with differences becoming more pronounced by 13 weeks. These implants also showed closer proximity to any bone (old or new), emphasising the role of new bone apposition. The enhanced bone formation within the recess supports the hypothesis that surgical preparation—such as periosteal elevation and cortical "scrubbing"—acts as a local osteogenic stimulus [215,216]. By elevating the periosteum and creating a defined defect, recess preparation not only introduces mechanical cues but also bleeding, which is a central driver of bone repair and remodelling [217,218].

Segmental analyses further revealed that recessed implants promoted more bone formation primarily in peripheral zones at 4 weeks, and in both peripheral and central zones by 13 weeks, suggesting that deposition is stimulated by load transfer or micro-motion at the implant margins. The significant negative correlation between bone–implant distance and new bone fraction in recessed implants supports this interpretation, indicating that reduced separation facilitates bridging.

By contrast, non-recessed implants maintained central BIC at early time points with little peripheral bone formation, likely reflecting mechanical loading from

the fixation band and soft tissue infiltration. At 13 weeks, measurable BIC persisted in only a few of the non-recessed implants, and the new bone area did not significantly increase. This pattern aligns with evidence that physiological loading promotes osteocyte-mediated signalling, osteoblast differentiation, and bone deposition [166,219,220], particularly through periosteal-related mechanisms [221]. Similarly, studies on osteoinductive bioceramics have shown substantial bone formation beyond the skeletal envelope in dome-shaped implants, even with the periosteum intact [222,223]. Although only a single point of contact is theoretically sufficient for vibration transmission, the mechanical stability of the implant remains essential. Excessive mobility or wobbling would compromise function and risk tissue irritation. Therefore, less invasive anchoring mechanisms or even minor surface scraping may be alternative strategies to provide sufficient mechanical interlocking and ensure stability without requiring extensive bone engagement.

Unlike screw-shaped implants, where laser ablation enhances osseointegration [29,224,225] , the transcutaneous disc model showed minimal surface-related effects in early healing, likely due to the small bone-contact area and the dominant influence of recess preparation. By 13 weeks, however, preliminary surface-dependent differences emerged: most recessed laser-ablated implants demonstrated BIC, and both non-recessed and recessed discs showed a trend toward greater new bone area compared with machined controls. This suggests that as implant–bone proximity increases over time, surface topography may exert a greater influence. Previous rabbit tibia studies support this, showing that roughened surfaces improve implant retention, with pull-out force correlating with as arithmetic mean height of the surface S_a up to an optimal threshold of ~3.6–3.9 μm [98,99,226]. The laser-modified discs in this study had an S_a of 2.18 ± 0.09 μm, a roughness associated with improved retention and potentially supportive of long-term stability.

Overall, the data indicate that while recess creation is more invasive and surgically demanding, it consistently enhances new bone ingrowth and reduces fibrous encapsulation. Conversely, the non-recessed approach is technically simpler and allows for some early BIC, but this is progressively replaced by fibrous tissue, with limited bone apposition over time. Surface modification effects appear modest in the early phase but become more evident at later stages, particularly when bone–implant proximity is improved.

5.4 Methodological considerations and limitations

Understanding complications and long-term outcomes of BAHS and tBCD requires an approach that goes beyond any single experimental technique or model. Retrieval analyses, performed in **Paper I**, provide invaluable insights into

how implants integrate in the human biological environment over time, revealing histological changes, inflammatory patterns, and evidence of microbial colonisation. Microbiological profiling in **Papers I** and **II** allowed us to identify the common bacterial species, antibiotic resistance profiles, and biofilm properties that influence infection and inflammation. In **Papers III** and **IV**, surgical evaluations—from *ex vivo* drilling studies to cadaveric and preclinical models—helped clarify the mechanical and thermal variables of osteotomy creation as well as the biological environment around implants. However, these findings are not without limitations.

Paper I was the largest retrospective multicentre case series to date of electively retrieved percutaneous implants, yet the cohort was highly heterogeneous. There was a broad range of implantation time (1-15 years). While this diversity increases the generalisability of the findings, it complicates broad comparisons across cases. Patient-specific factors such as diabetes, prior radiotherapy, smoking, or neurodevelopmental disorders were not systematically analysed in relation to tissue responses, limiting the ability to attribute outcomes to host-related factors. Furthermore, differences in retrieval procedures across centres constrained the number of implants retrieved with complete soft tissue, bone, and microbiological data. Longitudinal information on pain progression or resolution following explantation was also inconsistently available, restricting insights into symptom trajectories after device removal.

Paper II was limited by the relatively small cohort size and incomplete follow-up, as not all patients attended both the 3- and 12-month assessments. This restricted, in some cases, the ability to capture the temporal dynamics of staphylococcal colonisation, and characterisation of biofilm-forming ability, and AMR. In addition, multiple bacterial strains were sometimes isolated from the same patient, but potential synergistic or competitive interactions between strains were not assessed. Consequently, the attribution of clinical outcomes to specific isolates may oversimplify the underlying microbial ecology.

Paper III evaluated drilling systems in *ex vivo* and *in vitro* models, providing controlled mechanical and thermal measurements that cannot be ethically or practically obtained *in vivo*. While these experiments demonstrated the relative performance of MIPS versus MONO drilling, the conditions remain simplifications of clinical reality. The use of bovine bone and synthetic bone blocks differs in density, vascularity, and thermal conductivity from human temporal bone, limiting direct extrapolation of findings.

Paper IV was performed in a sheep calvarial model and carries important limitations. Analysis was restricted to two time points (4 and 13 weeks), precluding evaluation of long-term osseointegration, interface maturation, and implant stability. Functional outcomes, such as vibration transmission for recessed versus non-recessed implants, were not tested. Moreover, the sheep skull does not perfectly replicate the anatomy or biomechanics of the human temporal bone, and the modest sample size—chosen to minimise animal use—reduces statistical power and generalisability. Nonetheless, by directly comparing recessed and non-recessed surgical techniques and clinically relevant implant designs within the same animals, inter-animal variability was minimised, and detailed region-specific histomorphometric analyses were possible. These data provide a valuable foundation for the further refinement of tBCD systems.

The combination of these methodologies can therefore generate a much more robust framework than any technique in isolation. However, integrating multiple approaches inevitably increases complexity and raises challenges in clinical translation. A key question is how to balance experimental depth with clinical practicality. For example, while advanced microbiological assays such as MBEC testing provide valuable insights into biofilm antibiotic tolerance, their implementation in daily clinical workflows remains limited. Similarly, retrieval studies are rare and depend on coordinated networks of hospitals that are willing to collect and share materials systematically.

Ultimately, prioritisation is required: which surgical, diagnostic, and therapeutic interventions offer the greatest impact on patient care? Standardised pain and soft tissue scoring systems, coupled with consistent microbiological sampling, may be the most immediately applicable measures to integrate into clinical protocols. Meanwhile, *ex vivo* and animal models remain essential for preclinical testing of new surgical approaches and implant designs. By strategically combining methodologies, we can bridge the gap between experimental findings and clinical decision-making, ensuring that advances in BAHS research are justified ethically and translate into safer, more reliable outcomes for patients.

5.5 Translational aspects

The research questions addressed in this thesis are patient-centred, making them directly relevant and translatable to clinical practice. Some findings are rooted in retrospective and case series studies, while others are derived from preclinical investigations, together providing a continuum of knowledge from the bench to the bedside.

From **Papers I** and **II**, the importance of systematic microbiological sampling became evident, particularly in patients with severe symptoms that resulted in elective implant retrieval. These studies explored the role of biofilms and AMR in adverse clinical outcomes and revealed their connection to routine treatment practices. Currently, no consensus or clinical guidelines exist on whether peri-abutment bacterial sampling should be performed or how such results should inform antimicrobial treatment in BAHS. Consequently, clinicians lack standardised, evidence-based protocols for case management, and the evaluation of clinical status remains inconsistent, highlighting the need for validated assessment tools. Recommendations should be formulated through close collaboration between clinicians, researchers, and industry partners, following the model established by the International Consensus Meeting on Periprosthetic Joint Infection (ICM, https://www.icmortho.org/), which emphasises multidisciplinary consensus-building based on current evidence and expert opinion.

In **Paper III**, we evaluated a single-step drill system, MONO, as a prerequisite for clinical use, comparing it with the system already established in practice, and validated standardised *ex vivo* and *in vitro* techniques for assessing drilling performance. This work demonstrates how preclinical models of mechanical and thermal performance can provide a framework for evaluating future drilling systems before patient implementation.

Finally, **Paper IV** represents a critical step in translating the accumulated knowledge from percutaneous implant evolution into the field of transcutaneous systems. By demonstrating how surgical bone preparation influences tissue integration, this study lays the groundwork for future clinical applications and guides the ongoing refinement of transcutaneous implant design and surgical protocols. In this way, **Paper IV** serves as a bridge between experimental innovation and clinical practice, supporting the long-term goal of developing less invasive, more reliable, and patient-centred BAHS solutions.

6 SUMMARY AND CONCLUSIONS

This thesis contributes to the field of bone-anchored hearing systems (BAHS) by addressing key clinical, microbiological, and surgical questions through a combination of complementary methodologies. Central to this work were three overarching themes: the role of bacteria and adequacy of current treatment strategies; the safety and efficiency of simplified drilling procedures; and the future evolution of transcutaneous bone conduction systems (tBCD).

Paper I presented the largest cohort to date of retrieved percutaneous BAHS, identifying pain and infection as the most common reasons for implant removal. Importantly, implant survival did not consistently align with histological osseointegration, underscoring the complexity of interpreting patient-reported outcomes in relation to tissue integration.

Paper II correlated bacterial colonisation—most notably by *Staphylococcus aureus* and *Staphylococcus epidermidis*—with patient symptoms and peri-abutment tissue status. It indicated that biofilm formation and antimicrobial resistance are major contributors to soft tissue complications and should be central considerations in future treatment strategies.

Paper III compared the single-step MONO drill system to conventional clinically used multi-step protocols. It showed how drill geometry, torque, and irrigation influence mechanical forces, heat generation, and bone preservation, with direct implications for surgical safety and drilling efficiency.

Paper IV translated knowledge from percutaneous to transcutaneous systems by introducing a laser-modified surface and comparing recessed versus non-recessed implantation in an ovine model. Findings revealed that bone recess preparation, rather than surface modification, was the main determinant of early bone formation and reduced fibrous encapsulation—though this benefit came at the cost of greater surgical invasiveness.

Altogether, the work presented in this thesis shows that pain, infection, and biofilms constitute central challenges in BAHS and tBCD. At the same time, surgical technique and drilling protocols play a pivotal role in osseointegration and long-term implant stability. Insights from percutaneous implants are needed to inform the refinement of transcutaneous devices, as soft-tissue complications continue to pose limitations. Collectively, this work provides an evidence base for optimising implant design, improving surgical procedures and diagnostics, and informing both therapeutic strategies and the development of next-generation

BAHS—aimed at greater longevity, fewer complications, and more patient-centred outcomes.

7 FUTURE PERSPECTIVES

This thesis addresses a broad spectrum of research questions related to percutaneous and transcutaneous bone conduction devices. While the findings are complementary, they also point to several important avenues for future investigation.

Standardisation and registries

In **Paper I**, retrieval analyses provided unique insights into implant–tissue interactions in cases of severe complications. However, the lack of standardised protocols limits comparability across studies. Establishing harmonised procedures for retrieval analyses and consistent documentation of pain, inflammation, and infection would enable more robust comparative research. On a broader scale, the development of registry systems for hearing implants, including both bone-anchored and cochlear devices, could further advance the field by building cumulative knowledge, informing patient candidacy, and identifying risk factors for complications. Future work should define which clinical, surgical, and patient-reported parameters such registries must capture to be most effective.

Microbiome, biofilms, and clinical guidelines

Papers I and **II** highlighted the role of the microbiome, biofilm formation, and antimicrobial resistance in peri-implant complications. These findings stress the need for consensus guidelines on clinical management and hygiene care for bone-anchored hearing system (BAHS) recipients. Comparative studies across treatment centres could help identify best practices, while interventional studies may clarify the impact of structured patient instruction on reducing soft tissue complications. Ultimately, collaborative efforts should translate microbiological findings into practical recommendations for clinicians.

Data, prediction models, and antimicrobial stewardship

Larger multicenter studies could provide the statistical power needed to generate predictive models, identifying patients at higher risk of complications and tailoring treatment strategies accordingly. Given the global rise in antimicrobial resistance, future research should also monitor the environmental and clinical impact of routine antibiotic use in BAHS management. At the same time, the integration of antimicrobial biomaterials into implant design may offer promising preventive strategies.

Surgical innovation and implant design

The less invasive surgical approaches explored in **Papers III** and **IV** lay a foundation for simplifying BAHS procedures and expanding access to patients who may benefit from the treatment. Our *in vivo* study on modified transcutaneous implants also opens the debate on whether osseointegration is an absolute prerequisite for bone conduction. Further work is needed to determine whether retaining autologous bone chips in osteotomies may enhance osseointegration in screw implants and to explore how both percutaneous and transcutaneous implant designs can be refined for improved stability, reduced complications, and easier surgical handling.

ACKNOWLEDGEMENTS

When my friends used to say, *"A PhD is hard,"* and I saw them struggling, I thought I understood what they meant. In reality, I didn't. Doing a PhD is often an isolating journey that requires a great deal of human support, and to understand that, you actually need to go through it. It would take me hours to name everyone who has helped me during these four years, but I will try to do so in this section.

This PhD gave me a unique opportunity to work, learn, and contribute to the field of translational research, on a subject that directly helps people. This has been a major source of motivation for me and has also shaped the way I now approach scientific questions. I would call it *people-oriented research*, and I feel privileged to have been part of it. Along the way, I was supported by wonderful people, my supervisors: Martin Lars Johansson, Anders Palmquist, Margarita Trobos, and Peter Thomsen. I thank them all for being there for me, for deepening my research, sharing their expertise, and allowing me to grow independently. Thank you, Martin, for your knowledge, conversations, encouragement, and support in helping me stand on my own. From the very first moment you made me feel welcomed, and you were one of the main reasons I chose to pursue this PhD, a decision I have never regretted. Thank you, Anders, for your guidance, humor, and memorable trips to Daegu, Östersund, and Lyon. I hope that one day my understanding of Småländska will be good enough to fully appreciate your jokes. Thank you, Margarita, for turning me into a microbiologist in just about a year, for trusting me, being patient, and always giving thoughtful advice and feedback. Finally, thank you, Peter, the most knowledgeable person about Kazakhstan I have met abroad. We Kazakhs truly appreciate that. Thank you for sparking stimulating discussions, for teaching and supporting me—at times that support meant more than anything else.

I am deeply grateful to Lena Emanuelsson, Maria Hoffman, Birgitta Norlindh, Rose Maria Tschina and Anna Johansson-Loo. Without you, this thesis would not have come to life. You are the heart of the lab, your smiles, jokes, anfd warmth made us feel at home despite being far from the family. Thank you, Furqan Ali Shah, Farah Asa'ad, Reza Mokhtari and Christer Dahlin for all the nice discussions.

I am sincerely thankful to my colleagues at Oticon Medical, Thomas, Alfred, Anton, Emelie, and Nicole, for their support and collaboration. Whether we worked closely or only occasionally, your help and companionship were always

invaluable. I am equally thankful to my bachelor's and master's research supervisors, Dana Akilbekova, Sahar Salehi, Jianhua Zhang, and Cevat Erisken, for introducing me to the field of biomaterials science and setting me on this path.

My heartfelt gratitude goes to my dear friends and colleagues, Martina, Liliana, Heithem, Paula, Adam, Jincy, Chiara, Ana, and Nesrin, for standing by my side throughout this journey and making sure I not only survived but thrived. Martina and Lili, you truly are the light of my eyes; your hugs, smiles, and kindness carried me through many difficult days. Heithem, your feedback and support were invaluable, and it was a privilege to share an office with you. Adam, Paula, Jincy, and Chiara, I am grateful for the wonderful moments we shared, and I feel lucky to call you my friends. Ana, thank you for always being there and for working with Lena and Birgitta on my final histological sections during precious summer days in Gothenburg. And to Nesrin, thank you for the great hangouts and for helping me with the last-minute revisions of this thesis.

Last but not least, I want to thank my family and friends for their constant presence and encouragement. Nika, Aidana, Balu, Alina, Rollan, Martin, Dima, and Kevin, thank you for checking in on me and being there when I needed support. I am also grateful to Sabina, Arina, Ada, and Olesya for their kindness, and to Sabina A., Nera, Jax, Adam, Joshua, Viktor, and Isay for bringing variety into my days and helping me step away from science when I needed a break.

And to my parents and brothers, thank you for supporting me along this journey, for being there when I needed you most, and for asking once in a while with genuine curiosity: *"So, what is your project about?"*

This industrial PhD project was funded by the Swedish Foundation for Strategic Research (SSF; Industrial Doctoral Student funding ID20-0091, https://strategiska.se/en/) and the William Demant Fund (Case no. 20-1587, https://www.williamdemantfonden.dk/) and supported by Oticon Medical AB, Sweden. Additional funding was provided by the Swedish Research Council (2020-04715, 2022-00853), the Swedish State under the agreement between the Swedish Government and the county councils (the ALF-agreement; ALFGBG-725641, ALFGBG-1005762), Handlanden Hjalmar Svensson Foundation, Adlerbertska Forskningsstiftelsen, the IngaBritt and Arne Lundberg Foundation, Sylvan Foundation, and the Area of Advance Materials of Chalmers and GU Biomaterials within the Strategic Research Area initiative launched by the Swedish Government. Oticon Medical AB also provided support in the form of salary for MLJ but had no role in the study design, data collection and analysis, decision to publish, or preparation of the manuscripts and thesis.

REFERENCES

1 World Health Organization (WHO). *Global estimates on prevalence of hearing loss*, <http://www.who.int/pbd/deafness/estimates/en/ [cited 2025 May 27].> (2018).

2 Stenfelt, S. & Goode, R. L. Bone-conducted sound: physiological and clinical aspects. *Otol Neurotol* **26**, 1245-1261 (2005). https://doi.org/10.1097/01.mao.0000187236.10842.d5

3 Bento, R. F., Kiesewetter, A., Ikari, L. S. & Brito, R. Bone-anchored hearing aid (BAHA): indications, functional results, and comparison with reconstructive surgery of the ear. *Int Arch Otorhinolaryngol* **16**, 400-405 (2012). https://doi.org/10.7162/S1809-97772012000300017

4 Reinfeldt, S., Hakansson, B., Taghavi, H. & Eeg-Olofsson, M. New developments in bone-conduction hearing implants: a review. *Med Devices (Auckl)* **8**, 79-93 (2015). https://doi.org/10.2147/MDER.S39691

5 Tjellstrom, A., Lindstrom, J., Hallen, O., Albrektsson, T. & Branemark, P. I. Osseointegrated titanium implants in the temporal bone. A clinical study on bone-anchored hearing aids. *Am J Otol* **2**, 304-310 (1981).

6 Calon, T. G. A. *et al.* Percutaneous bone-anchored hearing system implant survival after 550 primary implant surgeries. *Clin Otolaryngol* **43**, 735-739 (2018). https://doi.org/10.1111/coa.13036

7 Lagerkvist, H. *et al.* Ten years of experience with the Ponto bone-anchored hearing system-A systematic literature review. *Clin Otolaryngol* **45**, 667-680 (2020). https://doi.org/10.1111/coa.13556

8 Osborne, M. S., Child-Hymas, A. & McDermott, A. L. Clinical evaluation and resonance frequency analysis of laser-ablated titanium bone-anchored hearing implant system in children with Down Syndrome. *Int. J. Pediatr. Otorhinolaryngol.* **151**, 110981 (2021). https://doi.org/10.1016/j.ijporl.2021.110981

9 Wallberg, E., Granstrom, G., Tjellstrom, A. & Stalfors, J. Implant survival rate in bone-anchored hearing aid users: long-term results. *J Laryngol Otol* **125**, 1131-1135 (2011). https://doi.org/10.1017/S0022215111001447

10 Hao, T., Ijaz, A., Cho, W. S. & Kasbekar, A. Percutaneous bone-anchored hearing rehabilitation in adults: the Nottingham experience over a five-year period. *J Laryngol Otol* **139**, 752-756 (2025). https://doi.org/10.1017/S002221512500043X

11 Verstraeten, N., Zarowski, A. J., Somers, T., Riff, D. & Offeciers, E. F. Comparison of the audiologic results obtained with the bone-anchored hearing aid attached to the headband, the testband, and to the "snap" abutment. *Otol Neurotol* **30**, 70-75 (2009). https://doi.org/10.1097/MAO.0b013e31818be97a

12 Cywka, K. B., Skarzynski, P. H., Krol, B., Hatzopoulos, S. & Skarzynski, H. Evaluation of the Bonebridge BCI 602 active bone conductive implant in adults: efficacy and stability of audiological, surgical, and functional outcomes. *Eur Arch Otorhinolaryngol* **279**, 3525-3534 (2022). https://doi.org/10.1007/s00405-022-07265-2

13 Albrektsson, T., Branemark, P. I., Hansson, H. A. & Lindstrom, J. Osseointegrated titanium implants. Requirements for ensuring a long-lasting,

direct bone-to-implant anchorage in man. *Acta Orthop Scand* **52**, 155-170 (1981). https://doi.org/10.3109/17453678108991776

14 Grandfield, K., Palmquist, A. & Engqvist, H. High-resolution three-dimensional probes of biomaterials and their interfaces. *Philos Trans A Math Phys Eng Sci* **370**, 1337-1351 (2012). https://doi.org/10.1098/rsta.2011.0253

15 Palmquist, A. A multiscale analytical approach to evaluate osseointegration. *J Mater Sci Mater Med* **29**, 60 (2018). https://doi.org/10.1007/s10856-018-6068-y

16 Branemark, R., Ohrnell, L. O., Nilsson, P. & Thomsen, P. Biomechanical characterization of osseointegration during healing: an experimental in vivo study in the rat. *Biomaterials* **18**, 969-978 (1997). https://doi.org/10.1016/s0142-9612(97)00018-5

17 Esposito, M., Hirsch, J. M., Lekholm, U. & Thomsen, P. Biological factors contributing to failures of osseointegrated oral implants. (II). Etiopathogenesis. *Eur J Oral Sci* **106**, 721-764 (1998). https://doi.org/10.1046/j.0909-8836..t01-6-.x

18 Nakatsuji, T., Cheng, J. Y. & Gallo, R. L. Mechanisms for control of skin immune function by the microbiome. *Curr Opin Immunol* **72**, 324-330 (2021). https://doi.org/10.1016/j.coi.2021.09.001

19 Shah, F. A., Thomsen, P. & Palmquist, A. Osseointegration and current interpretations of the bone-implant interface. *Acta Biomater* **84**, 1-15 (2019). https://doi.org/10.1016/j.actbio.2018.11.018

20 Han, X. *et al.* Surface modification techniques of titanium and titanium alloys for biomedical orthopaedics applications: A review. *Colloids Surf B Biointerfaces* **227**, 113339 (2023). https://doi.org/10.1016/j.colsurfb.2023.113339

21 Liu, X., Chu, P. K. & Ding, C. Surface modification of titanium, titanium alloys, and related materials for biomedical applications. *Mater Sci Eng R Rep* **47**, 49-121 (2004).

22 Palmquist, A., Omar, O. M., Esposito, M., Lausmaa, J. & Thomsen, P. Titanium oral implants: surface characteristics, interface biology and clinical outcome. *J R Soc Interface* **7 Suppl 5**, S515-527 (2010). https://doi.org/10.1098/rsif.2010.0118.focus

23 Shah, F. A., Trobos, M., Thomsen, P. & Palmquist, A. Commercially pure titanium (cp-Ti) versus titanium alloy (Ti6Al4V) materials as bone anchored implants - Is one truly better than the other? *Mater Sci Eng C Mater Biol Appl* **62**, 960-966 (2016). https://doi.org/10.1016/j.msec.2016.01.032

24 Textor, M., Sittig, C., Frauchiger, V., Tosatti, S. & Brunette, D. M. in *Titanium in Medicine: Material Science, Surface Science, Engineering, Biological Responses and Medical Applications* (eds Donald M. Brunette, Pentti Tengvall, Marcus Textor, & Peter Thomsen) 171-230 (Springer Berlin Heidelberg, 2001).

25 Forsgren, J., Svahn, F., Jarmar, T. & Engqvist, H. Formation and adhesion of biomimetic hydroxyapatite deposited on titanium substrates. *Acta Biomater* **3**, 980-984 (2007). https://doi.org/10.1016/j.actbio.2007.03.006

26 Colnot, C. *et al.* Molecular analysis of healing at a bone-implant interface. *J Dent Res* **86**, 862-867 (2007). https://doi.org/10.1177/154405910708600911

27 Teunissen, E. M., Caspers, C. J. I., Vijverberg, M. A., Mylanus, E. A. M. & Hol, M. K. S. Long-Term Follow-up of a Wide-Diameter Bone-Anchored Hearing Implant: 10-Year Experience on Stability, Survival, and Tolerability of an

Implant-Abutment Combination. *Otol Neurotol* **44**, 40-46 (2023). https://doi.org/10.1097/MAO.0000000000003763

28 Gottlow, J., Sennerby, L., Rosengren, A. & Flynn, M. An experimental evaluation of a new craniofacial implant using the rabbit tibia model: part I. Histologic findings. *Otol Neurotol* **31**, 832-839 (2010). https://doi.org/10.1097/MAO.0b013e3181dfbbab

29 Shah, F. A. *et al.* Laser-Modified Surface Enhances Osseointegration and Biomechanical Anchorage of Commercially Pure Titanium Implants for Bone-Anchored Hearing Systems. *PLoS One* **11**, e0157504 (2016). https://doi.org/10.1371/journal.pone.0157504

30 Osborne, M. S. *et al.* Clinical Evaluation of a Novel Laser-Ablated Titanium Implant System for Bone Anchored Hearing Systems in a Pediatric Population and the Relationship of Resonance Frequency Analysis With Implant Survival. *Otol Neurotol* **43**, 219-226 (2022). https://doi.org/10.1097/MAO.0000000000003435

31 Singer, A. J. Healing Mechanisms in Cutaneous Wounds: Tipping the Balance. *Tissue Eng Part B Rev* **28**, 1151-1167 (2022). https://doi.org/10.1089/ten.TEB.2021.0114

32 Klopfleisch, R. & Jung, F. The pathology of the foreign body reaction against biomaterials. *J Biomed Mater Res A* **105**, 927-940 (2017). https://doi.org/10.1002/jbm.a.35958

33 Holgers, K.-M., Thomsen, P., Tjellström, A., Ericson, L. E. & Bjursten, L.-M. Morphologic Evaluation of Clinical Long-Term Percutaneous Titanium Implants. *Int J Oral Maxillofac Implants* **9** (1994).

34 Hogsbro, M., Agger, A. & Johansen, L. V. Bone Anchored Hearing Implant Surgery: 1 Year Follow-Up Data Shows No Effect of Hydroxyapatite Coating on Soft Tissue Reaction After Loading at 1 Week. *Otol Neurotol* **38**, e152-e158 (2017). https://doi.org/10.1097/MAO.0000000000001442

35 Trobos, M. *et al.* The clinical outcome and microbiological profile of bone-anchored hearing systems (BAHS) with different abutment topographies: a prospective pilot study. *Eur Arch Otorhinolaryngol* **275**, 1395-1408 (2018). https://doi.org/10.1007/s00405-018-4946-z

36 Johansson, M. L. *et al.* Non-invasive sampling procedure revealing the molecular events at different abutments of bone-anchored hearing systems-A prospective clinical pilot study. *Front Neurosci* **16**, 1058689 (2022). https://doi.org/10.3389/fnins.2022.1058689

37 Calon, T. G. A. *et al.* Microbiome on the Bone-Anchored Hearing System: A Prospective Study. *Front Microbiol* **10**, 799 (2019). https://doi.org/10.3389/fmicb.2019.00799

38 Calon, T. G. A., van Tongeren, J., Omar, O., Johansson, M. L. & Stokroos, R. J. Cytokine expression profile in the bone-anchored hearing system: 12-week results from a prospective randomized, controlled study. *Clin Implant Dent Relat Res* **20**, 606-616 (2018). https://doi.org/10.1111/cid.12615

39 Jansen, J. A., van der Waerden, J. P., van der Lubbe, H. B. & de Groot, K. Tissue response to percutaneous implants in rabbits. *J Biomed Mater Res* **24**, 295-307 (1990). https://doi.org/10.1002/jbm.820240303

40 Kanzara, T., Walijee, H., Badar Sheikh, R., Lau, A. & Temple, R. Long-term soft tissue outcomes for hydroxyapatite-coated bone-anchored hearing implant

surgery. *Eur Arch Otorhinolaryngol* **276**, 3067-3072 (2019). https://doi.org/10.1007/s00405-019-05609-z

41 Larsson, A. *et al.* Soft Tissue Integration of Hydroxyapatite-Coated Abutments for Bone Conduction Implants. *Clin Implant Dent Relat Res* **17 Suppl 2**, e730-735 (2015). https://doi.org/10.1111/cid.12304

42 Mylanus, E. A. & Cremers, C. W. A one-stage surgical procedure for placement of percutaneous implants for the bone-anchored hearing aid. *J Laryngol Otol* **108**, 1031-1035 (1994). https://doi.org/10.1017/s002221510012883x

43 Nelissen, R. C., den Besten, C. A., Mylanus, E. A. & Hol, M. K. Erratum to: Stability, survival, and tolerability of a 4.5-mm-wide bone-anchored hearing implant: 6-month data from a randomized controlled clinical trial. *Eur Arch Otorhinolaryngol* **273**, 113-114 (2016). https://doi.org/10.1007/s00405-015-3798-z

44 Snik, A. F. *et al.* Consensus statements on the BAHA system: where do we stand at present? *Ann Otol Rhinol Laryngol Suppl* **195**, 2-12 (2005). https://doi.org/10.1177/0003489405114s1201

45 Tjellstrom, A. & Granstrom, G. One-stage procedure to establish osseointegration: a zero to five years follow-up report. *J Laryngol Otol* **109**, 593-598 (1995). https://doi.org/10.1017/s0022215100130816

46 Tjellstrom, A. & Granstrom, G. How we do it: Frequency of skin necrosis after BAHA surgery. *Clin Otolaryngol* **31**, 216-220 (2006). https://doi.org/10.1111/j.1749-4486.2006.01152.x

47 de Wolf, M. J., Hol, M. K., Huygen, P. L., Mylanus, E. A. & Cremers, C. W. Clinical outcome of the simplified surgical technique for BAHA implantation. *Otol Neurotol* **29**, 1100-1108 (2008). https://doi.org/10.1097/MAO.0b013e31818599b8

48 Kruyt, I. J. *et al.* Three-Year Clinical and Audiological Outcomes of Percutaneous Implants for Bone Conduction Devices: Comparison Between Tissue Preservation Technique and Tissue Reduction Technique. *Otol Neurotol* **40**, 335-343 (2019). https://doi.org/10.1097/MAO.0000000000002105

49 Soo, G., Tong, C., Tsang, S. & Van Hasselt, C. in *The 2nd International Symposium on Bone Conduction Hearing-Craniofacial osseo-integration.* 33-34.

50 Hultcrantz, M. Outcome of the bone-anchored hearing aid procedure without skin thinning: a prospective clinical trial. *Otol Neurotol* **32**, 1134-1139 (2011).

51 Lindeboom, J. J. *et al.* Long-Term Results of the Linear Incision Technique With Tissue Reduction Versus Tissue Preservation for Inserting Bone-Anchored Hearing Implants: The Ongoing Optimization in Bone Implant Surgery. *Otol Neurotol* **45**, 285-294 (2024). https://doi.org/10.1097/MAO.0000000000004101

52 Calon, T. G. A. *et al.* Minimally Invasive Ponto Surgery Versus the Linear Incision Technique With Soft Tissue Preservation for Bone Conduction Hearing Implants: A Multicenter Randomized Controlled Trial. *Otol Neurotol* **39**, 882-893 (2018). https://doi.org/10.1097/MAO.0000000000001852

53 Johansson, M. L., Eriksson, T. & Omar, O. In Vitro and Ex Vivo Evaluation of a Novel Guided Drill System for Bone-Anchored Hearing Implants. *Int J Oral Maxillofac Implants* **34**, e85-e98 (2019). https://doi.org/10.11607/jomi.7590

54 Becker, W., Goldstein, M., Becker, B. E. & Sennerby, L. Minimally invasive flapless implant surgery: a prospective multicenter study. *Clin Implant Dent Relat Res* **7 Suppl 1**, S21-27 (2005). https://doi.org/10.1111/j.1708-8208.2005.tb00071.x

55 Brodala, N. Flapless surgery and its effect on dental implant outcomes. *Int J Oral Maxillofac Implants* **24 Suppl**, 118-125 (2009).

56 Campelo, L. D. & Camara, J. R. Flapless implant surgery: a 10-year clinical retrospective analysis. *Int J Oral Maxillofac Implants* **17**, 271-276 (2002).

57 Moraschini, V., Velloso, G., Luz, D. & Barboza, E. P. Implant survival rates, marginal bone level changes, and complications in full-mouth rehabilitation with flapless computer-guided surgery: a systematic review and meta-analysis. *Int J Oral Maxillofac Surg* **44**, 892-901 (2015). https://doi.org/10.1016/j.ijom.2015.02.013

58 Berdougo, M., Fortin, T., Blanchet, E., Isidori, M. & Bosson, J. L. Flapless implant surgery using an image-guided system. A 1- to 4-year retrospective multicenter comparative clinical study. *Clin Implant Dent Relat Res* **12**, 142-152 (2010). https://doi.org/10.1111/j.1708-8208.2008.00146.x

59 Fortin, T., Bosson, J. L., Isidori, M. & Blanchet, E. Effect of flapless surgery on pain experienced in implant placement using an image-guided system. *Int J Oral Maxillofac Implants* **21**, 298-304 (2006).

60 De Bruyn, H., Atashkadeh, M., Cosyn, J. & van de Velde, T. Clinical outcome and bone preservation of single TiUnite implants installed with flapless or flap surgery. *Clin Implant Dent Relat Res* **13**, 175-183 (2011). https://doi.org/10.1111/j.1708-8208.2009.00200.x

61 Eriksson, R. A. & Albrektsson, T. The effect of heat on bone regeneration: an experimental study in the rabbit using the bone growth chamber. *J Oral Maxillofac Surg* **42**, 705-711 (1984). https://doi.org/10.1016/0278-2391(84)90417-8

62 Jeong, S. M. *et al.* The effect of guided flapless implant procedure on heat generation from implant drilling. *J Craniomaxillofac Surg* **42**, 725-729 (2014). https://doi.org/10.1016/j.jcms.2013.11.002

63 Katsoulis, J. *et al.* Comparison of implant stability by means of resonance frequency analysis for flapless and conventionally inserted implants. *Clin Implant Dent Relat Res* **14**, 915-923 (2012). https://doi.org/10.1111/j.1708-8208.2010.00326.x

64 Sclar, A. G. Guidelines for flapless surgery. *J Oral Maxillofac Surg* **65**, 20-32 (2007). https://doi.org/10.1016/j.joms.2007.03.017

65 Caspers, C. J. I., Kruyt, I. J., Mylanus, E. A. M. & Hol, M. K. S. A Clinical Evaluation of Minimally Invasive Ponto Surgery With a Modified Drill System for Inserting Bone-Anchored Hearing Implants. *Otol Neurotol* **42**, 1192-1200 (2021). https://doi.org/10.1097/MAO.0000000000003195

66 Holmes, S., Hamiter, M., Berry, C. & Mankekar, G. Tissue Preservation Techniques for Bone-Anchored Hearing Aid Surgery. *Otol Neurotol* **42**, 1044-1050 (2021). https://doi.org/10.1097/MAO.0000000000003157

67 Bezdjian, A. *et al.* Experience with Minimally Invasive Ponto Surgery and Linear Incision Approach for Pediatric and Adult Bone Anchored Hearing Implants. *Ann Otol Rhinol Laryngol* **129**, 380-387 (2020). https://doi.org/10.1177/0003489419891451

68 Johansson, M. L. *et al.* Short-term results from seventy-six patients receiving a bone-anchored hearing implant installed with a novel minimally invasive surgery technique. *Clin Otolaryngol* **42**, 1043-1048 (2017). https://doi.org/10.1111/coa.12803

69 Kim, H. H. S. *et al.* Standardization of the Punch Technique for the Implantation of Bone Anchored Auditory Devices: Evaluation of the MIPS Surgical Set. *Otol Neurotol* **40**, e631-e635 (2019). https://doi.org/10.1097/MAO.0000000000002291

70 Bennett, A. & Sawant, R. Comparison of soft tissue preservation techniques for BAHA insertion in 41 patients: 'Bus-stop' (open approach) vs MIPS (minimally invasive approach). *Clin Otolaryngol* **44**, 1120-1123 (2019). https://doi.org/10.1111/coa.13409

71 Limbrick, J. *et al.* Novel Minimal Access Bone Anchored Hearing Implant Surgery and a New Surface Modified Titanium Implant, the Birmingham Experience. *Otol Neurotol* **40**, 1326-1332 (2019). https://doi.org/10.1097/MAO.0000000000002423

72 Johansson ML, L. E., Omar O. in *International Congress on Bone Conduction Hearing and Related Technologies* (Miami Beach, Florida, United States, 2019).

73 Teunissen, E., Caspers, C., Kruyt, I., Mylanus, E. & Hol, M. Long-Term Clinical Outcomes for Bone-Anchored Hearing Implants: 3-Year Comparison Between Minimally Invasive Ponto Surgery and the Linear Incision Technique With Tissue Preservation. *Otol Neurotol* **46**, 161-169 (2025). https://doi.org/10.1097/MAO.0000000000004398

74 Cruz, L. D. S. *et al.* Minimally invasive surgery as a new clinical standard for bone anchored hearing implants-real-world data from 10 years of follow-up and 228 surgeries. *Front Surg* **10**, 1209927 (2023). https://doi.org/10.3389/fsurg.2023.1209927

75 Teunissen, E. M. *et al.* Evaluation of Clinical Performance of Ponto Implantation Using a Minimally Invasive Surgical Technique-A Prospective Multicenter Study. *Otol Neurotol* **45**, 1037-1044 (2024). https://doi.org/10.1097/MAO.0000000000004315

76 Eriksson, A. R. & Albrektsson, T. Temperature threshold levels for heat-induced bone tissue injury: a vital-microscopic study in the rabbit. *J Prosthet Dent* **50**, 101-107 (1983). https://doi.org/10.1016/0022-3913(83)90174-9

77 Bachus, K. N., Rondina, M. T. & Hutchinson, D. T. The effects of drilling force on cortical temperatures and their duration: an in vitro study. *Med Eng Phys* **22**, 685-691 (2000). https://doi.org/10.1016/s1350-4533(01)00016-9

78 Aghvami, M., Brunski, J. B., Serdar Tulu, U., Chen, C. H. & Helms, J. A. A Thermal and Biological Analysis of Bone Drilling. *J Biomech Eng* **140**, 1010101-1010108 (2018). https://doi.org/10.1115/1.4040312

79 Can, M., Koluacik, S., Bahce, E., Gokce, H. & Tecellioglu, F. S. Investigation of thermal damage in bone drilling: Hybrid processing method and pathological evaluation of existing methods. *J Mech Behav Biomed Mater* **126**, 105030 (2022). https://doi.org/10.1016/j.jmbbm.2021.105030

80 Ein-Afshar, M. J., Shahrezaee, M., Shahrezaee, M. H. & Sharifzadeh, S. R. Biomechanical Evaluation of Temperature Rising and Applied Force in Controlled Cortical Bone Drilling: an Animal in Vitro Study. *Arch Bone Jt Surg* **8**, 605-612 (2020). https://doi.org/10.22038/abjs.2020.45014.2233

81 Jung, O., Lindner, C., Pantermehl, S. & Barbeck, M. Heat Development During Medical Drilling: Influencing Factors and Examination Methods - Overview and First Results. *In Vivo* **35**, 3011-3017 (2021). https://doi.org/10.21873/invivo.12596

82 Tehemar, S. H. Factors affecting heat generation during implant site preparation: a review of biologic observations and future considerations. *Int J Oral Maxillofac Implants* **14**, 127-136 (1999).

83 Shah, F. A. & Palmquist, A. Evidence that Osteocytes in Autogenous Bone Fragments can Repair Disrupted Canalicular Networks and Connect with Osteocytes in de novo Formed Bone on the Fragment Surface. *Calcif Tissue Int* **101**, 321-327 (2017). https://doi.org/10.1007/s00223-017-0283-2

84 Timon, C. & Keady, C. Thermal Osteonecrosis Caused by Bone Drilling in Orthopedic Surgery: A Literature Review. *Cureus* **11**, e5226 (2019). https://doi.org/10.7759/cureus.5226

85 Pandey, R. K. & Panda, S. S. Drilling of bone: A comprehensive review. *J Clin Orthop Trauma* **4**, 15-30 (2013). https://doi.org/10.1016/j.jcot.2013.01.002

86 Hakansson, B., Eeg-Olofsson, M., Reinfeldt, S., Stenfelt, S. & Granstrom, G. Percutaneous versus transcutaneous bone conduction implant system: a feasibility study on a cadaver head. *Otol Neurotol* **29**, 1132-1139 (2008). https://doi.org/10.1097/MAO.0b013e31816fdc90

87 Hakansson, B. The future of bone conduction hearing devices. *Adv Otorhinolaryngol* **71**, 140-152 (2011). https://doi.org/10.1159/000323715

88 Magele, A., Schoerg, P., Stanek, B., Gradl, B. & Sprinzl, G. M. Active transcutaneous bone conduction hearing implants: Systematic review and meta-analysis. *PLoS One* **14**, e0221484 (2019). https://doi.org/10.1371/journal.pone.0221484

89 Mulla, O., Agada, F. & Reilly, P. G. Introducing the Sophono Alpha 1 abutment free bone conduction hearing system. *Clin Otolaryngol* **37**, 168-169 (2012). https://doi.org/10.1111/j.1749-4486.2012.02465.x

90 Rauch, A. K., Wesarg, T., Aschendorff, A., Speck, I. & Arndt, S. Long-term data of the new transcutaneous partially implantable bone conduction hearing system Osia(R). *Eur Arch Otorhinolaryngol* **279**, 4279-4288 (2022). https://doi.org/10.1007/s00405-021-07167-9

91 Ghoncheh, M. *et al.* Output performance of the novel active transcutaneous bone conduction implant Sentio at different stimulation sites. *Hear Res* **421**, 108369 (2022). https://doi.org/10.1016/j.heares.2021.108369

92 Lagerkvist, H. J., M. L. The Sentio™ System (Whitepaper 282508). Report No. 282508UK – Version B / 2024.10, (Oticon Medical, Research and Technology, Askim, Sweden, 2024).

93 Sprinzl, G. M. & Wolf-Magele, A. The Bonebridge Bone Conduction Hearing Implant: indication criteria, surgery and a systematic review of the literature. *Clin Otolaryngol* **41**, 131-143 (2016). https://doi.org/10.1111/coa.12484

94 Willenborg, K., Avallone, E., Maier, H., Lenarz, T. & Busch, S. A New Active Osseointegrated Implant System in Patients with Single-Sided Deafness. *Audiol Neurootol* **27**, 83-92 (2022). https://doi.org/10.1159/000515489

95 Fierens, G., Standaert, N., Peeters, R., Glorieux, C. & Verhaert, N. Safety of active auditory implants in magnetic resonance imaging. *J Otol* **16**, 185-198 (2021). https://doi.org/10.1016/j.joto.2020.12.005

96 Rigato, C. *et al.* Direct bone conduction stimulation: Ipsilateral effect of different transducer attachments in active transcutaneous devices. *Hear Res* **361**, 103-112 (2018). https://doi.org/10.1016/j.heares.2018.01.007

97 Schurzig, D. *et al.* Clinical Evidence on the Influence of Implant Position onto Maximum Output with the Bonebridge Bone Conduction Implant. *Otol Neurotol* **46**, 725-732 (2025). https://doi.org/10.1097/MAO.0000000000004533

98 Ronold, H. J., Lyngstadaas, S. P. & Ellingsen, J. E. A study on the effect of dual blasting with TiO2 on titanium implant surfaces on functional attachment in bone. *J Biomed Mater Res A* **67**, 524-530 (2003). https://doi.org/10.1002/jbm.a.10580

99 Ronold, H. J., Lyngstadaas, S. P. & Ellingsen, J. E. Analysing the optimal value for titanium implant roughness in bone attachment using a tensile test. *Biomaterials* **24**, 4559-4564 (2003). https://doi.org/10.1016/s0142-9612(03)00256-4

100 Eeg-Olofsson, M. *et al.* Evaluation of Bone Tissue Formation in a Flat Surface Attachment of a Bone Conduction Implant: A Pilot Study in a Sheep Model. *Audiol Neurotol Extra* **4**, 62-76 (2014).

101 Taghavi, H. *et al.* A vibration investigation of a flat surface contact to skull bone for direct bone conduction transmission in sheep skulls in vivo. *Otol Neurotol* **34**, 690-698 (2013). https://doi.org/10.1097/MAO.0b013e3182877aee

102 Azevedo, C. *et al.* Functional and patient-reported outcomes of bone-anchored hearing aids (BAHA): A prospective case series study. *J Otol* **18**, 7-14 (2023). https://doi.org/10.1016/j.joto.2022.11.002

103 Badran, K., Arya, A. K., Bunstone, D. & Mackinnon, N. Long-term complications of bone-anchored hearing aids: a 14-year experience. *J Laryngol Otol* **123**, 170-176 (2009). https://doi.org/10.1017/S0022215108002521

104 Bates, T. *et al.* Complications and Outcomes of Bone-Anchored Prostheses of the Hand: A Systematic Review. *J Hand Surg Am* (2024). https://doi.org/10.1016/j.jhsa.2024.09.017

105 Holgers, K. M., Roupe, G., Tjellstrom, A. & Bjursten, L. M. Clinical, immunological and bacteriological evaluation of adverse reactions to skin-penetrating titanium implants in the head and neck region. *Contact Dermatitis* **27**, 1-7 (1992). https://doi.org/10.1111/j.1600-0536.1992.tb05189.x

106 Wazen, J. J., Wycherly, B. & Daugherty, J. Complications of bone-anchored hearing devices. *Adv Otorhinolaryngol* **71**, 63-72 (2011). https://doi.org/10.1159/000323583

107 Genc, S. *et al.* [Chronic pain in bone anchored hearing aids]. *Agri* **33**, 200-202 (2021). https://doi.org/10.14744/agri.2019.84704

108 Siau, D. *et al.* Bone-anchored hearing aids and chronic pain: a long-term complication and a cause for elective implant removal. *J Laryngol Otol* **126**, 445-449 (2012). https://doi.org/10.1017/S0022215112000394

109 Mylanus, E. A., Johansson, C. B. & Cremers, C. W. Craniofacial titanium implants and chronic pain: histologic findings. *Otol Neurotol* **23**, 920-925 (2002). https://doi.org/10.1097/00129492-200211000-00018

110 Fontaine, N., Hemar, P., Schultz, P., Charpiot, A. & Debry, C. BAHA implant: implantation technique and complications. *Eur Ann Otorhinolaryngol Head Neck Dis* **131**, 69-74 (2014). https://doi.org/10.1016/j.anorl.2012.10.006

111 Verheij, E., Bezdjian, A., Grolman, W. & Thomeer, H. G. A Systematic Review on Complications of Tissue Preservation Surgical Techniques in Percutaneous Bone Conduction Hearing Devices. *Otol Neurotol* **37**, 829-837 (2016). https://doi.org/10.1097/MAO.0000000000001091

112 Kiringoda, R. & Lustig, L. R. A meta-analysis of the complications associated with osseointegrated hearing aids. *Otol Neurotol* **34**, 790-794 (2013). https://doi.org/10.1097/MAO.0b013e318291c651

113 Johansson, M. L. *et al.* Multimodal Analysis of the Tissue Response to a Bone-Anchored Hearing Implant: Presentation of a Two-Year Case Report of a Patient With Recurrent Pain, Inflammation, and Infection, Including a Systematic Literature Review. *Front Cell Infect Microbiol* **11**, 640899 (2021). https://doi.org/10.3389/fcimb.2021.640899

114 Vijverberg, M. A., Caspers, C. J. I., Kruyt, I. J., Mylanus, E. A. M. & Hol, M. K. S. Prospective 5 year outcomes of different implant designs and surgical techniques in 68 patients with bone anchored hearing implants. *Clin Otolaryngol* **48**, 65-69 (2023). https://doi.org/10.1111/coa.13974

115 Tjellstrom, A. & Stalfors, J. Bone-anchored hearing device surgery: a 3- to 6-year follow-up with life table and worst-case scenario calculation. *Otol Neurotol* **33**, 891-894 (2012). https://doi.org/10.1097/MAO.0b013e3182565b2e

116 Holgers, K. M., Thomsen, P. & Tjellstrom, A. Persistent irritation of the soft tissue around an osseointegrated titanium implant. Case report. *Scand J Plast Reconstr Surg Hand Surg* **28**, 225-230 (1994). https://doi.org/10.3109/02844319409015984

117 Holgers, K. M., Thomsen, P., Tjellstrom, A. & Bjursten, L. M. Immunohistochemical study of the soft tissue around long-term skin-penetrating titanium implants. *Biomaterials* **16**, 611-616 (1995). https://doi.org/10.1016/0142-9612(95)93858-b

118 Holgers, K. M., Thomsen, P., Tjellstrom, A. & Ericson, L. E. Electron microscopic observations on the soft tissue around clinical long-term percutaneous titanium implants. *Biomaterials* **16**, 83-90 (1995). https://doi.org/10.1016/0142-9612(95)98267-i

119 Anderson, J. M. Biological responses to materials. *Annu Rev Mater Res* **31**, 81-110 (2001).

120 Koh, T. J. & DiPietro, L. A. Inflammation and wound healing: the role of the macrophage. *Expert Rev Mol Med* **13**, e23 (2011).

121 Gretzer, C., Emanuelsson, L., Liljensten, E. & Thomsen, P. The inflammatory cell influx and cytokines changes during transition from acute inflammation to fibrous repair around implanted materials. *J Biomater Sci Polym Ed* **17**, 669-687 (2006).

122 Thomsen, P. & Gretzer, C. Macrophage interactions with modified material surfaces. *Curr Opin Solid State Mater Sci* **5**, 163-176 (2001).

123 Broggini, N. *et al.* Peri-implant inflammation defined by the implant-abutment interface. *J Dent Res* **85**, 473-478 (2006). https://doi.org/10.1177/154405910608500515

124 Wilgus, T. A., Roy, S. & McDaniel, J. C. Neutrophils and Wound Repair: Positive Actions and Negative Reactions. *Adv Wound Care (New Rochelle)* **2**, 379-388 (2013). https://doi.org/10.1089/wound.2012.0383

125 Holgers, K. M. & Ljungh, A. Cell surface characteristics of microbiological isolates from human percutaneous titanium implants in the head and neck. *Biomaterials* **20**, 1319-1326 (1999). https://doi.org/10.1016/s0142-9612(99)00033-2

126 Flemming, H. C., Neu, T. R. & Wozniak, D. J. The EPS matrix: the "house of biofilm cells". *J Bacteriol* **189**, 7945-7947 (2007). https://doi.org/10.1128/JB.00858-07

127 Hoiby, N., Bjarnsholt, T., Givskov, M., Molin, S. & Ciofu, O. Antibiotic resistance of bacterial biofilms. *Int J Antimicrob Agents* **35**, 322-332 (2010). https://doi.org/10.1016/j.ijantimicag.2009.12.011

128 Arciola, C. R., Campoccia, D., Ravaioli, S. & Montanaro, L. Polysaccharide intercellular adhesin in biofilm: structural and regulatory aspects. *Front Cell Infect Microbiol* **5**, 7 (2015). https://doi.org/10.3389/fcimb.2015.00007

129 Flemming, H. C. & Wingender, J. The biofilm matrix. *Nat Rev Microbiol* **8**, 623-633 (2010). https://doi.org/10.1038/nrmicro2415

130 Liu, H. Y., Prentice, E. L. & Webber, M. A. Mechanisms of antimicrobial resistance in biofilms. *NPJ Antimicrob Resist* **2**, 27 (2024). https://doi.org/10.1038/s44259-024-00046-3

131 Brown, M. R., Allison, D. G. & Gilbert, P. Resistance of bacterial biofilms to antibiotics: a growth-rate related effect? *J Antimicrob Chemother* **22**, 777-780 (1988). https://doi.org/10.1093/jac/22.6.777

132 Costerton, J. W., Stewart, P. S. & Greenberg, E. P. Bacterial biofilms: a common cause of persistent infections. *Science* **284**, 1318-1322 (1999). https://doi.org/10.1126/science.284.5418.1318

133 Gerdes, K. & Semsey, S. Microbiology: Pumping persisters. *Nature* **534**, 41-42 (2016). https://doi.org/10.1038/nature18442

134 Hall, C. W. & Mah, T. F. Molecular mechanisms of biofilm-based antibiotic resistance and tolerance in pathogenic bacteria. *FEMS Microbiol Rev* **41**, 276-301 (2017). https://doi.org/10.1093/femsre/fux010

135 Lewis, K. Persister cells, dormancy and infectious disease. *Nat Rev Microbiol* **5**, 48-56 (2007). https://doi.org/10.1038/nrmicro1557

136 Monksfield, P. *et al.* Biofilm formation on bone-anchored hearing aids. *J Laryngol Otol* **125**, 1125-1130 (2011). https://doi.org/10.1017/S0022215111002143

137 Holgers, K. M., Tjellstrom, A., Bjursten, L. M. & Erlandsson, B. E. Soft tissue reactions around percutaneous implants: a clinical study on skin-penetrating titanium implants used for bone-anchored auricular prostheses. *Int J Oral Maxillofac Implants* **2**, 35-39 (1987).

138 Kruyt, I. J., Nelissen, R. C., Johansson, M. L., Mylanus, E. A. M. & Hol, M. K. S. The IPS-scale: A new soft tissue assessment scale for percutaneous and transcutaneous implants for bone conduction devices. *Clin Otolaryngol* **42**, 1410-1413 (2017). https://doi.org/10.1111/coa.12922

139 Gillett, D., Fairley, J. W., Chandrashaker, T. S., Bean, A. & Gonzalez, J. Bone-anchored hearing aids: results of the first eight years of a programme in a

district general hospital, assessed by the Glasgow benefit inventory. *J Laryngol Otol* **120**, 537-542 (2006). https://doi.org/10.1017/S0022215106001277

140 Chu, T. S. M., Mather, M. & Banerjee, A. Complications of bone-conduction hearing implants (BCHI) implantation surgery. *Am J Otolaryngol* **41**, 102378 (2020). https://doi.org/10.1016/j.amjoto.2019.102378

141 Zheng, Y. N., Sarah, A., Imran, M., Sue, A. & Melanie, G. Decision-making: Bone conducting hearing implants for adults. (The Ear Foundation, 2017).

142 Trobos, M. *et al.* Genomics of Staphylococcus aureus and Staphylococcus epidermidis from Periprosthetic Joint Infections and Correlation to Clinical Outcome. *Microbiol Spectr* **10**, e0218121 (2022). https://doi.org/10.1128/spectrum.02181-21

143 Svensson Malchau, K. *et al.* Biofilm properties in relation to treatment outcome in patients with first-time periprosthetic hip or knee joint infection. *J Orthop Translat* **30**, 31-40 (2021). https://doi.org/10.1016/j.jot.2021.05.008

144 Zaborowska, M. *et al.* Biofilm formation and antimicrobial susceptibility of staphylococci and enterococci from osteomyelitis associated with percutaneous orthopaedic implants. *J Biomed Mater Res B Appl Biomater* **105**, 2630-2640 (2017). https://doi.org/10.1002/jbm.b.33803

145 Barbara, M., Perotti, M., Gioia, B., Volpini, L. & Monini, S. Transcutaneous bone-conduction hearing device: audiological and surgical aspects in a first series of patients with mixed hearing loss. *Acta Otolaryngol* **133**, 1058-1064 (2013). https://doi.org/10.3109/00016489.2013.799293

146 Doshi, J., Schneiders, S., Foster, K., Reid, A. & McDermott, A. L. Magnetic resonance imaging and bone anchored hearing implants: pediatric considerations. *Int J Pediatr Otorhinolaryngol* **78**, 277-279 (2014). https://doi.org/10.1016/j.ijporl.2013.11.023

147 Steinmetz, C. *et al.* MRI artefacts after Bonebridge implantation. *Eur Arch Otorhinolaryngol* **271**, 2079-2082 (2014). https://doi.org/10.1007/s00405-014-3001-y

148 Utrilla, C., Gavilan, J., Garcia-Raya, P., Calvino, M. & Lassaletta, L. MRI after Bonebridge implantation: a comparison of two implant generations. *Eur Arch Otorhinolaryngol* **278**, 3203-3209 (2021). https://doi.org/10.1007/s00405-020-06380-2

149 Yang, J. *et al.* BoneBridge implantation in patients with single-sided deafness resulting from vestibular schwannoma resection: objective and subjective benefit evaluations. *Acta Otolaryngol* **138**, 877-885 (2018). https://doi.org/10.1080/00016489.2018.1469789

150 Godbehere, J., Carr, S. D., Moraleda, J., Edwards, P. & Ray, J. A comparison study of complications and initial follow-up costs of transcutaneous and percutaneous bone conduction devices. *J Laryngol Otol* **131**, 667-670 (2017). https://doi.org/10.1017/S002221511700127X

151 Lavilla Martin de Valmaseda, M. J. *et al.* Clinical guideline on bone conduction implants. *Acta Otorrinolaringol Esp (Engl Ed)* **70**, 105-111 (2019). https://doi.org/10.1016/j.otorri.2017.12.001

152 de Souza, M. A., Riart, S. L. V., de Souza, S. R., de Brito, R. & Bento, R. F. Complications of transcutaneous protheses–a systematic review of publications over the past 10 years. *Int Arch Otorhinolaryngol* **26**, e505-e512 (2022).

153 Crowder, H. R., Bestourous, D. E. & Reilly, B. K. Adverse events associated with Bonebridge and Osia bone conduction implant devices. *Am J Otolaryngol* **42**, 102968 (2021). https://doi.org/10.1016/j.amjoto.2021.102968

154 Hernandez, S., Ospina, J. C., Gutierrez-Gomez, E., Rodriguez-Ruiz, M. T. & Escobar, J. L. Long term cutaneous complications related to bone conduction hearing implants. A retrospective study (2004-2018). *Auris Nasus Larynx* **48**, 878-884 (2021). https://doi.org/10.1016/j.anl.2021.01.020

155 Baer, D. R. *et al.* Comparison of the sputter rates of oxide films relative to the sputter rate of SiO2. *J Vac Sci Technol A* **28**, 1060-1072 (2010).

156 Baldassarri, L., Bertuccini, L., Ammendolia, M. G., Arciola, C. R. & Montanaro, L. Effect of iron limitation on slime production by Staphylococcus aureus. *Eur J Clin Microbiol Infect Dis* **20**, 343-345 (2001). https://doi.org/10.1007/pl00011274

157 Arciola, C. R. *et al.* Detection of slime production by means of an optimised Congo red agar plate test based on a colourimetric scale in Staphylococcus epidermidis clinical isolates genotyped for ica locus. *Biomaterials* **23**, 4233-4239 (2002). https://doi.org/10.1016/s0142-9612(02)00171-0

158 Holgers, K. M., Bjursten, L. M., Thomsen, P., Ericson, L. E. & Tjellstrom, A. Experience with percutaneous titanium implants in the head and neck: a clinical and histological study. *J Invest Surg* **2**, 7-16 (1989). https://doi.org/10.3109/08941938909016500

159 Byrd, A. L. *et al.* Staphylococcus aureus and Staphylococcus epidermidis strain diversity underlying pediatric atopic dermatitis. *Sci Transl Med* **9** (2017). https://doi.org/10.1126/scitranslmed.aal4651

160 Harris-Tryon, T. A. & Grice, E. A. Microbiota and maintenance of skin barrier function. *Science* **376**, 940-945 (2022). https://doi.org/10.1126/science.abo0693

161 Kulalert, W. *et al.* The neuroimmune CGRP-RAMP1 axis tunes cutaneous adaptive immunity to the microbiota. *Proc Natl Acad Sci U S A* **121**, e2322574121 (2024). https://doi.org/10.1073/pnas.2322574121

162 Chiu, I. M. *et al.* Bacteria activate sensory neurons that modulate pain and inflammation. *Nature* **501**, 52-57 (2013). https://doi.org/10.1038/nature12479

163 Blake, K. J. *et al.* Staphylococcus aureus produces pain through pore-forming toxins and neuronal TRPV1 that is silenced by QX-314. *Nat Commun* **9**, 37 (2018). https://doi.org/10.1038/s41467-017-02448-6

164 de Tommaso, M. *et al.* Effects of affective pictures on pain sensitivity and cortical responses induced by laser stimuli in healthy subjects and migraine patients. *Int J Psychophysiol* **74**, 139-148 (2009). https://doi.org/10.1016/j.ijpsycho.2009.08.004

165 van Wamel, W. J., Rooijakkers, S. H., Ruyken, M., van Kessel, K. P. & van Strijp, J. A. The innate immune modulators staphylococcal complement inhibitor and chemotaxis inhibitory protein of Staphylococcus aureus are located on beta-hemolysin-converting bacteriophages. *J Bacteriol* **188**, 1310-1315 (2006). https://doi.org/10.1128/JB.188.4.1310-1315.2006

166 Al Kindi, A. *et al.* Staphylococcus aureus Internalized by Skin Keratinocytes Evade Antibiotic Killing. *Front Microbiol* **10**, 2242 (2019). https://doi.org/10.3389/fmicb.2019.02242

167 Campoccia, D., Montanaro, L. & Arciola, C. R. The significance of infection related to orthopedic devices and issues of antibiotic resistance. *Biomaterials* **27**, 2331-2339 (2006). https://doi.org/10.1016/j.biomaterials.2005.11.044

168 Albavera-Gutierrez, R. R. *et al.* Prevalence of Staphylococcus aureus Infections in the Implantation of Orthopedic Devices in a Third-Level Hospital: An Observational Cohort Study. *Pathogens* **13** (2024). https://doi.org/10.3390/pathogens13080620

169 Teterycz, D. *et al.* Outcome of orthopedic implant infections due to different staphylococci. *Int J Infect Dis* **14**, e913-918 (2010). https://doi.org/10.1016/j.ijid.2010.05.014

170 Antonelli, P. J., Lee, J. C. & Burne, R. A. Bacterial biofilms may contribute to persistent cochlear implant infection. *Otol Neurotol* **25**, 953-957 (2004). https://doi.org/10.1097/00129492-200411000-00015

171 Im, G. J. *et al.* Analysis of Bacterial Biofilms on a Cochlear Implant Following Methicillin-Resistant Staphylococcus Aureus Infection. *J Audiol Otol* **19**, 172-177 (2015). https://doi.org/10.7874/jao.2015.19.3.172

172 Pawlowski, K. S., Wawro, D. & Roland, P. S. Bacterial biofilm formation on a human cochlear implant. *Otol Neurotol* **26**, 972-975 (2005). https://doi.org/10.1097/01.mao.0000169047.38759.8b

173 Brown, E. M. & Thomas, P. Fusidic acid resistance in Staphylococcus aureus isolates. *Lancet* **359**, 803 (2002). https://doi.org/10.1016/S0140-6736(02)07869-8

174 Castanheira, M., Watters, A. A., Bell, J. M., Turnidge, J. D. & Jones, R. N. Fusidic acid resistance rates and prevalence of resistance mechanisms among Staphylococcus spp. isolated in North America and Australia, 2007-2008. *Antimicrob Agents Chemother* **54**, 3614-3617 (2010). https://doi.org/10.1128/AAC.01390-09

175 Castanheira, M., Watters, A. A., Mendes, R. E., Farrell, D. J. & Jones, R. N. Occurrence and molecular characterization of fusidic acid resistance mechanisms among Staphylococcus spp. from European countries (2008). *J Antimicrob Chemother* **65**, 1353-1358 (2010). https://doi.org/10.1093/jac/dkq094

176 Hajikhani, B. *et al.* The global prevalence of fusidic acid resistance in clinical isolates of Staphylococcus aureus: a systematic review and meta-analysis. *Antimicrob Resist Infect Control* **10**, 75 (2021). https://doi.org/10.1186/s13756-021-00943-6

177 Alsterholm, M., Flytstrom, I., Bergbrant, I. M. & Faergemann, J. Fusidic acid-resistant Staphylococcus aureus in impetigo contagiosa and secondarily infected atopic dermatitis. *Acta Derm Venereol* **90**, 52-57 (2010). https://doi.org/10.2340/00015555-0771

178 Chen, H. J. *et al.* Fusidic acid resistance determinants in Staphylococcus aureus clinical isolates. *Antimicrob Agents Chemother* **54**, 4985-4991 (2010). https://doi.org/10.1128/AAC.00523-10

179 McLaws, F., Chopra, I. & O'Neill, A. J. High prevalence of resistance to fusidic acid in clinical isolates of Staphylococcus epidermidis. *J Antimicrob Chemother* **61**, 1040-1043 (2008). https://doi.org/10.1093/jac/dkn071

180 Mitra, A., Mohanraj, M. & Shah, M. High levels of fusidic acid-resistant Staphylococcus aureus despite restrictions on antibiotic use. *Clin Exp Dermatol* **34**, 136-139 (2009). https://doi.org/10.1111/j.1365-2230.2008.02790.x

181 Shah, M. & Mohanraj, M. High levels of fusidic acid-resistant Staphylococcus aureus in dermatology patients. *Br J Dermatol* **148**, 1018-1020 (2003). https://doi.org/10.1046/j.1365-2133.2003.05291.x

182 Olsen, L. B., Larsen, S., Wanscher, J. H., Faber, C. E. & Jeppesen, J. Postoperative infections following cochlear implant surgery. *Acta Otolaryngol* **138**, 956-960 (2018). https://doi.org/10.1080/00016489.2018.1482422

183 Shapira, Y., Yaar-Soffer, Y., Hildesheimer, M., Migirov, L. & Henkin, Y. Pain in cochlear implant recipients: an uncommon, yet serious, consequence of cochlear implantation. *Laryngoscope* **125**, 1946-1951 (2015). https://doi.org/10.1002/lary.25272

184 Vijendren, A. *et al.* Cochlear Implant Infections and Outcomes: Experience From a Single Large Center. *Otol Neurotol* **41**, e1105-e1110 (2020). https://doi.org/10.1097/MAO.0000000000002772

185 Weder, S., Shaul, C., Wong, A., O'Leary, S. & Briggs, R. J. Management of Severe Cochlear Implant Infections-35 Years Clinical Experience. *Otol Neurotol* **41**, 1341-1349 (2020). https://doi.org/10.1097/MAO.0000000000002783

186 Zhang, A. *et al.* Effect of feed condition on thrust force and torque during continuous and step-by-step drilling of cortical bone. *Procedia CIRP* **89**, 201-206 (2020). https://doi.org/10.1016/j.procir.2020.05.143

187 Fujiwara, S. *et al.* Effect of low-speed drilling without irrigation on osseointegration: an experimental study in dogs. *Oral Maxillofac Surg* **26**, 595-601 (2022). https://doi.org/10.1007/s10006-021-01023-0

188 Alam, K. *et al.* Effect of drill quality on biological damage in bone drilling. *Sci Rep* **13**, 6234 (2023). https://doi.org/10.1038/s41598-023-33381-y

189 Korkmaz, M. E., Gupta, M., Ross, N. S. & Sivalingam, V. Implementation of green cooling/lubrication strategies in metal cutting industries: a state of the art towards sustainable future and challenges. *Sustain Mater Technol* **36**, e00641 (2023).

190 Zhao, J., Liu, Z., Wang, B., Hu, J. & Wan, Y. Tool coating effects on cutting temperature during metal cutting processes: Comprehensive review and future research directions. *Mech Syst Signal Proces* **150**, 107302 (2021).

191 Mohlhenrich, S. C. *et al.* Thermal evaluation by infrared measurement of implant site preparation between single and gradual drilling in artificial bone blocks of different densities. *Int J Oral Maxillofac Surg* **45**, 1478-1484 (2016). https://doi.org/10.1016/j.ijom.2016.05.020

192 Koutiech, T., Ahmad Heshmeh, O., Alkerdi, K., Toumi, J. & Al Sabek, L. Comparison of Maximum Heat Generation during Implant Site Preparation between Single and Gradual Drilling Protocols in Artificial D1 Bone Blocks: An In Vitro Study. *Int J Dent* **2022**, 9370395 (2022). https://doi.org/10.1155/2022/9370395

193 Cseke, A. & Heinemann, R. The effects of cutting parameters on cutting forces and heat generation when drilling animal bone and biomechanical test materials. *Med Eng Phys* **51**, 24-30 (2018). https://doi.org/10.1016/j.medengphy.2017.10.009

194 Jacob, C. H. & Berry, J. T. A study of the bone machining process--drilling. *J Biomech*, 343-349 (1976).
195 Augustin, G. *et al.* Temperature changes during cortical bone drilling with a newly designed step drill and an internally cooled drill. *Int Orthop* **36**, 1449-1456 (2012). https://doi.org/10.1007/s00264-012-1491-z
196 Augustin, G. *et al.* Thermal osteonecrosis and bone drilling parameters revisited. *Arch Orthop Trauma Surg* **128**, 71-77 (2008). https://doi.org/10.1007/s00402-007-0427-3
197 Migliorati, M. *et al.* Internal bone temperature change during guided surgery preparations for dental implants: an in vitro study. *Int J Oral Maxillofac Implants* **28**, 1464-1469 (2013). https://doi.org/10.11607/jomi.2854
198 Pupulin, F., Oresta, G., Sunar, T. & Parenti, P. On the thermal impact during drilling operations in guided dental surgery: An experimental and numerical investigation. *J Mech Behav Biomed Mater* **150**, 106327 (2024). https://doi.org/10.1016/j.jmbbm.2023.106327
199 Ali, A., Brintouch, I., Romanos, G. & Delgado-Ruiz, R. Cooling Efficiency of Sleeveless 3D-Printed Surgical Guides with Different Cylinder Designs. *Medicina (Kaunas)* **60** (2024). https://doi.org/10.3390/medicina60020239
200 Kniha, K. *et al.* Temperature Threshold Values of Bone Necrosis for Thermo-Explantation of Dental Implants-A Systematic Review on Preclinical In Vivo Research. *Materials (Basel)* **13** (2020). https://doi.org/10.3390/ma13163461
201 Bonfield, W. & Li, C. H. The temperature dependence of the deformation of bone. *J Biomech* **1**, 323-329 (1968). https://doi.org/10.1016/0021-9290(68)90026-2
202 Thompson, H. C. Effect of drilling into bone. *J Oral Surg (Chic)* **16**, 22-30 (1958).
203 Augustin, G., Davila, S., Udiljak, T., Vedrina, D. S. & Bagatin, D. Determination of spatial distribution of increase in bone temperature during drilling by infrared thermography: preliminary report. *Arch Orthop Trauma Surg* **129**, 703-709 (2009). https://doi.org/10.1007/s00402-008-0630-x
204 Bertollo, N. *et al.* A comparison of the thermal properties of 2- and 3-fluted drills and the effects on bone cell viability and screw pull-out strength in an ovine model. *Clin Biomech (Bristol)* **25**, 613-617 (2010). https://doi.org/10.1016/j.clinbiomech.2010.02.007
205 Addendum to Surgical Manual including the MONO procedure. Report No. 223523UK / 2021.06, (Oticon Medical, Askim, Sweden, 2021).
206 Coyac, B. R. *et al.* A novel system exploits bone debris for implant osseointegration. *J Periodontol* **92**, 716-726 (2021). https://doi.org/10.1002/JPER.20-0099
207 Coyac, B. R. *et al.* Optimizing autologous bone contribution to implant osseointegration. *J Periodontol* **91**, 1632-1644 (2020). https://doi.org/10.1002/JPER.19-0524
208 Bolind, P. *et al.* Histologic evaluation of retrieved craniofacial implants. *Otolaryngol Head Neck Surg* **123**, 140-146 (2000). https://doi.org/10.1067/mhn.2000.104667
209 Bolind, P., Johansson, C. B., Johansson, P., Granstrom, G. & Albrektsson, T. Retrieved implants from irradiated sites in humans: a histologic/histomorphometric investigation of oral and craniofacial implants.

Clin Implant Dent Relat Res **8**, 142-150 (2006). https://doi.org/10.1111/j.1708-8208.2006.00010.x

210 Granstrom, G. Microradiographic study of retrieved craniofacial osseointegrated implants. *ORL J Otorhinolaryngol Relat Spec* **62**, 26-32 (2000). https://doi.org/10.1159/000027711

211 Tjellstrom, A., Jacobsson, M. & Albrektsson, T. Removal torque of osseointegrated craniofacial implants: a clinical study. *Int J Oral Maxillofac Implants* **3**, 287-289 (1988).

212 van der Pouw, C. T., Johansson, C. B., Mylanus, E. A., Albrektsson, T. & Cremers, C. W. Removal of titanium implants from the temporal bone: histologic findings. *Am J Otol* **19**, 46-51 (1998).

213 Albrektsson, T., Jemt, T., Molne, J., Tengvall, P. & Wennerberg, A. On inflammation-immunological balance theory-A critical apprehension of disease concepts around implants: Mucositis and marginal bone loss may represent normal conditions and not necessarily a state of disease. *Clin Implant Dent Relat Res* **21**, 183-189 (2019). https://doi.org/10.1111/cid.12711

214 Hakansson, B. *et al.* A novel bone conduction implant (BCI): engineering aspects and pre-clinical studies. *Int J Audiol* **49**, 203-215 (2010). https://doi.org/10.3109/14992020903264462

215 Lutz, R. *et al.* Periosteal elevation induces supracortical peri-implant bone formation. *J Craniomaxillofac Surg* **45**, 1170-1178 (2017). https://doi.org/10.1016/j.jcms.2017.05.009

216 Yin, X., Zhang, C., Hze-Khoong, E. P., Wang, Y. & Xu, L. Influence of periosteal coverage on distraction osteogenesis with dental implant distractors. *J Oral Maxillofac Surg* **72**, 1921-1927 (2014). https://doi.org/10.1016/j.joms.2014.06.440

217 Stegen, S., van Gastel, N. & Carmeliet, G. Bringing new life to damaged bone: the importance of angiogenesis in bone repair and regeneration. *Bone* **70**, 19-27 (2015). https://doi.org/10.1016/j.bone.2014.09.017

218 Tomlinson, R. E. & Silva, M. J. Skeletal Blood Flow in Bone Repair and Maintenance. *Bone Res* **1**, 311-322 (2013). https://doi.org/10.4248/BR201304002

219 Sapir-Koren, R. & Livshits, G. Osteocyte control of bone remodeling: is sclerostin a key molecular coordinator of the balanced bone resorption-formation cycles? *Osteoporos Int* **25**, 2685-2700 (2014). https://doi.org/10.1007/s00198-014-2808-0

220 Uda, Y., Azab, E., Sun, N., Shi, C. & Pajevic, P. D. Osteocyte Mechanobiology. *Curr Osteoporos Rep* **15**, 318-325 (2017). https://doi.org/10.1007/s11914-017-0373-0

221 Watanabe-Takano, H. *et al.* Mechanical load regulates bone growth via periosteal Osteocrin. *Cell Rep* **36**, 109380 (2021). https://doi.org/10.1016/j.celrep.2021.109380

222 Shah, F. A. *et al.* Bone without borders - Monetite-based calcium phosphate guides bone formation beyond the skeletal envelope. *Bioact Mater* **19**, 103-114 (2023). https://doi.org/10.1016/j.bioactmat.2022.03.012

223 Jolic, M. *et al.* Pyrophosphate-Containing Calcium Phosphates Negatively Impact Heterotopic Bone Quality. *Adv Healthc Mater*, e2405171 (2025). https://doi.org/10.1002/adhm.202405171

224 Palmquist, A., Johansson, A., Suska, F., Branemark, R. & Thomsen, P. Acute inflammatory response to laser-induced micro- and nano-sized titanium surface features. *Clin Implant Dent Relat Res* **15**, 96-104 (2013). https://doi.org/10.1111/j.1708-8208.2011.00361.x

225 Lackington, W. A. *et al.* Bio-Inspired Micro- and Nano-Scale Surface Features Produced by Femtosecond Laser-Texturing Enhance TiZr-Implant Osseointegration. *Adv Healthc Mater* **13**, e2400810 (2024). https://doi.org/10.1002/adhm.202400810

226 Ronold, H. J. & Ellingsen, J. E. Effect of micro-roughness produced by TiO2 blasting--tensile testing of bone attachment by using coin-shaped implants. *Biomaterials* **23**, 4211-4219 (2002). https://doi.org/10.1016/s0142-9612(02)00167-9